SYNTHESIS AND CHARACTERIZATION OF NOVEL ORGANIC MATERIAL FOR DYE SENSITIZED SOLAR CELLS AND ORGANIC LIGHT EMITTING DIODES

TEADKAIT KAEWPUANG

THESIS SUBMITTED IN PARTIAL FULFILLMENT OF THE REQUIREMENTS FOR THE DEGREE OF MASTER OF SCIENCE
MAJOR IN CHEMISTRY FACULTY OF SCIENCE
UBON RATCHATHANI UNIVERSITY
YEAR 2012

THESIS APPROVAL

UBON RATCHATHANI UNIVERSITY

MASTER OF SCIENCE

MAJOR IN CHEMISTRY FACULTY OF SCIENCE

TITLE SYNTHESIS AND CHARACTERIZATION OF NOVEL ORGANIC MATERIAL FOR DYE SENSITIZED SOLAR CELLS AND ORGANIC LIGHT EMITTING DIODES

NAME MR.TEADKAIT KAEWPUANG

THIS THESIS HAS BEEN ACCEPTED BY

V. Promarak ..... CHAIR

(ASSOC.PROF.DR.VINICH PROMARAK)

Chanokporn Phaosiri ..... COMMITTEE

(ASST.PROF.DR.CHANOKPORN PHAOSIRI)

T. Sudyoadsuk ..... COMMITTEE

(ASST.PROF.DR.TAWEESAK SUDYOADSUK)

..... DEAN

(ASST.PROF.DR.JANPEN INTARAPRASERT)

APPROVAL BY UBON RATCHATHANI UNIVERSITY

Utith Inprasit .....

(ASSOC.PROF.DR.UTITH INPRASIT)

VICE PRESIDENT FOR ACADEMIC AFFAIRS

FOR THE PRESIDENT OF UBON RATCHATHANI UNIVERSITY

ACADEMIC YEAR 2012

ACKNOWLEDGMENTS

I wish to express my admiration and appreciation to Assoc.Prof.Dr.Vinich Promarak, my advisor, for his excellent suggestions, supervision, and understanding throughout my study.

I would also like to thank the many people who contributed their time, instrumentation, and advice to my project. In particular, Dr.Tinnagon Keawin for NMR experiments, Dr.Taweesak Sudyoadsuk for optoelectronic devices, Asst.Prof.Dr.Siriporn Jungsuttiwong for molecular orbital calculation, Assoc.Prof.Dr.Sayant Saengsuwan for TGA and DSC data. Moreover, I would like to thank Ubon Ratchathani Rajabhat University for IR spectroscopy.

I wish to acknowledge Asst.Prof.Dr.Chanokporn Phaosiri for constructive comments and suggestion.

Thanks so much to the Center of excellence for Innovation in Chemistry (PERCH-CIC) and Ubon Ratchathani University for financial support. Gratitude is expressed to all my teachers for showing me a different line in life, as a Chemistry graduate student. My sincere thankful is also express to the Department of Chemistry, Faculty of Science, Ubon Ratchathani University for providing a wonderful academic environment during the course work.

My appreciation is extended to all the staff of the Department of Chemistry. Furthermore, I feel thankful to my friends, sisters, brothers here in Center for Organic Electronics and Alternative Energy.

Most of all, I feel appreciate and grateful to my beloved family for their inculcation and encouragement that found me to be a fortitude person.

Teadkait Kaewpuang

(Mr Teadkait Kaewpuang)

Reseacher

บทคัดย่อ

ชื่อเรื่อง : การสังเคราะห์และการพิสูจน์ เอกลักษณ์วัสดุอินทรีย์ชนิดใหม่เพื่อใช้ในอุปกรณ์เซลล์แสงอาทิตย์ชนิดสีย้อมไวแสงและอุปกรณ์ไดโอดสารเรืองแสง

โดย : เทอดเกียรติ แก้วพวง

ชื่อปริญญา : วิทยาศาสตรมหาบัณฑิต

สาขาวิชา : เคมี

ประธานกรรมการที่ปรึกษา : รองศาสตราจารย์ ดร.วินิช พรมอารักษ์

ศัพท์สำคัญ : โอลิโกไธโอฟีน คาร์บาโซล ดี-ดี-ไพ-เอ เซลล์แสงอาทิตย์ชนิดสีย้อมไวแสง ไดโอดเรืองแสงสารอินทรีย์ อุปกรณ์ออปโตอิเล็กทรอนิกส์

ในงานวิจัยนี้รายงานการสังเคราะห์และพิสูจน์เอกลักษณ์อนุพันธ์คาร์บาโซล สำหรับใช้ในอุปกรณ์ออปโตอิเล็กทรอนิกส์ โดยได้ออกแบบโมเลกุลสีย้อมประเภท D-D-π-A ซึ่งมีความแตกต่างของ หมู่ไพ-คอนจูเกต และหมู่รับอิเล็กตรอน สำหรับใช้ในอุปกรณ์เซลล์แสงอาทิตย์ชนิดสีย้อมไวแสง โมเลกุลสีย้อมประเภท D-D-π-A ที่ทำได้สังเคราะห์ **CFTAn-A** n=1-3 ประกอบด้วย 3 ส่วน คือ (1) หมู่คาร์บาโซลทำหน้าที่เป็นหมู่ให้อิเล็กตรอน (2) หมู่โอลิโกไธโอฟีน และโอลิโกไธโอฟีน-ฟีนิลทำหน้าที่เป็นไพ-คอนจูเกตและ (3) หมู่กรดไซยาโนอะคริลิคทำหน้าที่เป็นหมู่รับอิเล็กตรอนและหมู่ยึดเกาะ สมบัติทางแสง ทางเคมีไฟฟ้า และทางความร้อนของสีย้อมขึ้นกับจำนวนของไธโอฟีนและหมู่รับอิเล็กตรอน จากการคำนวณการกระจายตัวของอิเล็กตรอนในโมเลกุลของสีย้อมที่สภาวะพื้นพบอิเล็กตรอนสะสมอยู่ที่หมู่ให้อิเล็กตรอนที่เป็นหมู่คาร์บาร์โซล-คาร์บาร์โซล และโอลิโกไธโอฟีน และที่สภาวะกระตุ้นมีการเคลื่อนที่ของอิเล็กตรอนไปยังหมู่ให้อิเล็กตรอนพบว่าโมเลกุลสีย้อมมีค่าสัมประสิทธิ์การดูดกลืนแสงโมลาร์สูงอยู่ในช่วงของสีน้ำเงินถึงสีเขียวเมื่อจำนวนของหมู่ไธโอฟีนเพิ่มขึ้นทำให้สเปกตรัมการดูดกลืนแสงกว้างเกิดการเรดชิฟท์ สีย้อม **CFTA3-A** เหมาะสมสำหรับเป็นวัสดุในอุปกรณ์เซลล์แสงอาทิตย์ โมเลกุลสารเรืองแสง **C_2TnG1** n=0-2 และ **PFC**, **PFCdi-Py** และ **PFCdi-CPy** สำหรับใช้เป็นสารเรืองแสงในอุปกรณ์ไดโอดเปล่งแสงสารอินทรีย์ สมบัติทางแสง และความร้อนของสีย้อมขึ้นกับจำนวนของไธโอฟีน และหมู่เดนดรอนที่ยึดติด จำนวนของหมู่ไธโอฟีนและเดนดรอนเพิ่มขึ้นทำให้สเปกตรัมการดูดกลืนแสงเกิดการเรดชิฟท์และกว้าง พบว่าโมเลกุลเป้าหมายมีการเรืองแสงอยู่ในช่วงสีน้ำเงินถึงสีเขียว สารเรืองแสงเป้าหมายมีคุณสมบัติทางเคมีไฟฟ้าและมีความเสถียรทางความร้อนที่ดี จึงคาดว่าโมเลกุลเหล่านี้สามารถนำไปใช้เป็นสารเรืองแสงในอุปกรณ์ไดโอดเปล่งแสงสารอินทรีย์ได้อย่างมีประสิทธิภาพ

ABSTRACT

TITLE : SYNTHESIS AND CHARACTERIZATION OF NOVEL ORGANIC MATERIAL FOR DYE SENSITIZED SOLAR CELLS AND ORGANIC LIGHT EMITTING DIODES

BY : TEADKAIT KAEWPUANG

DEGREE : MASTER OF SCIENCE

MAJOR : CHEMISTRY

CHAIR : ASSOC.PROF.VINICH PROMARAK, Ph.D.

KEYWORDS : OLIGOTHIOPHENE / CARBAZOLE / D-D-π-A/ DYE SENSITIZED SOLAR CELLS / ORGANIC LIGHT-EMITTING DIODES / OPTOELECTRONIC DEVICES

This thesis deals with synthesis and characterization of novel carbazole derivatives for using as dye molecules in optoelectronic devices. The designed D-D-π-A organic dyes containing different linker and acceptor units for using as dye molecules in dye-sensitized solar cell (DSCs). The D-D-π-A type organic dyes **CFTATn-A** n=1-3 composed of three parts: (1) cabarzole donating groups (D); (2) an oligothiophenes and oligothiophene-phenylenes (π); and (3) cyanoacrylic acid anchoring groups (A). The electronic, electrochemical, and thermal properties of these compounds can be tuned by varying the number of thiophene rings and anchoring groups. The electron distribution before the light irradiation (HOMO) is delocalized mainly over carbazole-carbazole donor and oligothiophene; whereas after light irradiation (LUMO) it moves to the acceptor units close to the anchoring groups. These compounds exhibited a high molar absorptivity in the blue/green region of solar light. The number of thiophene increased the conjugation length of compounds resulting a red-shift and broad in absorption solution spectra. The dye **CFTAT3-A** should be promising materials for DSCs devices. The target emitting materilals **C_2TnG1** n=0-2 and **PFC**, **PFCdi-Py** and **PFCdi-CPy** for using as emitting molecules in OLEDs devices. The electronic, electrochemical, and thermal properties of these compounds can be tuned by varying the number of thiophene rings and dendron moieties. The number of thiophene and dendron units increased the conjugation length of compounds resulting a red-shift and broad in absorption solution spectra. All compounds in this study are fluorescent with the

color ranging from blue to green. All targets have good electrochemical and thermal stabilities and could be used as emissive layers in OLEDs. The performance of OLEDs using these materials as light-emitting layer is under investigation and will be reported in the future.

CONTENTS

CONTENTS (CONTINUED)

LIST OF TABLES

LIST OF SCHEMES

LIST OF FIGURES

LIST OF FIGURES (CONTINUED)

LIST OF FIGURES (CONTINUED)

LIST OF FIGURES (CONTINUED)

LIST OF FIGURES (CONTINUED)

LIST OF FIGURES (CONTINUED)

LIST OF ABBREVIATIONS

ABBREVIATION	FULL WORD
DMF	Dimethylformamide
THF	Tetrahydrofuran
DMSO	Dimethylsulphoxide
NBS	N-Bromosuccinimide
RT/rt	Room temperature
d	Doublet
dd	Doublet of doublets
td	Triplet of doublets
ε	Molar absorption
eV	Electron volt
h	Hour/hours
HOMO	Highest occupied molecular orbital
LUMO	Lowest unoccupied molecular orbital
IPCE	Incident photon to current efficiency
η	Overall light-to-electric power conversion efficiency
ITO	Indium-tin oxide
FT-IR	Fourier transform Infrared
J	Coupling constant
M	Molar concentration
MHz	Megahertz
min	Minutes
μA	Microamperes
μm	Micrometers
mol	Moles
mmol	Milimoles
m	unresolved multiple
N	Normality concentration

LIST OF ABBREVIATIONS (CONTINUED)

ABBREVIATION	FULL WORD
nm	Nanometers
NMR	Nuclear magnetic resonance
δ	Chemical shift in ppm relative to tetramethylsilane
ppm	Parts per million
s	Singlet
t	Triplet
TLC	Thin-layer chromatography
UV	Ultra-violet
n-Bu_4NPF_6	Tetrabutylammonium hexafluorophosphate
TD-DFT	Time-dependent density functional theory
GBL	Gamma-butyrolactone
NMP	*N*-methyl-2-pyrrolidone
S^+	Excited dye
S^o	Original state
AM 1.5	Air Mass 1.5
K	Kilo
W	Watt
V	Voltage (V)
s	second
I	Current (A)
A	Ampere
V_{oc}	Open circuit voltage
J_{sc}	Short circuit current
ff	Fill factor
J-V	Current density-voltage

CHAPTER 1

INTRODUCTION

1.1 Optoelectronics

Optoelectronics is a technology that the interaction between optics and electronics and the devices based on this technology are known as the optoelectronic devices. Consequently these materials were used as nonconductor in the electronic industry. Since 1977, Alan J. Heeger, Alan G. MacDiarmid and Hideki Shirakawa found that the conductivity of poly(acetylene) can be increased by eleven orders of magnitude when it is doped with halogens [1, 2]. The discovery and development of conductive polymers they received the Nobel Prize for Chemistry in 2000. Therefore, the possibility of using organic semiconducting materials for applications in optoelectronics and the semiconductor has been of great scientific and technological interest [3-5]. An important advantage of organic semiconducting materials is easy processability, i.e. form solution, large area coverage and the possibility to use flexible substrates make organic semiconductors ideal candidates for low cost electronic applications. During, the last 15 years rapid progress took place in the field of materials developments, device design, deposition processes and molecular modeling [6]. In the area of organic thin film devices vary active research is going on spanning many subjects such as organic light emitting diode (OLEDs) [7], organic field-effect transistors (OFETs) [8], sensors [9], organic photovoltaic [10] and dye solar cells (DSCs).

1.2 Dye Sensitized Solar cells

1.2.1 Introduction

Today, most solar cells manufactured in the world are silicon solar cells. There are several types of silicon solar cells, one of which is bulk silicon solar cells, which provide high conversion efficiency but require expensive materials and costly fabrication process. Then there are thin-film solar cells, which significantly reduce costs at the expense of decreased conversion efficiency. Non-silicon compound semiconductor solar cells are expected to provide

conversion efficiency as same as silicon crystal solar cells, but increased concerns about environmental load and the use of scarce metals. There is demand for the development of new low-cost high-efficiency non-silicon solar cells. One of next-generation solar cells expected to satisfy these demands is dye-sensitized solar cells (as follows called DSCs). Grätzel et al. reported high-efficiency cells using nanoporous titanium oxide semiconductor electrodes, ruthenium (Ru) metal complex dyes and iodine electrolyte solutions in the journal of Nature in 1991. consequently, many studies have been actively carried out on DSCs and revealed their performance comparable to amorphous silicon thin films. These DSCs have the advantages of low cost, lightweight, easy to be fabricated and friendly to the environment, but issues include durability and further improvement of their properties. To respond to these issues, many researcher have been made, such as solidifying electrolytes and improving materials and design structures.

In 1972 Honda and Fujishima reported that water splitting was possible by illumination of TiO_2 [11]. The large bandgap of TiO_2 yielded quite low conversion efficiencies due to the ability to absorb photons only in the ultraviolet region. Gerischer and Memming further showed that the enhanced light harvesting could be attained by sensitizing flat semiconductor electrodes [12]. In 1976 Tsubomura et al. presented a working dye-sensitized porous zinc oxide photocell using a platinum counter electrode and a iodide/triidodie redox couple [13]. In 1985, Desilvestro et al. used a rough TiO_2 electrode sensitized with a ruthenium complex yielding enhanced photo conversion efficiency [14]. The breakthrough for DSCs occurred in 1991, [15] when Grätzel and O'Regan managed to build a, 7.1%, photovoltaic device based on a dye-sensitized 10 μm thick porous TiO_2 electrode. The DSC research has since then expanded and today there is a quite large research community trying to understand and improve the photovoltaic efficiency of the DSC. DSCs manufacturing facility, G24 innovations, started up with a capacity of 25 MW located in Cardiff, Wales. The DSC technology may be considered among the most advanced solar cell techniques on the verge of commercialization. DSC is an appropriate candidate in the view of materials and production cost and device performance trade off. In the near future, the venture of DSCs as a competitive technology will thus be revealed.

1.2.1 Principle of DSCs

The DSCs, or the Grätzel cell, is a complex system where three different components, the semiconductor, the chromophore and the electrolyte are brought together to generate electric power from light without suffering any permanent chemical transformation (Figure 1.1) [16].

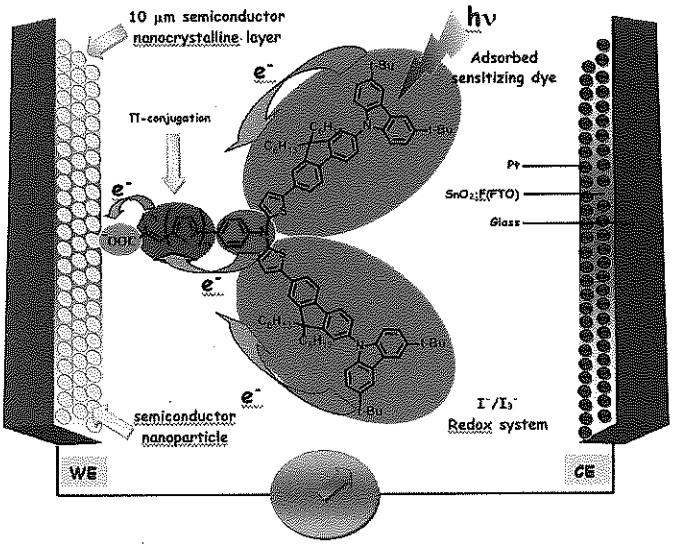

Figure 1.1 Schematic picture of the dye sensitized solar cell.

The nanocrystalline semiconductor is usually the anatase TiO_2, although alternative wide band gap oxides such as ZnO can be used. A monolayer of the chromophore, i.e. the sensitizer, is attached to the surface of the semiconductor. Photoexcitation of the chromophore results in the injection of an electron into the conduction band of the semiconductor (Figure 1.2). The chromophore is regenerated by the electrolyte, usually an organic solvent containing a redox couple, such as iodide/triiodide. The electron donation to the chromophore by iodide is compensated by the reduction of triiodide at the counter electrode and the circuit is completed by electron migration through the external load. The overall voltage generated corresponds to the difference between the Fermi level of the semiconductor and the redox potential of the electrolyte.

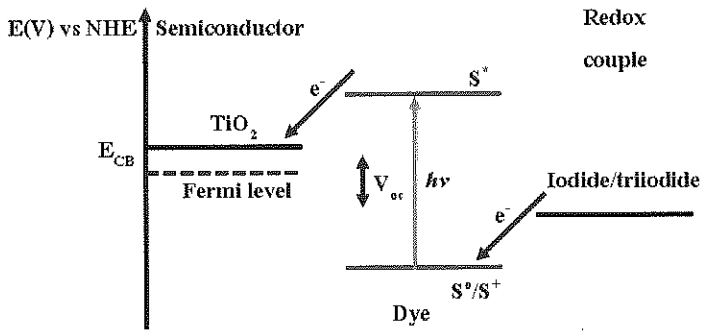

Figure 1.2 Schematic picture of the electron flow in the DSC.

The performance of the solar cell can be quantified with parameters such as incident photon to current efficiency (IPCE), open circuit photovoltage (V_{oc}) and the overall efficiency of the photovoltaic cell (η). The efficiency of the DSC is related to a large number of parameters. This thesis will only focus on the development of efficient sensitizers and their synthesis, even so, it is important to have the general concepts in mind.

1.2.2 Overall Efficiency of the Photovoltaic Cell (η)

The solar energy to electricity conversion efficiency under white-light irradiation (e.g., AM 1.5 G) can be obtained from the following equation:

$$\eta = \frac{J_{sc} \cdot V_{oc} \cdot \mathrm{ff}}{I_0} \qquad (1.1)$$

Where I_0 (mW/cm^2) is the photon flux (e.g., ca. 100 mW/cm^2 for AM 1.5 G), J_{sc} (A) is the short-circuit current density under irradiation, V_{oc} (V) is the open-circuit voltage, *ff* represents the cell fill factor. The fill factor measures the squareness of the *J*-V curve (Figure 1.3).

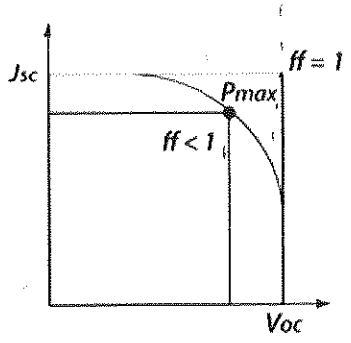

Figure 1.3 *J*-V curve.

1.2.3 Chromophores

The efficiencies of the sensitizers are related to some basic criteria [17]. The HOMO potential of the dye should be sufficiently positive compared to the electrolyte redox potential for efficient dye regeneration. The LUMO potential of the dye should be sufficiently negative to match the potential of the conduction band edge of the TiO_2 and the light absorption in the visible region should be efficient. However, by broadening the absorption spectra, the difference in the potentials of the HOMO and the LUMO energy levels is decreased. If the HOMO and LUMO energy levels are too close in potential, the driving force for electron injection into the semiconductor or regeneration of the dye from the electrolyte could be hindered. The sensitizer should also exhibit small reorganization energy for excited- and ground-state redox processes, in order to minimize free energy losses in primary and secondary electron transfer steps.

1.2.3.1 Ruthenium Based Chromophores

Chromophores of ruthenium complexes such as the **N3**, **N719** and black dyes have been intensively investigated and show record solar energy-to-electricity conversion efficiencies (η) of 10, 11.2 and 10.8%, respectively (Figure 1.4) [18].

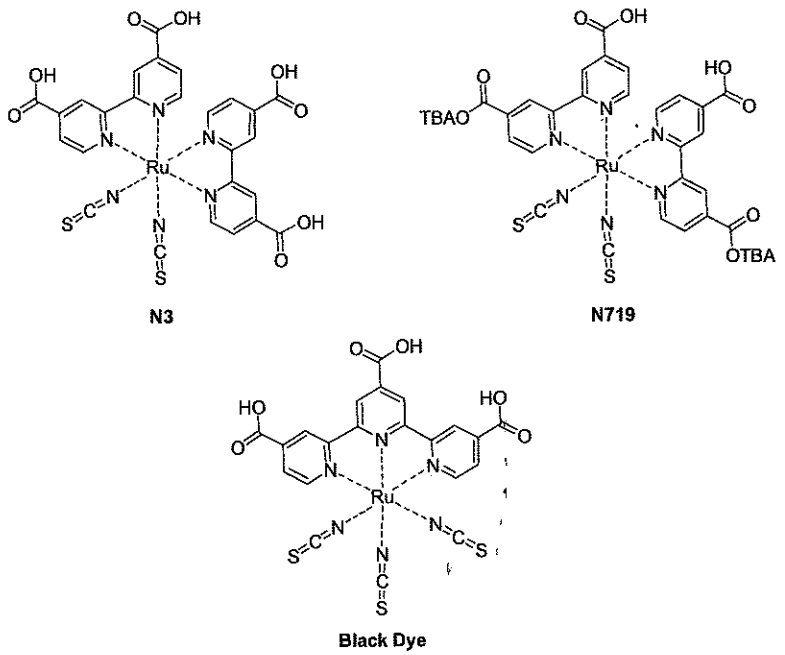

Figure 1.4 chemical structures of **N3**, **N719** and black dyes.

A large number of different ruthenium based sensitizers have been investigated in order to improve the photovoltaic performance and stability of the DSCs. Amongst them especially four (**K19**, **K73**, **K77** and **Ru-1**) have shown interesting properties in that they are competing in efficiency and have higher molar extinction coefficients than the three former. The enhanced absorption observed is expected from the extended conjugated system.

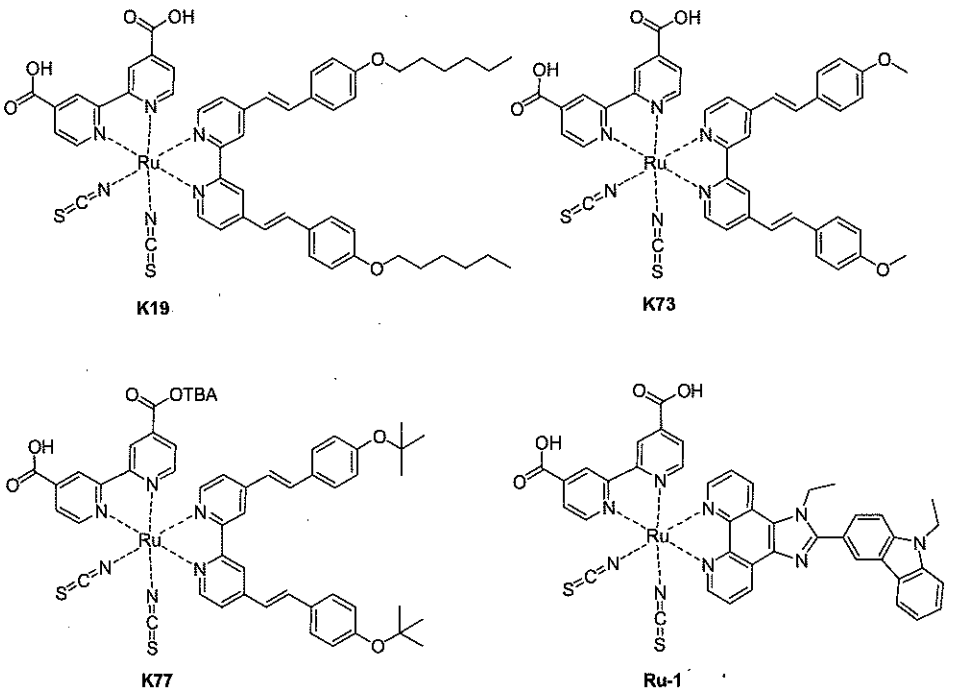

Figure 1.5 chemical structures of **K19**, **K73**, **K77** and **Ru-1** dyes.

1.2.3.2 Organic Chromophores

Recently, performances of DSCs based on metal-free organic dyes have been remarkably improved by several groups. The first transient studies on a coumarin dye in DSCs was performed in 1996, when Grätzel et al. found injection rates of 200 fs from C**343** into the conduction band of TiO_2. Since **C343** has a narrow absorption spectrum, the conversion efficiency of this specific compound was low. By introduction of a methine unit, the π-system could be expanded and in 2001 a respectable efficiency of 5.6% was obtained with **NKX-2311** [19]. Adding more methine units (up to three) and introducing bulky substituents to prevent dye-aggregation could push the efficiency to 6.7% in 2005 **(NKX-2753)**. Currently other building

blocks like thiophene are tested, which are believed to give a higher stability. First results of 7.4% for **NKX-2677** are encouraging [20].

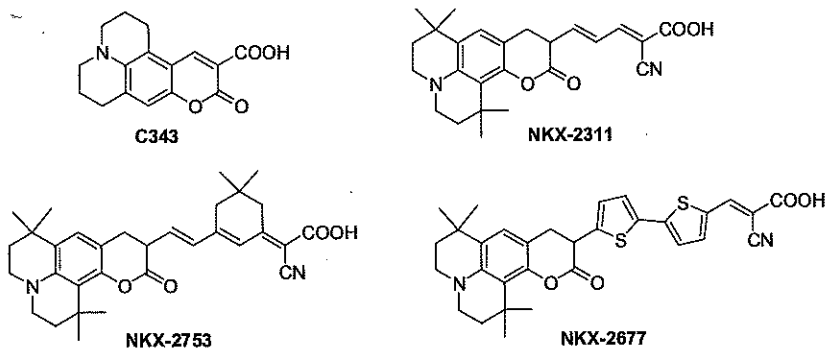

Figure 1.6 chemical structures of **C343, NKX-2311, NKX-2753** and **NKX-2677** dyes.

In 2003, an indoline dye **D102** and **D149** discovered by Ito et al. These indoline dyes gave solar-to-electrical energy conversion efficiency of 6.1 and 9%, respectively, in full sunlight. A highest efficiency for organic dyes has been achieved by an indoline dye **D149** [21].

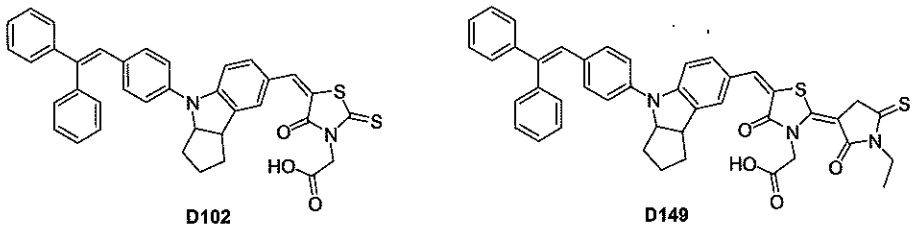

Figure 1.7 chemical structures of **D102** and **D149** dyes.

In 2007, Yuanzuo Li et al. [22] reported that the highly efficient and stable organic dyes **JK-1** and **JK-2** composed of bis-dimethylfluoreneaniline moiety as the electron donor and cyanoacrylic acid moiety as the electron acceptor with an overall conversion efficiency of 8.01%.

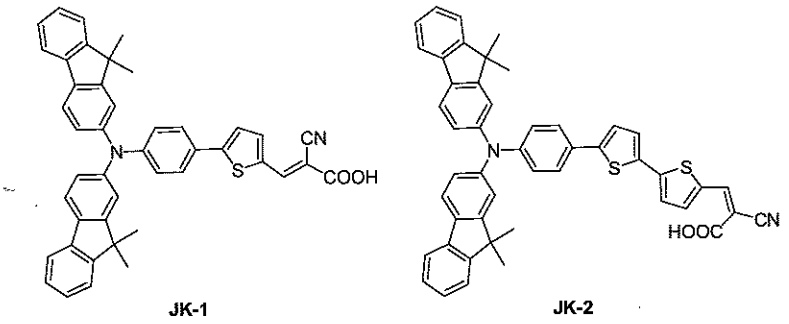

Figure 1.8 chemical structures of **JK-1** and **JK-2** dyes.

In 2007, Duckhyun Kim et al. [23] investigated that the organic dyes **JK-24** and **JK-25** containing *N*-(9,9-dimethylfluoren-2-yl)carbazole as electron donor and cyanoacrylic acid as electron acceptor bridged by thiophene units, gave an overall conversion efficiency (η) of 5.15%. Although many structure frameworks such as coumarin, aniline, and indoline have been employed as good electron donor unit, the small molecular organic dyes containing the *N*-substituted carbazole structural motif have been little explored for DSCs.

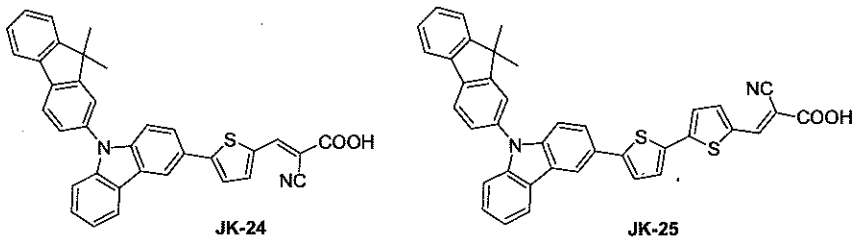

Figure 1.9 chemical structures of **JK-24** and **JK-25** dyes.

Carbazoles represent the second strategy, starting from highly photo-stable sensitizers, dealing with the efficiency issue by introducing different substituents on the carbazole framework. This class of dye has high absorption coefficients in the visible region, and the fluorescence quantum yields of the singlet state are near unity. Electron injection from dye singlet states into the conduction band of a semiconductor is generally faster than that from triplet and it conserves more potential from the light capture. Some carbazole compounds have been used as sensitizer in DSC but their efficiency was low. Recently, the carbazole compounds-based dye-sensitized solar cells have reached efficiencies around 5.15-8.30% [24-26].

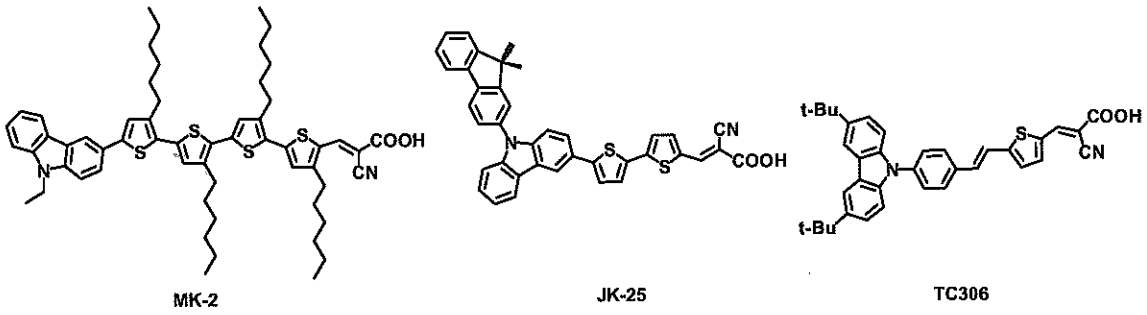

Figure 1.10 Chemical structure of some carbazole derivatives used as sensitizer in DSCs.

Most of the dyes employed in DSCs have carboxylic acid groups to anchor on the TiO_2-surface. The binding is reversible with high binding equilibrium constants ($K = 10^5\ M^{-1}$). At a pH > 9 the equilibrium is typically shifted to the reactant side and the dye molecules desorb. This somewhat fragile linkage triggered the development of dyes with different anchoring groups. In general the binding strength to a metal oxide surface decreases in the order phosphonic acid > carboxylic acid > ester > acid chloride > carboxylate salts > amides [27] due to its strong electronic withdrawing properties, the most widely used and successful to date being the carboxylic acid and phosphonic acid functionalities. The carboxylic acid groups, while ensuring efficient adsorption of the dye on the surface also promote electronic coupling between the donor levels of the excited chromophores and the acceptor levels of the TiO_2 semiconductor. Some of the possible modes of chelation/derivatization, ranging from chemical bonding (chelating or bridging mode) to H-bonding, are shown in Figure 1.11 [28].

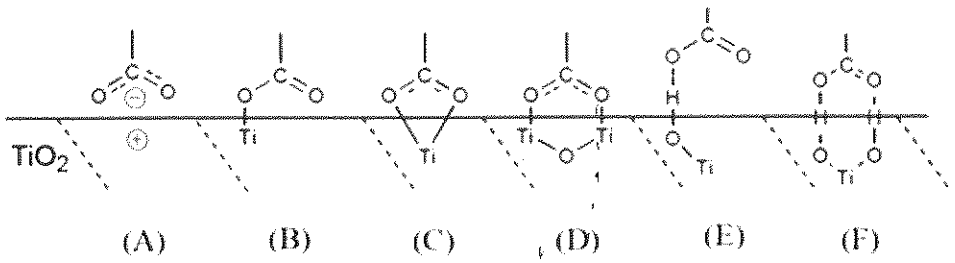

Figure 1.11 Possible binding modes for carboxylic acid groups on TiO_2.

1.3 Organic light emitting diodes (OLEDs)

The most promising organic-based electro-optic devices are OLEDs. They have recently received a great deal of attention because of their application for a wide range of display applications as well as from the standpoint of scientific interest. They are attractive because of low voltage driving, high brightness, capability of multicolor emission by the selection of emitting materials and easy fabrication of large-area and thin-film devices. Following the reports on OLEDs using single crystals of anthracene, recent pioneering works on OLEDs using low molecular-weight organic materials and a conjugated polymer have triggered extensive research and development within this field. Recent years have witnessed significant progress with regard to brightness, multi- or full-color emission, and durability and thermal stability of OLEDs. The OLEDs fall into two competing technologies based on the materials used: small molecule devices are fabricated using vacuum evaporation techniques, whereas polymer structures can be applied using spin-casting or ink-jet techniques. The screen-printing technique has recently been introduced and is presumed to be applicable to both polymer and small molecule devices [29].

1.3.1 Structure

The basic OLED cell structure consists of a stack of thin organic layers sandwiched between a transparent anode and a metallic cathode. The organic layers comprise a hole-injection layer, a hole-transport layer, an emissive layer and an electron-transport layer. When an appropriate voltage (typically a few volts) is applied to the cell, the injected positive and negative charges recombine in the emissive layer to produce light (electroluminescence). The structure of OLED the organic layers and the choice of anode and cathode are designed to maximize the recombination process in the emissive layer, thus maximizing the light output from the OLED device. Both the electroluminescent efficiency and control of color output can be significantly enhanced by "doping" the emissive layer with a small amount of highly fluorescent molecules [30,31].

An OLED consists of the following parts:

Substrate (clear plastic, glass, foil) - The substrate supports the OLED.

Anode (transparent) - The anode removes electrons (adds electron "holes") when a current flows through the device.

Organic layers - These layers are made of organic molecules or polymers.

Conducting layer - This layer is made of organic plastic molecules that transport "holes" from the anode. One conducting polymer used in OLEDs is polyaniline.

Emissive layer - This layer is made of organic plastic molecules (different ones from the conducting layer) that transport electrons from the cathode; this is where light is made. One polymer used in the emissive layer is polyfluorene.

Cathode (may or may not be transparent depending on the type of OLED) - The cathode injects electrons when a current flows through the device.

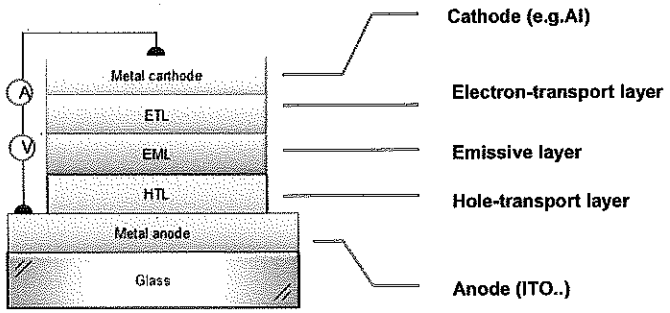

Figure 1.12 Organic light emitting diodes (OLEDs) Structure

1.3.2 Working Principle

When a voltage is applied to the electrodes the charges start moving in the device under the influence of the electric field. Electrons leave the cathode and holes move from the anode in opposite direction. The recombination of this charges leads to the creation of a photon with a frequency given by the energy gap ($E = hv$) between the LUMO and HOMO levels of the emitting molecules. Therefore, the electrical power applied to the electrodes is transformed into light. Different materials and dopants can be used to generate different colors and the combination of them allows building up a white light source [32].

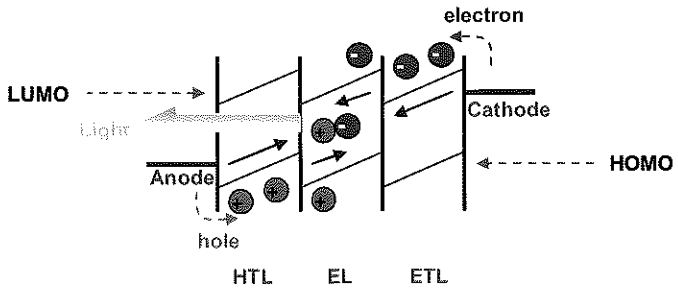

Figure 1.13 Organic light emitting diodes (OLEDs) working principle

1.3.3 Material Technologies

The development of new materials, particularly for achieving emission in the blue region of the spectrum, for organic light-emitting devices is the focus of intense investigation throughout the world. Scientists have developed a new class of materials that demonstrate exceptional promise for use as electron transport materials within an OLED device. The successful development of practical blue OLED devices would significantly impact advancement of OLED technology in both display devices and energy-efficient solid-state lighting. These materials address the critical issue of achieving high quantum efficiency (photons generated per electron injected into an OLED device) at low voltages. Devices built at PNNL using the new materials have produced external quantum efficiencies at a brightness of 800 cd/m^2 as high as 11% at only 6.3 V without using conductivity doping. One class of new OLED materials developed at PNNL are based on organic phosphine oxide compounds while another is based on organic phosphine sulfides.

In the following passage some basics on materials used in OLEDs are given [11-13]. The colour of the emitted light can be tuned by the molecular structure of the organic emissive material (see Figure 1.14). Typical emitters for different colours can either be well-defined low molecular compounds such as DPVBI (4,40-bis(2,2-diphenylethene-1-yl)diphenyl) for blue emission, Alq_3 (tris(8-oxychinolinato)aluminum)

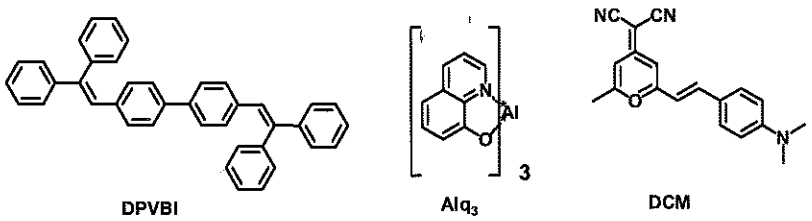

Figure 1.14 Chemical structures of various emitting materials small molecules used in OLEDs

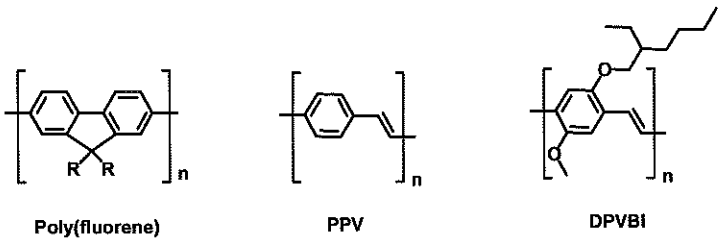

Figure 1.15 Chemical structures of various emitting materials polymers used in OLEDs

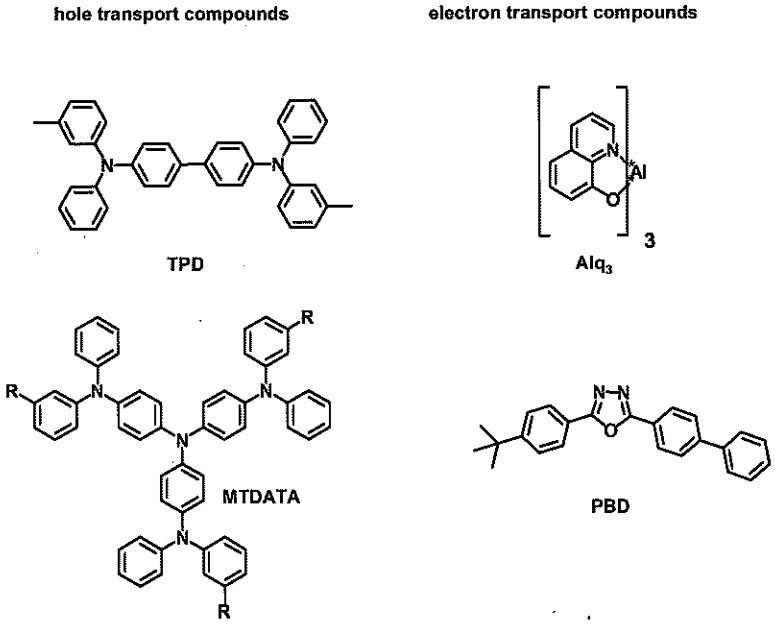

Figure 1.16 Various hole transport and electron transport materials used in OLEDs

For green emission [33], and DCM (4-(dicyanomethylene)-2-methyl-6-(*p*-dimethylaminostyryl)-4*H*-pyrane) for red emission, or polymers such as polyfluorenes (blue) [34], PPV (poly(p-phenylenvinylene)) (green) [35], and MEH-PPV (poly[(2-(2-ethylhexyloxy)-5-methoxy-p-phenylen)vinylene]) (orange) [36]. Typical hole transporters are materials based on the triarylamine motive like TPD (*N,N*-bis(3-methylphenyl)-*N,N*-diphenylbenzidine) or MTDATA (m-methyltris(diphenylamine)triphenylamin), while compounds like Alq_3 and PBD (2-(4-biphenyl)-5-(4-*tert*-butylphenyl)-1,3,4-oxadiazole) are able to transport electrons especially well (Figure 1.16).

1.3.4 Aim of the thesis

In recent years, the development of novel organic materials for optoelectronic applications has been attracted a lot of interest both in industry and academics. Especially in the area of dye solar cells (DSCs) and organic light emitting diodes (OLEDs) huge progress has been made. One of the main technological attraction of organic electronics is that the active layers can be deposited at low temperatures by liquid phase techniques. This makes organic semiconductors ideal candidates for low-cost, large-area electronic applications on flexible substrates.

The aims of this work are:

(1) To synthesize a novel donor-donor-π-conjugate acceptor (D-D-π-A) organic material based on *t*-Bu carbazole, fluorene and thiophene as the donor group, with an thiophene and thiophene-phenylene linker and a cyanoacrylic acid moiety as acceptor/anchor group that would be an interesting starting point for further modifications as show in Figure 1.17.

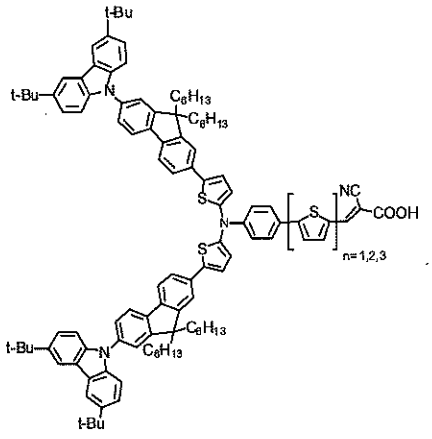

Figure 1.17 Organic dye structures of D-D-π-A type organic dyes (**CFTAnT-A** n=1-3).

(2) To synthesize a series of *t*-butylcarbazole, thiophene-substituted di-carbazole derivatives as both emitting and hole-transporting materials for OLEDs.

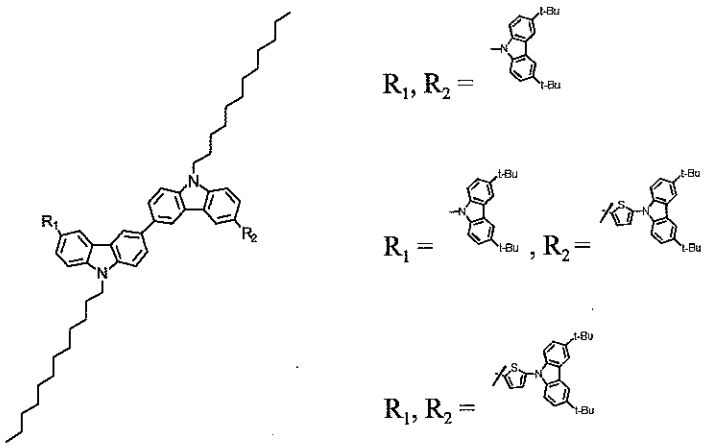

Figure 1.18 Structure emitting materials of *t*-butylcarbazole-substituted di-carbazole derivatives

(3) To synthesize a series of pyrene, di-pyrenecarbazole-substituted fluorene derivatives as both emitting and hole-transporting materials for OLEDs.

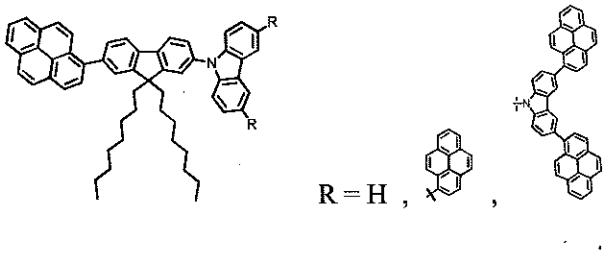

Figure 1.19 Emitting materials structure of pyrene, di-pyrenecarbazole-substituted fluorene derivatives

(4) To characterize and study the electronic, photophysical, electrochemical and thermal properties of the target molecules.

(5) To investigate their potential applications as both dye sensitizers and emitters for DSCs and OLEDs devices, respectively.

CHAPTER 2

SYNTHESIS AND CHARACTERIZATION OF D-D-π-A TYPE ORGANIC DYES FOR DYE SOLAR CELLS (CFTATn-A, n = 1-3)

2.1 Introduction

Organic sensitizers were divided into three parts; donor, linker and acceptor. This is a convenient method to systematise the sensitizers. There are several basic criteria that an efficient sensitizer should fulfill, and these criteria can be used when designing a new organic sensitizer. First of all, light excitation should be associated with vectorial electron flow from the light harvesting moiety of the dye, i.e. the donor and the linker, towards the proximity of the semiconductor, i.e. the acceptor/anchoring group of the dye. This can be seen as the HOMO is located over the donor and the linker, while the LUMO is located over the acceptor, i.e. a pronounced push-pull effect. Second, the HOMO potential of the dye should be sufficiently positive compared to the electrolyte redox potential for efficient dye regeneration [37]. Third, the LUMO potential of the dye should be sufficiently negative to match the potential of the conduction band edge of the TiO_2. Fourth, a strong conjugation and electronic coupling across the donor and the acceptor to ensure high electron transfer rates. Finally, to obtain a dye with efficient photocurrent generation, π-stacked aggregation on the semiconductor should be avoided [38]. Aggregation may lead to intermolecular quenching or molecules residing in the system not functionally attached to the semiconductor surface and thus acting as filters.

2.1.1 Carbazole in Conducting Materials

Due to the electron-donating nature of carbazoles, they have been widely used as hole-transporting materials for a number of applications, such as xerography, organic field-effect transistors, photorefractive systems, light emitting diodes; etc. Long-lived charge separate states and multiphoton absorbing abilities have been reported for some of these carbazole based materials. In photovoltaic cells the interest of using carbazole based sensitizers has increased in recent years. Studies of ruthenium complexes with carbazole as electron donor moiety have shown interesting results promising for DSC applications. However, organic sensitizers with carbazole donor moieties published when this project started (Figure 2.1), included in some cases relatively long

synthetic procedures which would have yielded high production costs and their efficiencies in the DSC was relatively low (η = 5.15-8.30%) compared to for instance some indoline sensitizers [36, 39].

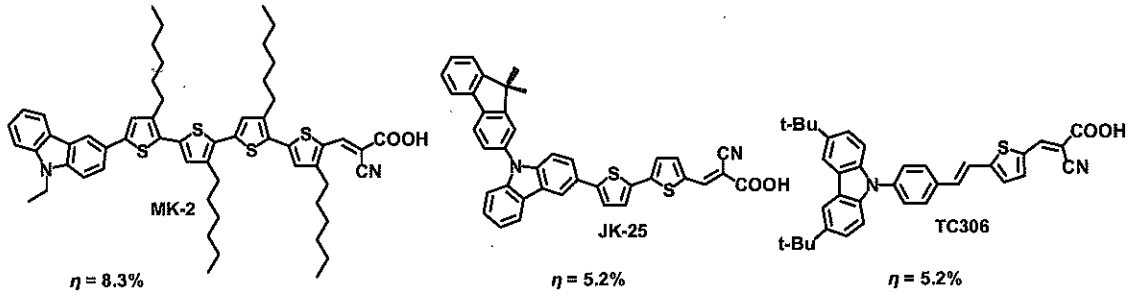

Figure 2.1 Examples of carbazole sensitizers published at the start of the project.

At this point in time, the number of carbazole based sensitizers has increased and modifications have been made both at the carbazole moiety, with different substituents and at the linker unit, where different π-conjugated systems have been investigated. The carbazole moiety is non-planar and can suppress aggregation due to the disturbance of the π-π stacking.

2.1.2 π-Conjugated Linker

2.1.2.1 Oligothiophenes as π-Conjugated Linker

Expansion of the π-conjugated C=C backbone to extend the absorption spectrum and broaden it to the red region, is one way to decrease the HOMO/LUMO energy level differences and thereby increase the solar cell performance. This would, however, complicate the synthetic procedure and affect the stability of the dye due to photoinduced *trans* to *cis* isomerisation. The introduction of different π-conjugated ring moieties, such as thiophene, benzene or pyrrole is an elegant way of extending the π-conjugated system without affecting the stability of the dye. In 2003 Hara et al. reported a series of coumarine dyes with different linker units (Figure 2.2) [40].

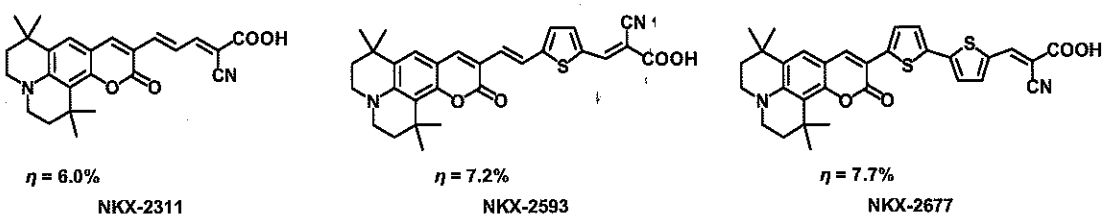

Figure 2.2 π-conjugated extension by thiophene introduction in the linker.

Broadened toward the red region when the dyes are adsorbed on the surface of TiO_2, leading to an increase of the photocurrent. **NKX-2593** and **NKX-2677** both show efficiencies over 7% and have almost identical absorption spectra. From a synthetic point of view, **NKX-2593** requires a slightly shorter synthetic route than **NKX-2677** to obtain approximately the same efficiency.

2.1.2.2 Thiophenes-phenylene as π-Conjugated Linker

The function of a bridge group is twofold, i.e. acting both as a part of the light absorbing chromophore and also as a channel for transporting charges. A good bridge group should promote the absorption of light over a wide wavelength region, yet retards the rate of internal charge recombination. Linearly connected arylenes serve both purposes quite well. The flexible dihedral angles between adjacent aryl groups are twisted to a greater extend upon excitation to the CT state, while the electronic resonance is reduced and the rate of charge recombination slows down. In 2009 Tahsin J. Chow et al. reported a series of naphthylphenylamine dyes with different linker units (Figure 2.3) [41].

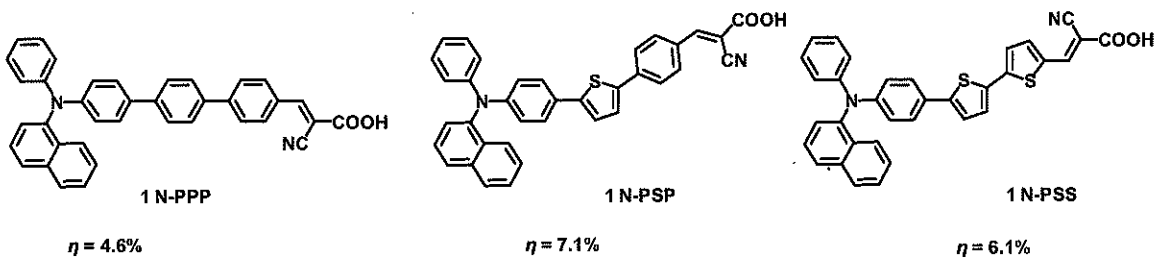

Figure 2.3 π-conjugated extension by thiophene-phenylene introduction in the linker.

The triarylene bridges consist of phenyl and/or thiophenyl groups linked together in a linear fashion. These compounds exhibited a high absorptivity in the blue/green region of solar light. **1N-PSP** and **1N-PSS** both show efficiencies over 6% and have almost identical absorption spectra. From a synthetic point of view, **1N-PSS** a slightly shorter synthetic route than **1N-PSP** to obtain approximately the same efficiency.

2.1.3 Cyanoacrylic Acid as Acceptor and Anchoring Group.

The carboxylic acid group is by far the most employed group for attachment of the sensitizers to the semiconductor surface. The binding modes (Figure 2.4) have been investigated by Galoppini and co-workers [42].

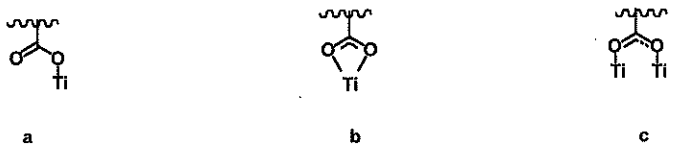

Figure 2.4 Main binding modes of carboxylate group to TiO_2, a) regular monodentate, b) regular bidentate chelating, c) bidging bidentate.

When it comes to the slightly wider term acceptor groups, cyanoacrylic acid is by far most commonly used due to its strong electronic withdrawing properties. There is a number of different acceptor groups reported and some show promising results (Figure 2.5). In some cases, the ending of the linker and the beginning of acceptor, since the increased conjugation that some acceptor groups provided will broaden the absorption spectra. However, in this thesis a synthetic point of view will be used to differentiate the linker and the acceptor depending on the reactants used [24, 43, 44].

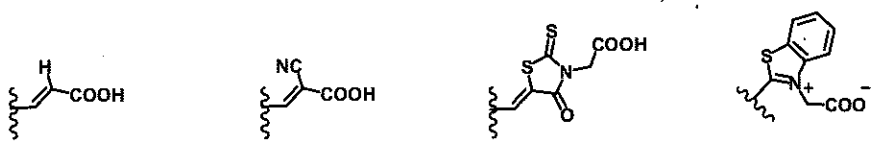

Figure 2.5 Examples of different acceptor groups.

2.2 Aim of the Study

We designed an organic chromophore based on di(carbazole fluorenethiophenyl)amine as the bulky donor group for decrease π-π stacking of molecules, with oligothiophenes because increase π-conjugated bridge for increase range of absorption of molecule and cyanoacrylic acid was used electron-withdrawing anchoring group, respectively. That would be an interesting starting point for further modifications (Figure 2.6). The D-D-π-A type organic dyes were

synthesized using a combination of Alkylation, Bromination, Ullmann coupling, Suzuki cross-coupling and Knoevenagel condensation reactions.

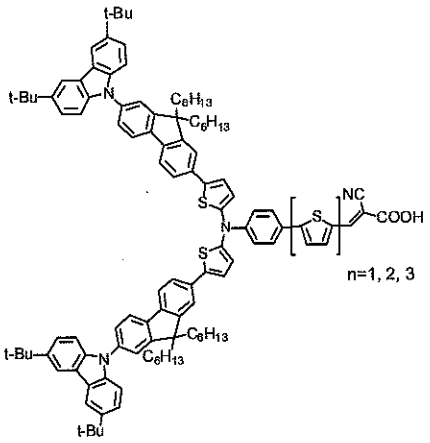

Figure 2.6 Organic dye structure of D-D-π-A typ organic dyes.

2.3 Results and Discussion

2.3.1 Synthesis

To synthetic approach to a series of dye sensitized solar cells for organic materials, first dibromofluorene was prepared from bromination of fluorene using bromine as electrophile in the present of $FeCl_3$ as afford dibromofluorene in 80% yield.

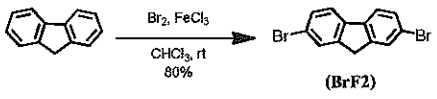

Figure 2.7 Bromination reaction to form dibromofluorene (**BrF2**).

The mechanism of bromination of fluorene is shown in Figure 2.8.

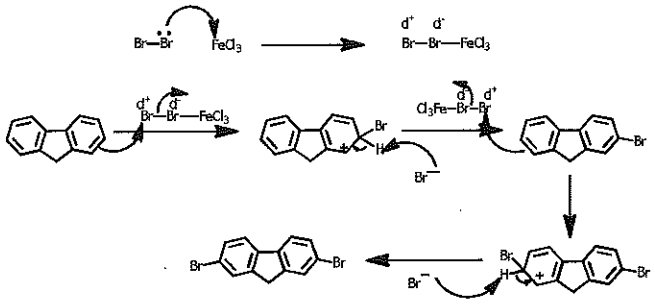

Figure 2.8 The proposed mechanism of bromination of fluorene.

Bromination follows the same general mechanism for the electrophilic aromatic substitution (EAS). Bromine itself is not electrophilic enough to react with benzene. But the addition of a strong Lewis acid (electron pair acceptor), such as $FeCl_3$, catalyses the reaction, and leads to the substitution product. The bromine molecule reacts with $FeCl_3$ by donating a pair of its electrons to the Lewis acid, which creates a more polar Br-Br bond, and thus a more reactive electrophile. In the Figure 2.8 show mechanism of bromination of fluorene by first step,

The bromine reacts with the Lewis acid to form a complex that makes the bromine more electrophilic. Next step, The π electrons of the aromatic **C=C** act as a nucleophile, attacking the electrophilic **Br**, and displacing iron bromo-trichloride. This step destroys the aromaticity giving the cyclohexadienyl cation intermediate and final step, Removal of the proton from the sp^3 **C** bearing the bromo-group reforms the **C=C** and the aromatic system, generating **HBr** and regenerating the active catalyst.

The chemical structure of **BrF2** was confirmed by ^{1}H-NMR analysis. The ^{1}H-NMR spectrum of product **BrF2** shows a singlet signal at chemical shift 7.7 ppm (2H) assigning as 1-H and 8-H position of fluorene ring, a doublet signal at chemical shift 7.65 ppm (2H, J = 7.45 Hz) assigning as 3-H and 4-H of fluorene adduct and a singlet signal at chemical shift 3.9 ppm (2H) assigning as methylene proton of fluorene.

Dialkylation at the C-9 position to increase the solubility of the resultant compound **BrF(2)** was accomplished by generation of the fluorenyl anion with an aqueous NaOH solution in DMSO and subsequent dihexylation with 1-bromohexane in the presence of *n*-Bu_4NCl as phase transfer catalyst at room temperature. The desired 2,7-dibromo-9,9-dihexyl-*9H*-fluorene was isolated by silica-gel column chromatography as brown solid in 86% yield.

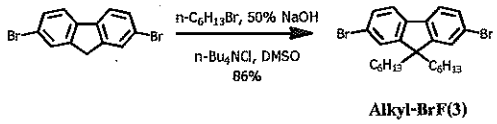

Alkyl-BrF(3)

Figure 2.9 Alkylation reaction to form 2,7-dibromo-9,9-dihexyl-*9H*-fluorene **(Alkyl-BrF(3))**.

The mechanism of alkylation with phase transfer catalyst to explain the critical role of tetraalkylammonium salts (Q^+X^-) in the reactions between two substances located in different immiscible phase is shown in Figure 2.10. Key to this tremendous enhancement in reactivity is the generation of a quaternary ammonium hydroxide, which makes the hydroxide anion soluble in organic solvents and sufficiently nucleophilic. The high rate of displacement is mainly due to two of the three characteristic features of the pairing cation (Q^+): high lipophilicity and the large ionic radius.

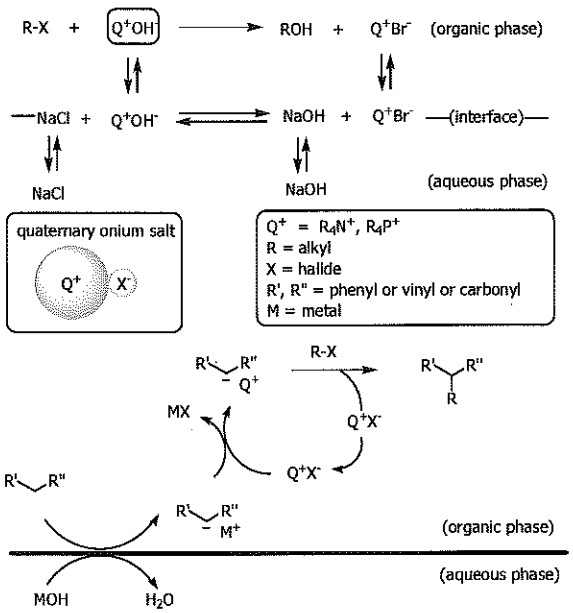

Figure 2.10 The proposed mechanism of alkylation.

The chemical structure of **Alkyl-BrF(3)** was confirmed by ^{1}H-NMR analysis. The ^{1}H-NMR spectrum of product **Alkyl-BrF(3)** shows a singlet signal at chemical shift 7.60 ppm (2H) assigning as 1-H and 8-H position of fluorene ring, a doublet signal at chemical shift 7.55 ppm (4H, J = 7.45 Hz) assigning as 3-H and 4-H of fluorene adduct, a triplet signal at chemical shift 2.0 ppm (4H) assigning as methylene proton of hexyl unit.

Subsequently, the key intermediate *N*-carbazole fluorene was synthesized by using Ullmann coupling of 2,7-dibromo-9,9-bis-*n*-hexylfluorene with 1 equivalent of 3,6-di-*tert*-carbazole in the presence of copper(I) iodide as catalyst, potassium phosphate as base and (±)-*trans*-diaminocyclohexane as co-catalyst in toluene at 170°C under N_2 in 70% yield.

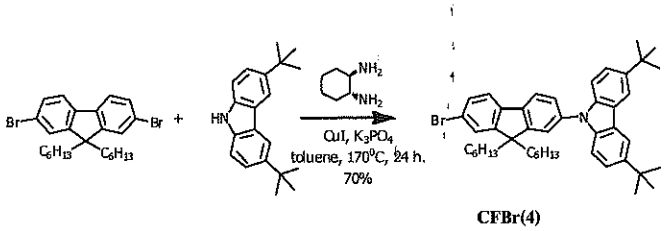

CFBr(4)

Figure 2.11 Ullmann coupling reaction to form 9-(7-bromo-9,9-dihexyl-9*H*-fluoren-2-yl)-3,6-di-*tert*-butyl-9*H*-cabazole **(CFBr(4))**.

The proposed mechanism of Ullmann coupling reaction is shown in Figure 2.12. his catalytic cycle, the first step is an oxidative addition of the aryl halide to copper, to form a copper(III) intermediate. Subsequently, the halide on copper is exchanged for the nucleophile and the obtained intermediate, *via* a reductive elimination step, releases the coupling product and the active Cu(I) catalyst is regenerated.

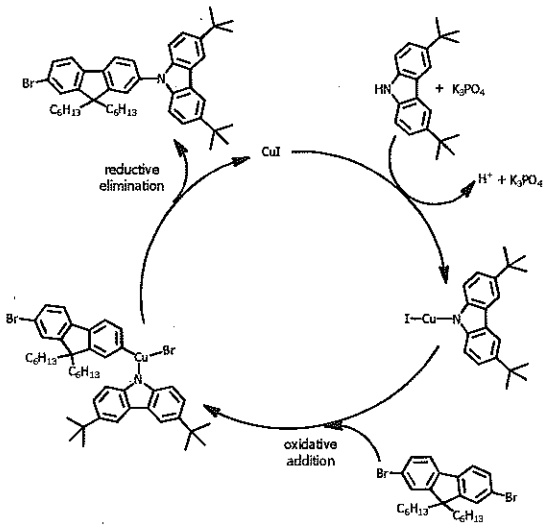

Figure 2.12 The proposed mechanism of Ullmann coupling reaction.

The chemical structure of **CFBr(4)** was confirmed by ^{1}H-NMR analysis. The ^{1}H-NMR spectrum of product **CFBr(4)** shows a singlet signal at chemical shift 8.36 ppm (2H)(**a**) assigning as 4-H and 5-H of *t*-Bu carbazole, a doublet signal at chemical shift 8.01 ppm (1H, J = 8.10 Hz)(**b**) assigning as 4-H of fluorene, a doublet signal at chemical shift 7.88 ppm (1H, J = 6.00 Hz)(**c**) 4-H of fluorene adduct, a multiplet signal at chemical shift between 7.49 to 7.71 ppm (9H) assigning as proton of fluorene and carbazole unit. Moreover, IR spectrum reveals the absorption at 1364 cm^{-1} which is consistent with the presence of C-N bond.

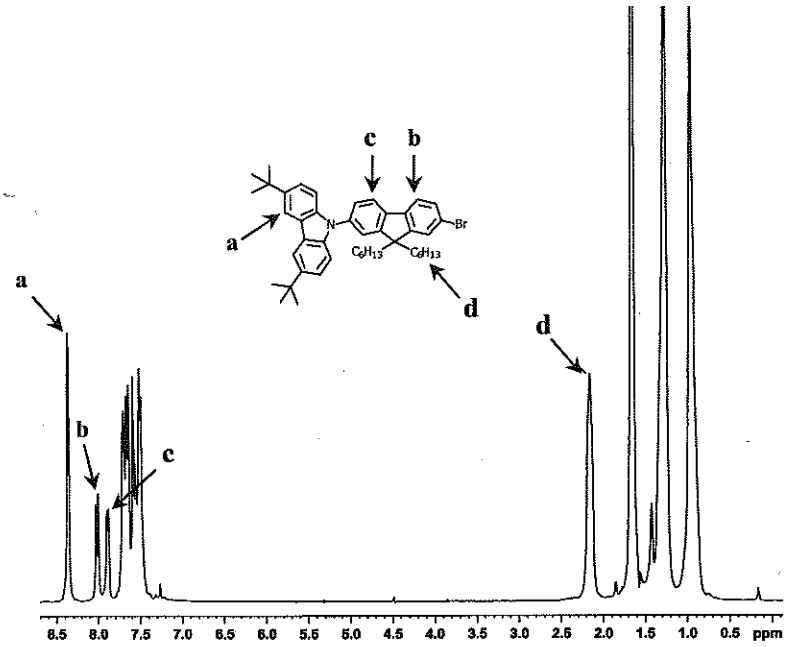

Figure 2.13 H^1-NMR spectrum of 9-(7-bromo-9,9-dihexyl-*9H*-fluoren-2-yl)-3,6-di-*tert*-butyl-*9H*-cabazole (**CFBr(4)**) in $CDCl_3$.

Suzuki cross-coupling reaction of 2-thiophenboronic acid. The thiophene intermediates were prepared by using $Pd(PPh_3)_4$ as catalyst in the presence of aqueous sodium carbonate solution in THF at refluxing temperature afforded the thiophene gave 77 % yield, show in Figure 2.14.

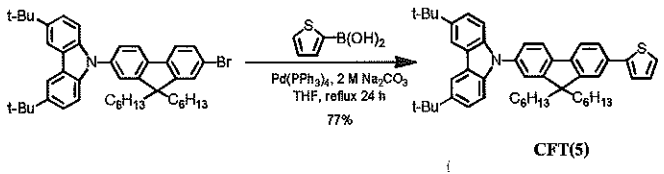

Figure 2.14 Suzuki cross-coupling reaction to form 3,6-di-tert-butyl-9-(9,9-dihexyl-7-(thiophen-2-yl)-9H-fluoren-2-yl)-9H-carbazole (**CFT(5)**).

The proposed mechanism of Suzuki cross-coupling mechanism of thiophene intermediate, show in Figure 2.15. The mechanism for the Suzuki cross-coupling involves three steps: 1) oxidative addition; 2) ligand substitution (transmetallation); 3) reductive elimination. The palladium(0) species is generated under the reaction conditions from palladium acetate and triphenylphosphine. The boronic acid reduces the Pd(II) to Pd(0). The palladium(0) complex then oxidatively adds the aryl halide. The halide is then substituted by phenylboronic acid to give a palladium diaryl complex. Reductive elimination from this complex occurs to give the new organic product and regenerate the Pd(0) catalyst.

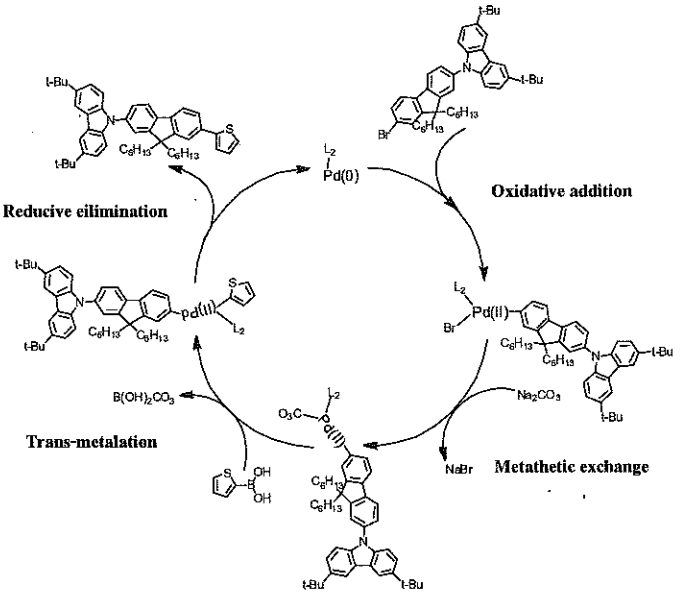

Figure 2.15 The proposed mechanism of Suzuki cross-coupling reaction.

The chemical structure of **CFT(5)** was confirmed by ^{1}H-NMR analysis. The ^{1}H-NMR spectrum of product **CFT(5)** shows a doublet signal at chemical shift 8.18 ppm (2H, J = 8.70 Hz)(**a**) assigning as 4-H and 5-H position of *t*-Bu carbazole, whereas the doublet signal at chemical shift 7.91 ppm (2H J = 8.70 Hz)(**b**) was assigned as two protons in fluorene ring. The overlapping peaks at chemical shift around 7.12 to 7.67 ppm (11H) are assigned as other protons in carbazole, fluorene and thiophene moieties, a triplet signal at chemical shift 2.03 ppm (4H, J = 5.70 Hz)(c) assigning as methylene proton of hexyl unit, show in Figure 2.16.

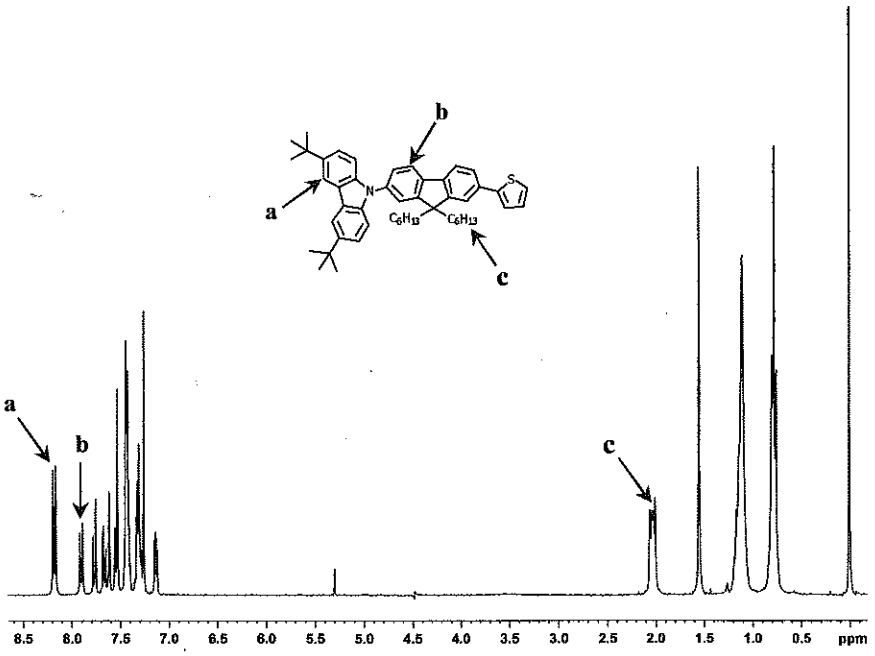

Figure 2.16 H^1-NMR spectrum of 3,6-di-*tert*-butyl-9-(9,9-dihexyl-7-(thiophen-2-yl)-9*H*-fluoren-2-yl)-9*H*-carbazole **CFT (5)** in $CDCl_3$.

Iodination reaction of **CFT (5)** with NIS in mixed solvent of choroform:acetic acid (1:1) to gave **CFTIodo (6)** in 90% yield. Iododination reaction in the Figure 2.17 was used to explain the observed order I > Br > Cl for the ease of halogen displacement from the aromatic ring and the better reactivity shown by electron-deficient aryl halides. Then we choose Iodine because Iodine is good living group more than Br and Cl.

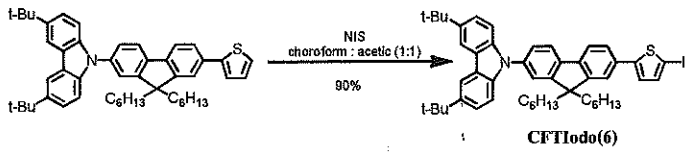

Figure 2.17 Iododination reaction to form 3,6-di-*tert*-butyl-9-(9,9-dihexyl-7-(5-iodothiophen-2-yl)-9*H*-fluoren-2-yl)-9*H*-carbazole **(CFTIodo(6))**.

The chemical structure of **CFTIodo(6)** was confirmed by ^{1}H-NMR analysis, show in Figure 2.18. The ^{1}H-NMR spectrum of product **CFTIodo(6)** shows a single signal at chemical shift 8.33 ppm (2H) assigning as 4-H position of *t*-Bu carbazole ring, a triplet signal at chemical shift 7.94 ppm (1H, J = 7.80 Hz) assigning 4-H position of fluorene ring connection with thiophene, a multiple signal at chemical shift between 7.14 to 7.82 ppm (11H) assigning proton on aromatic ring, a doublet signal at chemical shift 2.14 ppm (4H, J = 4.50 Hz) assigning as methylene proton of hexyl unit, show in Figure 2.18.

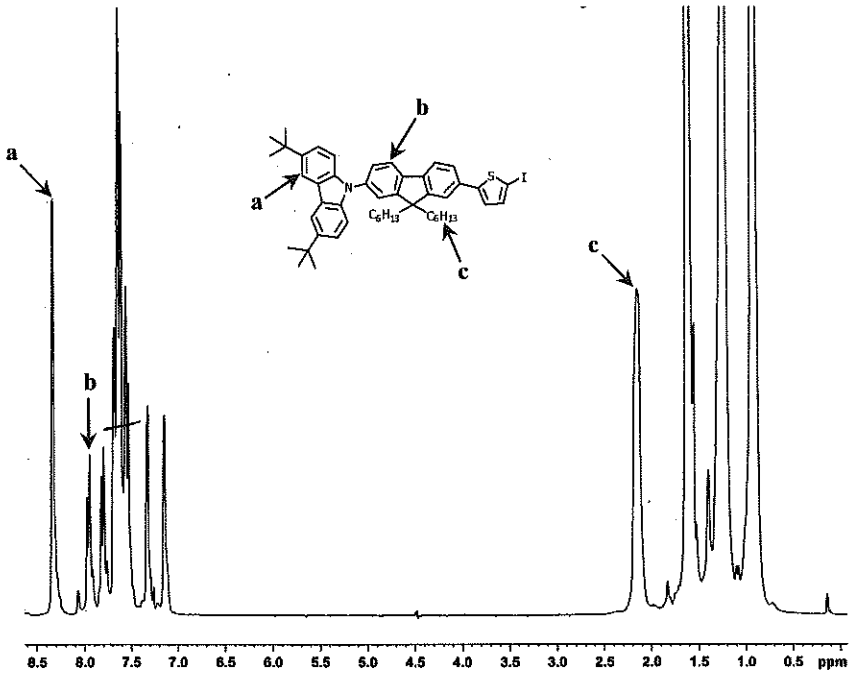

Figure 2.18 H^1-NMR spectrum of 3,6-di-*tert*-butyl-9-(9,9-dihexyl-7-(5-iodothiophen-2-yl)-9*H*-fluoren-2-yl)-9*H*-carbazole **(CFTIodo(6))** in $CDCl_3$.

Ullmann coupling of **CFTIodo (6)** with 1 equivalent of 4-bromoaniline in the presence of copper(I) iodide as catalyst, potassium phosphate as base and (±)-*trans*-diaminocyclohexane as co-catalyst in toluene at 170°C under N_2 in 45% yield, show in Figure 2.19.

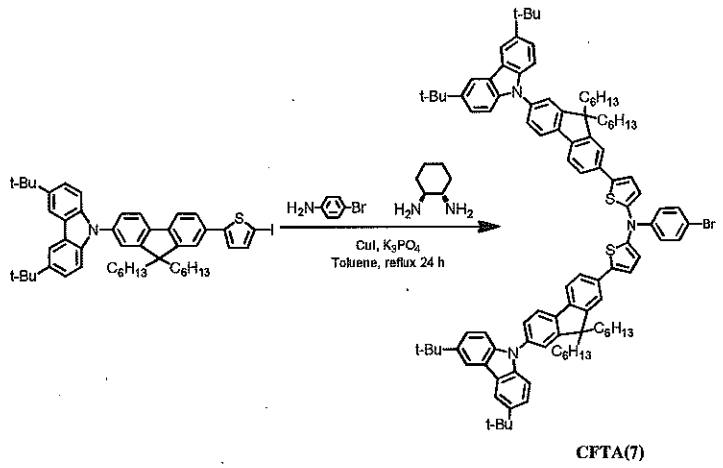

Figure 2.19 Ullmann coupling reaction to form *N*-(4-bromophenyl)-5-(7-(3,6-di-tert-butyl-9*H*-carbazol-9-yl)-9,9-dihexyl-9*H*-fluoren-2-yl)-N-(5-(7-(3,6-di-tert-butyl-9*H*-carbazol-9-yl)-9,9-dihexyl-9*H*-fluoren-2-yl)thiophen-2-yl)thiophen-2-amine **(CFTA(7))**.

The chemical structure of **CFTA(7)** was confirmed by ^{1}H-NMR analysis. The ^{1}H-NMR spectrum of product **CFTA(7)** shows a single signal at chemical shift 8.20 ppm (4H)(**a**) assigning as 4-H and 5-H position of *t*-Bu carbazole, a multiple signal at chemical shift between 7.15 to 7.90 ppm(28H)(**b**) assigning proton on aromatic ring. The triplet signal at chemical shift 2.05 ppm (8H, J = 7.92 Hz)(**c**) was assigned proton in hexyl unit.

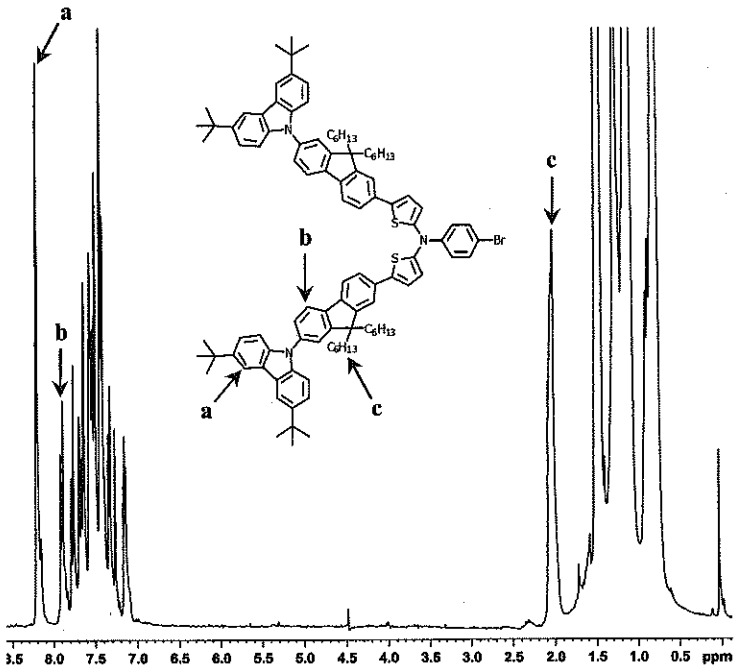

Figure 2.20 H^1-NMR spectrum of *N*-(4-bromophenyl)-5-(7-(3,6-di-tert-butyl-9*H*-carbazol-9-yl)-9,9-dihexyl-9*H*-fluoren-2-yl)-N-(5-(7-(3,6-di-tert-butyl-9*H*-carbazol-9-yl)-9,9-dihexyl-9*H*-fluoren-2-yl)thiophen-2-yl)thiophen-2-amine **(CFTA(7))** in $CDCl_3$.

Suzuki cross-coupling reaction of (5-formylthiophen-2-yl)boronic acid.

The aldehyde intermediates were prepared by using $Pd(PPh_3)_4$ as catalyst in the presence of aqueous sodium carbonate solution in THF at refluxing temperature afforded the thiophene-aldehyde gave 32 % yield, show in Figure 2.21.

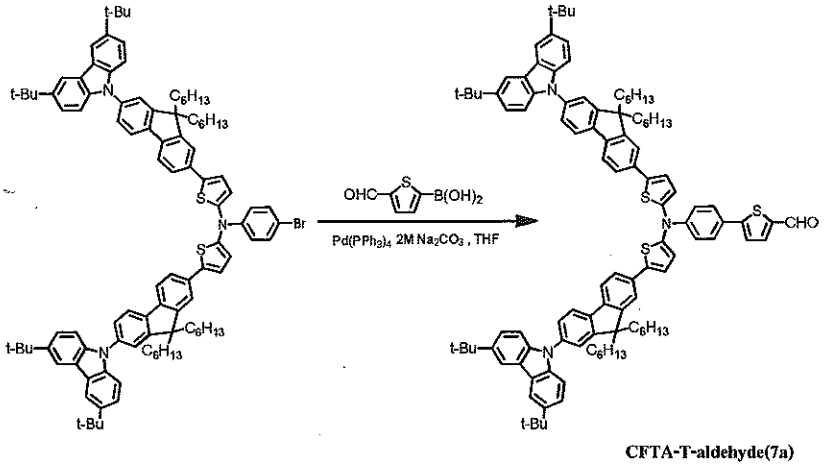

Figure 2.21 Suzuki cross-coupling reaction to form 5-(4-(bis(5-(7-(3,6-di-*tert*-butyl-9*H*-carbazol-9-yl)-9,9-dihexyl-9*H*-fluoren-2-yl)thiophen-2-yl)amino)phenyl)thiophene-2-carbaldehyde.

The chemical structure of **CFTA-T-aldehyde(7a)** was confirmed by ^{1}H-NMR analysis. The ^{1}H-NMR spectrum of product **CFTA-T-aldehyde(7a)** shows symbol peak of aldehyde. Whereas the single signal at chemical shift 9.89 ppm (1H)(**a**) assigning as proton of aldehyde group, a doublet signal at chemical shift 8.17 ppm (4H, J = 1.20 Hz)(**b**) assigning as 4-proton and 5-H of *t*-Bu carbazole, a multiple signal at chemical shift between 7.26 to 7.91 ppm(31H) assigning proton on aromatic ring, a doublet of doublet signal at chemical shift 2.03 ppm (8H, J = 10.05 Hz)(**c**) assigning as methylene proton of hexyl unit, show in Figure 2.22.

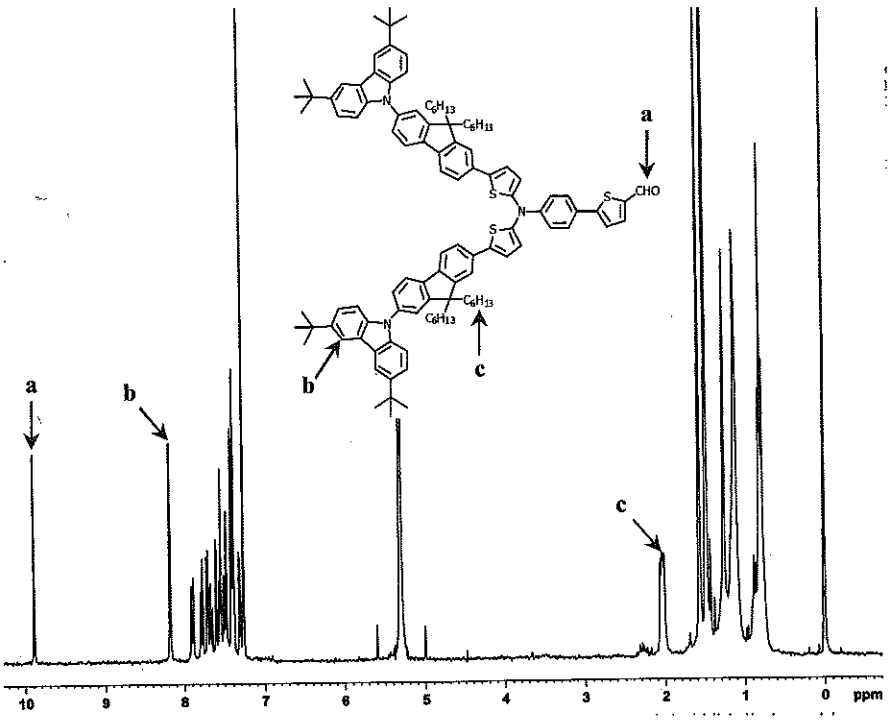

Figure 2.22 H^1-NMR spectrum of 5-(4-(bis(5-(7-(3,6-di-*tert*-butyl-9H-carbazol-9-yl)-9,9-dihexyl-9*H*-fluoren-2-yl)thiophen-2-yl)amino)phenyl)thiophene-2-carbaldehyde **(CFTA-T-aldehyde(7a))** in $CDCl_3$

Knovenagel condensation reaction of **CFTA-T-aldehyde (7a)** with 2-cyanoacetic acid using piperidine catalyst in Chloroform reflux 24h resulting in **CFTAT1-A** in 97% yield, show in Figure 2.23.

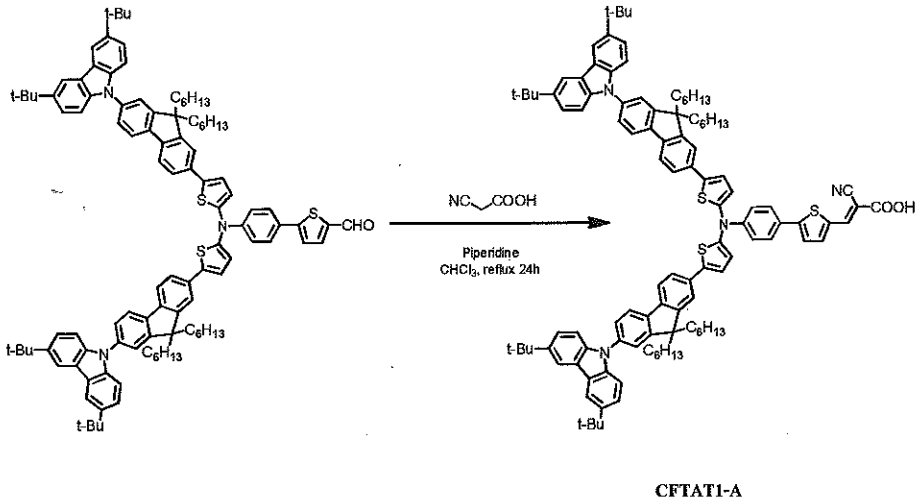

Figure 2.23 Knoevenagel condensation reaction of **CFTA-T-aldehyde(7)** with cynoacetic acid.

Suzuki cross-coupling reaction of 2-thiophenboronic acid. The thiophene intermediates were prepared by using $Pd(PPh_3)_4$ as catalyst in the presence of aqueous sodium carbonate solution in THF at refluxing temperature afforded the thiophene gave 66% yield, show in Figure 2.24.

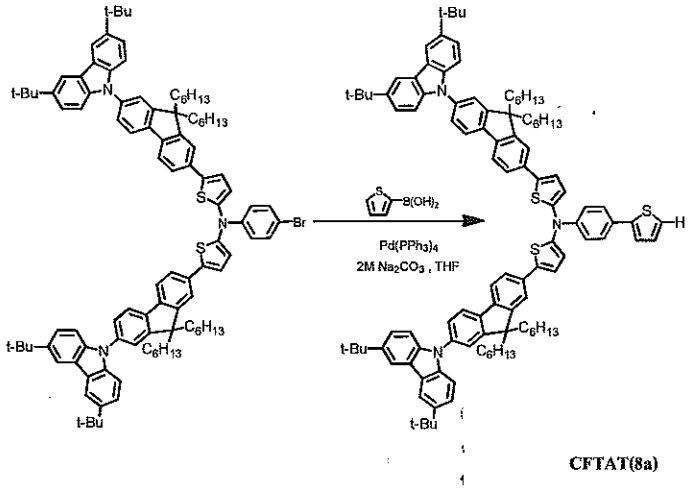

Figure 2.24 Suzuki cross-coupling reaction of **CFTA(7)** with 2-thiopheneboronic acid.

The chemical structure of **CFTAT(8a)** was confirmed by ^{1}H-NMR analysis. The ^{1}H-NMR spectrum of product **CFTAT(8a)** shows a singlet signal at chemical shift 8.21 ppm (4H)(**a**) assigning as 4-H and 5-H of *t*-Bu carbazole. Whereas the multiple signal at chemical

shift between 7.05 to 7.91 ppm (35H)(**b**) was assigned proton in carbazole, fluorene and phenyl ring. The multiplet signal at chemical shift 2.06 ppm (8H)(**c**) was assigned proton in hexyl unit, show in Figure 2.25.

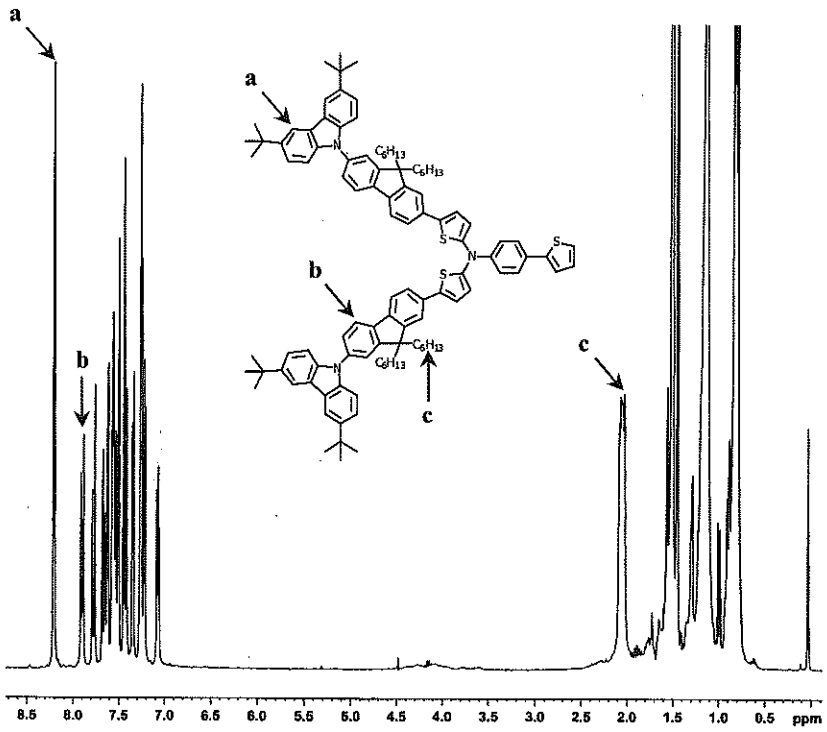

Figure 2.25 H^1-NMR spectrum of 5-(7-(3,6-di-*tert*-butyl-9*H*-carbazol-9-yl)-9,9-dihexyl-9*H*-fluoren-2-yl)-*N*-(5-(7-(3,6-di-*tert*-butyl-9*H*-carbazol-9-yl)-9,9-dihexyl-9*H*-fluoren-2-yl)thiophen-2-yl)-*N*-(4-(thiophen-2-yl)phenyl)thiophen-2-amine **(CFTAT(8a))** in $CDCl_3$.

Suzuki cross-coupling reaction of 2-thiophenboronic acid and the corresponding bromo-compound employed in order to increase the number of thiophene units in the molecules. The thiophene intermediates were prepared by using $Pd(PPh_3)_4$ as catalyst in the presence of aqueous sodium carbonate solution in THF at refluxing temperature afforded **CFTATBr(9a)** **CFTAdi-TBr(9b)** resulting in 86 and 99% yield, Respectively. The bromination reaction was carried out in THF as solvent with NBS. The reaction mixture was stirred at room temperature for 30 min to directly yield bromocompound as show in Figure 2.26.

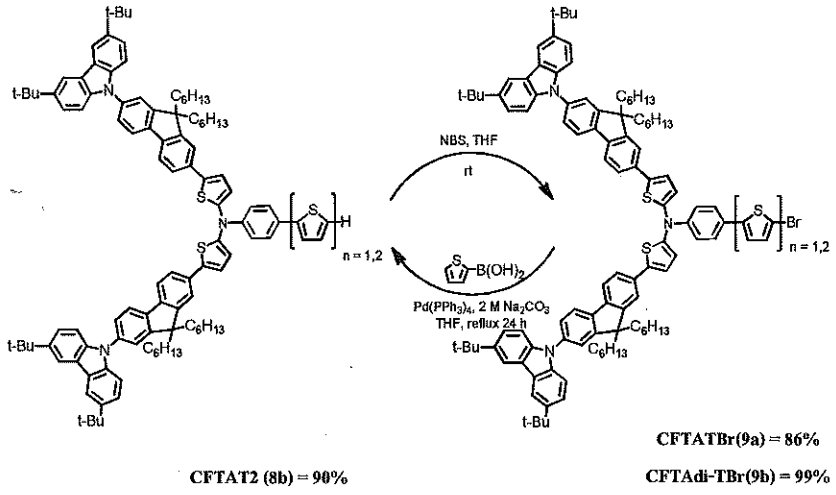

Figure 2.26 Suzuki cross-coupling reaction and bromination reaction to form bromocompounds.

Suzuki cross-coupling reaction of (5-formylthiophen-2-yl)boronic acid employed in order to increase the number of thiophene units in the molecules. The thiophene-aldehyde intermediates were prepared by using $Pd(PPh_3)_4$ as catalyst in the presence of aqueous sodium carbonate solution in THF at refluxing temperature afforded the thiophene-aldehyde adduct in 98 and 88% yield. Show in Figure 2.27.

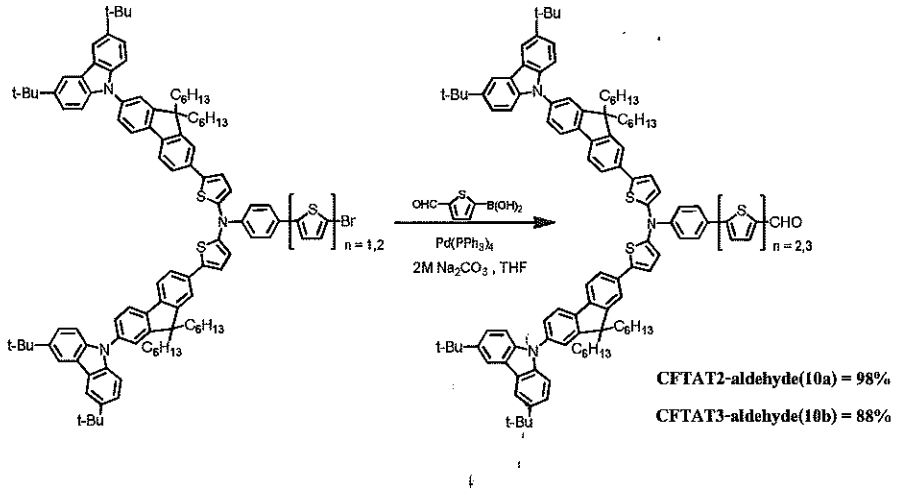

Figure 2.27 Suzuki cross-coupling reaction of bromocompounds.

The chemical structures of **CFTAT2-aldehyde(10a)** and **CFTAT3-aldehyde(10b)** were confirmed by ^{1}H-NMR analysis. The ^{1}H-NMR spectrum of product **CFTAT2-aldehyde(10a)** and **CFTAT3-aldehyde(10b)** shows symbol of aldehyde peak a singlet signal at chemical shift 9.88 ppm (1H)(**a**) assigning as proton position of aldehyde group, a singlet signal at chemical shift 8.18 ppm (4H)(**b**) assigning as 4-H position of *t*-Bu carbazole, a multiple signal at chemical shift between 7.19 to 7.91 ppm(33H) assigning proton on aromatic ring. The triplet signal at chemical shift 2.03 ppm (8H, J = 3.90 Hz)(**c**) was assigned proton in hexyl unit, show in Figure 2.28.

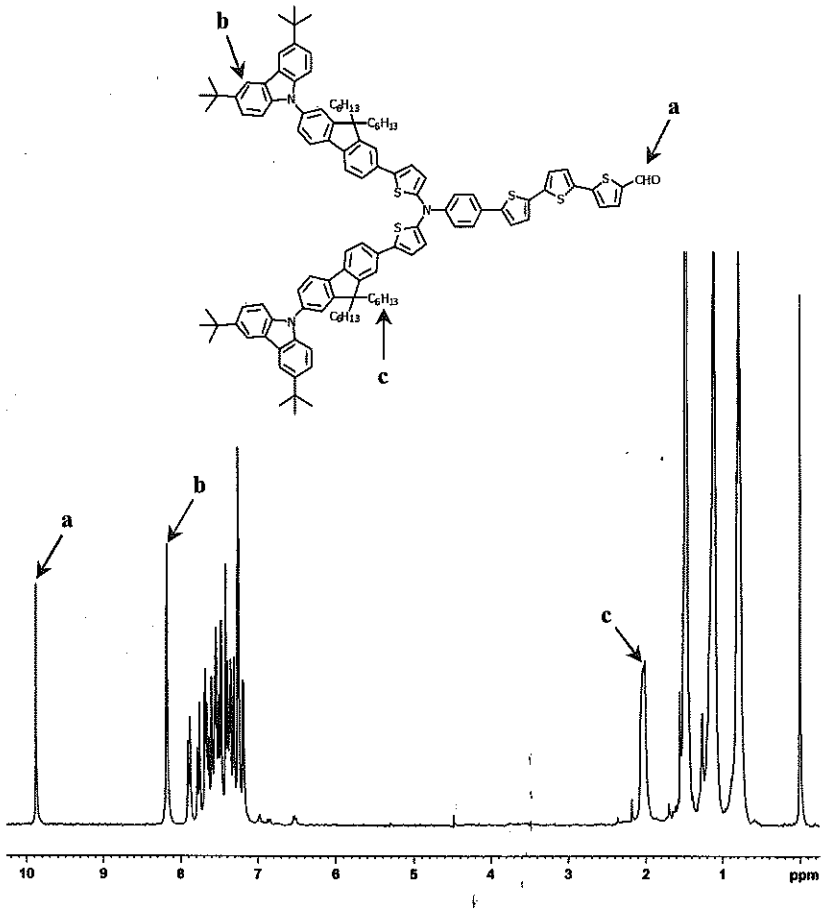

Figure 2.28 H^{1}-NMR spectrum of **CFTAT3-aldehyde(10b)** in $CDCl_3$.

Knovenagel condensation reaction of **CFTAT2-aldehyde(10a)** and **CFTAT3-aldehyde(10b)** with 2-cyanoacetic acid using piperidine catalyst in Chloroform reflux 24h resulting in **CFTAT2-A** and **CFTAT3-A** in 97 and 98% yield, show in Figure 2.29.

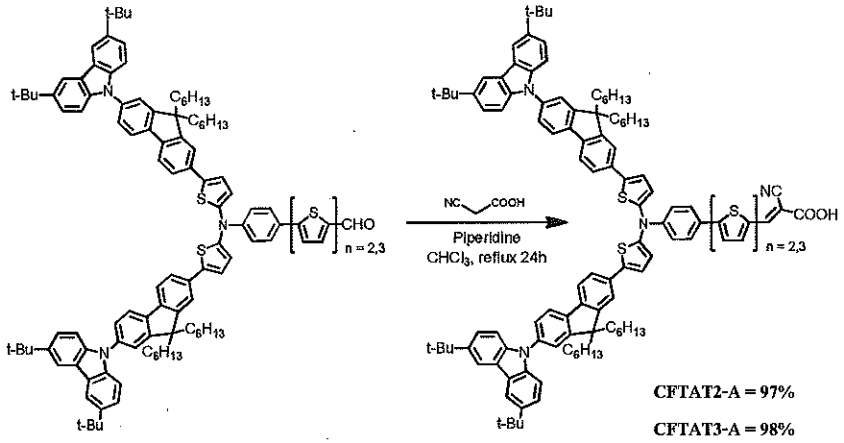

Figure 2.29 Knoevenagel condensation reaction of **CFTAT2-aldehyde(10a)** and **CFTAT3-aldehyde(10b)** with cynoacetic acid.

The chemical structure of **CFTAT2-A** was confirmed by ^{1}H-NMR analysis. The ^{1}H-NMR spectrum of product **CFTAT2-A** shows a triplet signal at chemical shift 8.19 ppm (6H, J = 6.00 Hz)(**a**) assigning as proton position of *t*-Bu carbazole and proton of cyanoacitic acid, a multiple signal at chemical shift between 7.24 to 7.90 ppm(32H) assigning proton on aromatic ring. The singlet signal at chemical shift 3.24 ppm (8H)(**c**) was assigned proton in hexyl unit, show in Figure 2.30.

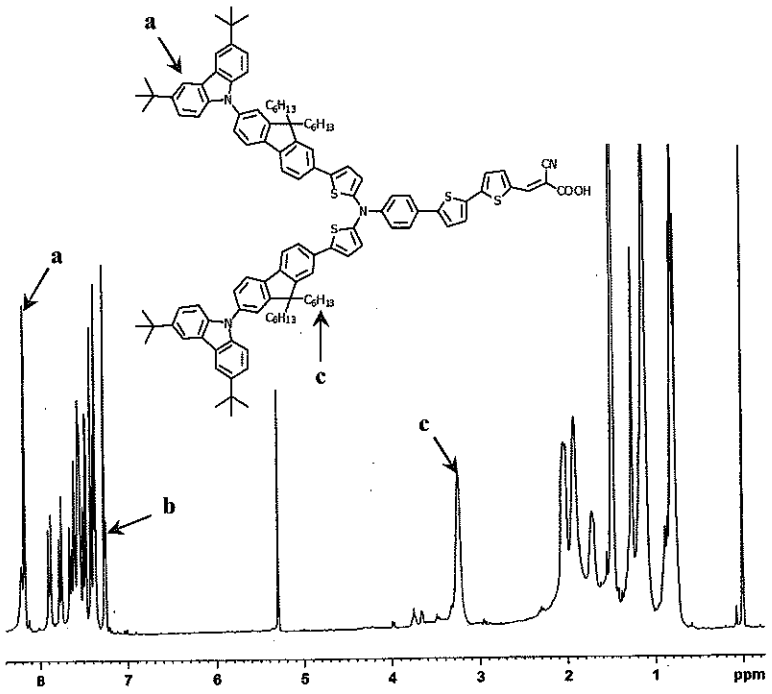

Figure 2.30 H^1-NMR spectrum of **CFTAT2-A** in $CDCl_3$.

The chemical structure of **CFTAT3-A** was confirmed by ^{1}H-NMR analysis. The ^{1}H-NMR spectrum of product **CFTAT3-A** shows a singlet signal at chemical shift 8.18 ppm (6H)(**a**) assigning as proton position of *t*-Bu carbazole and proton of cyanoacitic acid, a multiple signal at chemical shift between 7.16 to 7.89 ppm(32H) assigning proton on aromatic ring. The singlet signal at chemical shift 3.22 ppm (8H)(**c**) was assigned proton in hexyl unit, show in Figure 2.31.

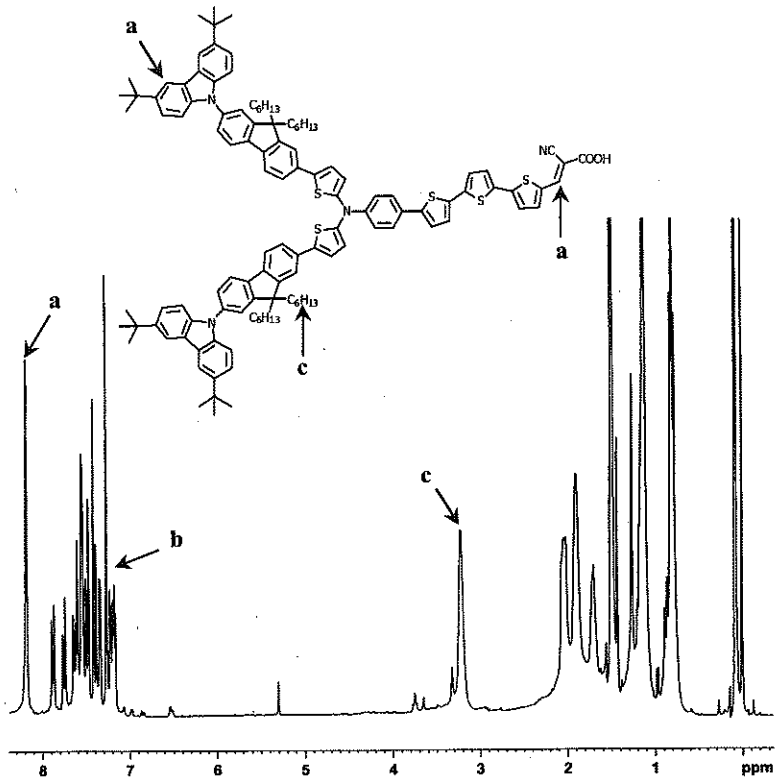

Figure 2.31 H^1-NMR spectrum of **CFTAT3-A** in $CDCl_3$.

Knoevenagel condensation is addition reaction of the methylene components, activated with two electron withdrawing groups, to aldehydes can be performed with secondary amines. A reasonable variation of the mechanism, in which piperidine acts as organocatalyst, involves the corresponding iminium intermediate as the acceptor is shown in Figure 2.32. [47]

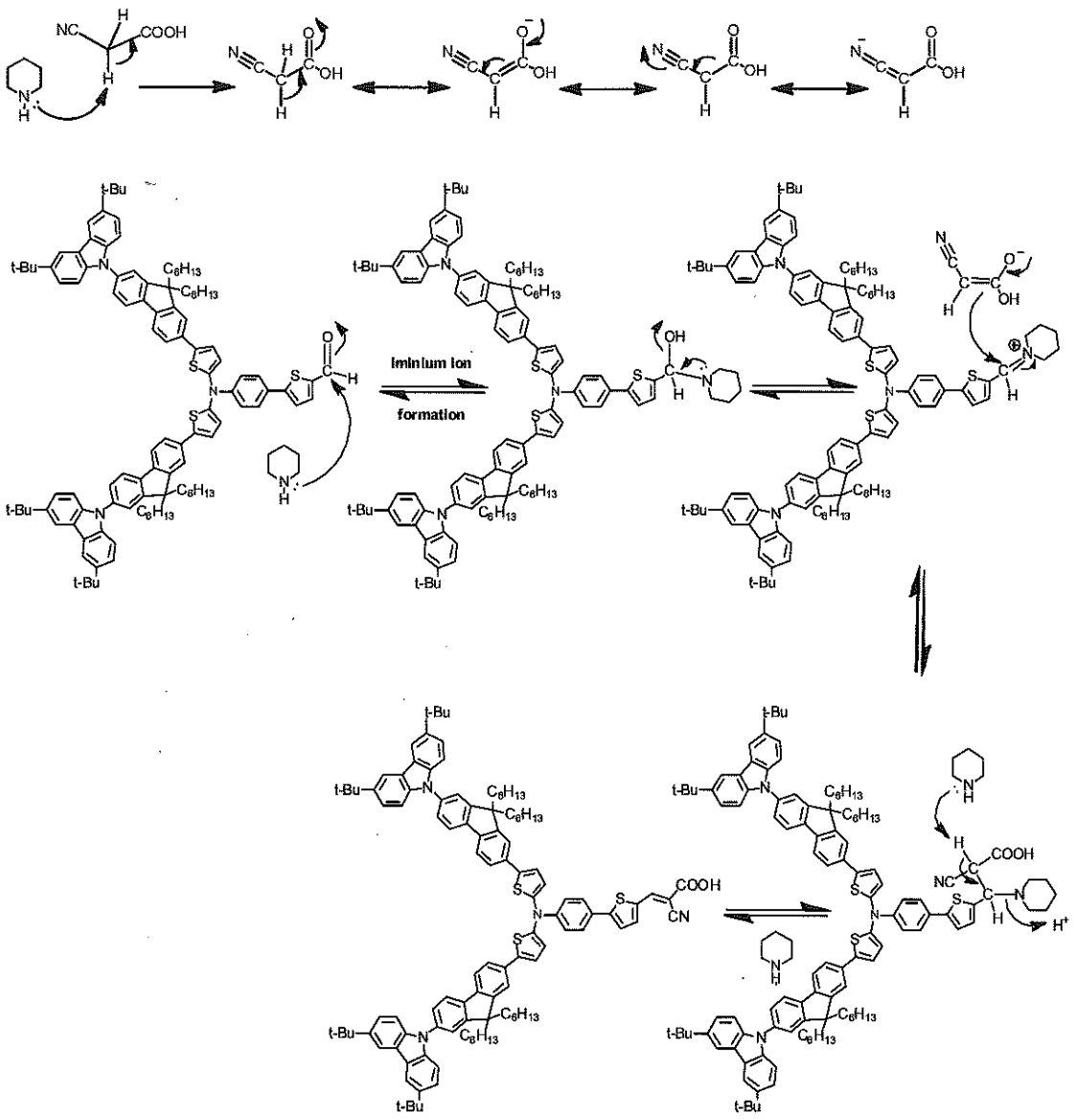

Figure 2.32 The proposed mechanism of Knoevenagel condensation reaction.

3.2.2. Total Synthesis

The target D-D-π-A type organic dyes **CFTATn-A, n = 1-3** were synthesized as shown in Scheme 2.1. Bromination reaction of fluorene (**F1**) with Br_2 using $FeCl_3$ as catalyst in chloroform gave **BrF(2)** in 80% yield. Alkylation reaction of **BrF(2)** with 1-bromohexane using NaOH as base and tetrabutyl ammonium bromide co-catalyst in DMSO to give **Alkyl-BrF (3)** in 86% yield. Ullmann coupling reaction of **Alkyl-BrF (3)** with *t*-Bu-carbazole using K_3PO_4 as base, CuI catalyst and used *trans*-diaminocyclohexane as co-catalyst in toluene gave **CFBr (4)** in 72% yield. Suzuki cross coupling reaction of **CFBr (4)** with 2-thiopheneboronic acid was carried out using $Pd(PPh_3)_4$ as a catalyst, Na_2CO_3 as a base in THF resulting in **CFT (5)** in 77% yield. Iodination reaction of **CFT (5)** with NIS in mixed solvent of choroform:acetic acid (1:1) to gave **CFTIodo (6)** in 90% yield. Ullmann coupling reaction between **CFTIodo (6)** and 4-bromoaniline afforded **CFTA (7)** in 45% yield. Suzuki cross coupling reaction of **CFTA (7)** with (5-formylthiophen-2-yl)boronic acid was carried out using $Pd(PPh_3)_4$ as a catalyst, Na_2CO_3 as a base in THF resulting in **CFTA-T- aldehyde (7a)** in 68% yield. Knovenagel condensation reaction of **CFTA-T- aldehyde (7a)** with 2-cyanoacetic acid using piperidine catalyst in Chloroform reflux 24h resulting in **CFTAT1-A** in 87% yield. Suzuki cross coupling reaction of **CFTA (7)** with 2-thiopheneboronic acid was carried out using $Pd(PPh_3)_4$ as a catalyst, Na_2CO_3 as a base in THF resulting in **CFTAT (8a)** in 66% yield. Bromination reaction **CFTAT (8a)** with NBS in THF gave **CFTATBr (9a)** in 86% yield. Suzuki cross coupling reaction of **CFTATBr (9a)** with 2-thiopheneboronic acid gave **CFTAdi-T (8b)** in 90% yield followed by bromination of the resultant with NBS in THF gave **CFTAdi-TBr (9b)** in 99% yield. Suzuki cross coupling reaction of **CFTATBr (9a)** and **CFTAdi-TBr (9b)** with 5-formyl(thiophen-2-yl)boronic acid yielded **CFTAdi-T-aldehyde (10a)** and **CFTAtri-T-aldehyde (10b)** in 98% and 88% yields, respectively. Finally, Knovenagel condensation reaction of **CFTAdi-T-aldehyde (10a)** and **CFTAtri-T-aldehyde (10b)** with 2-cyanoacetic acid using piperidine catalyst in chloroform produced **Dye2** and **Dye3** in 97% and 98% yields, respectively.

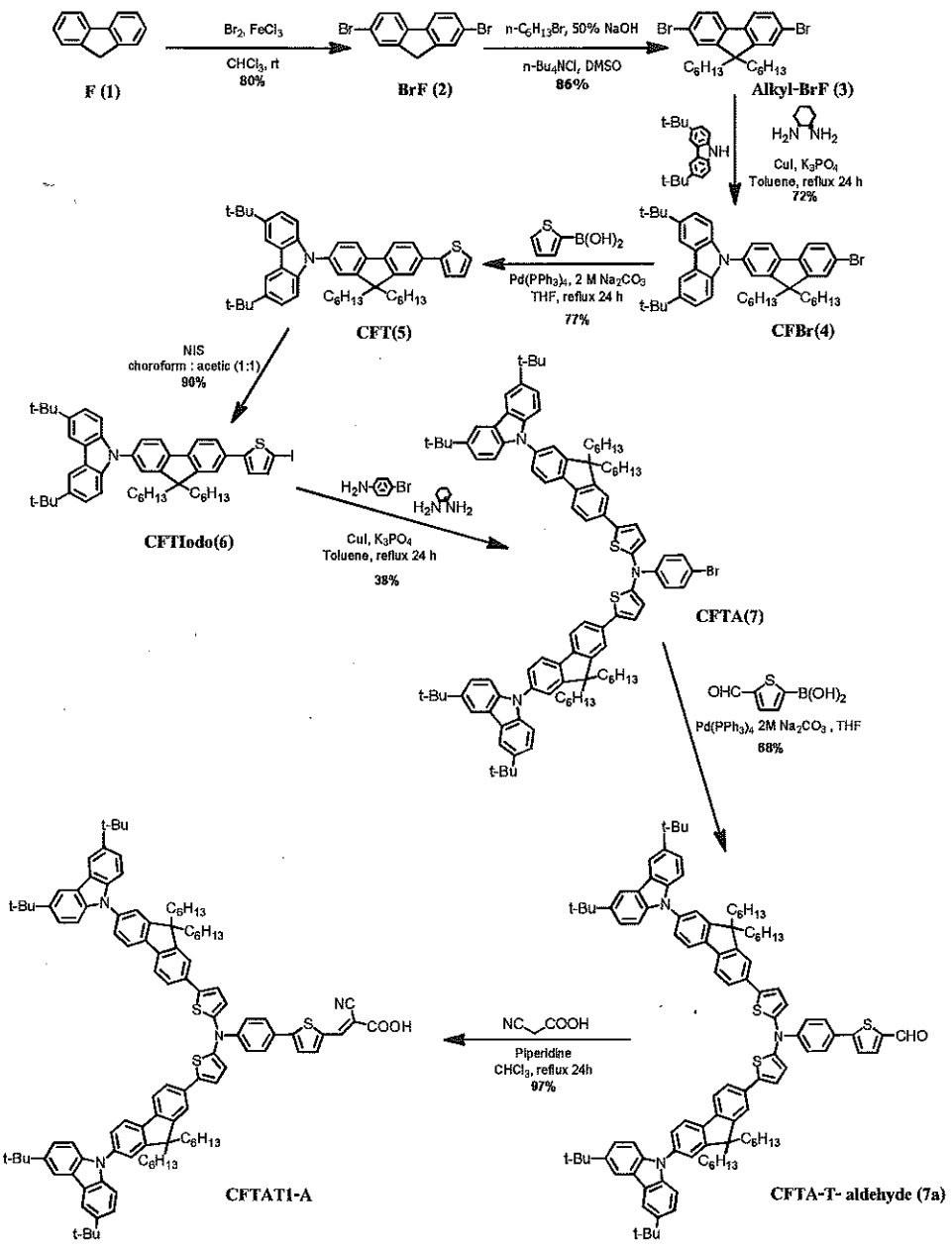

Scheme 2.1 Synthetic route to D-D-π-A type organic dyes (**CFTATn-A, n = 1-3**).

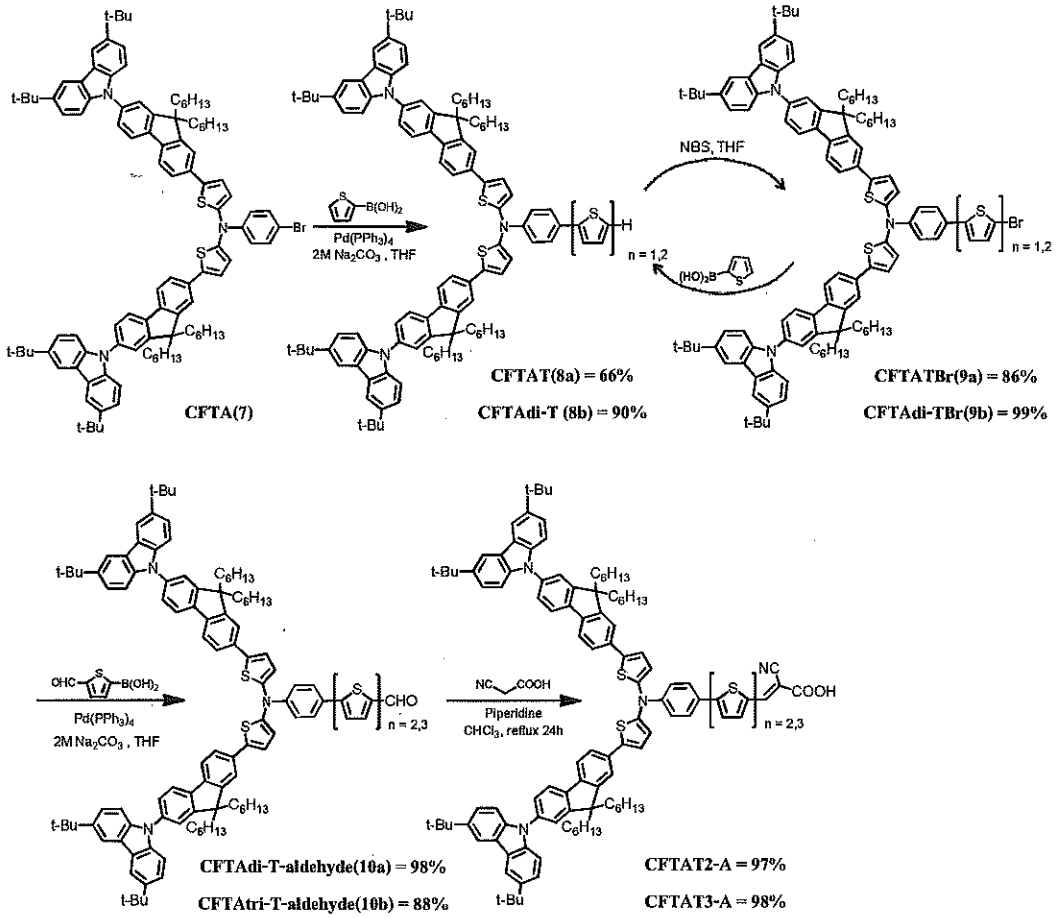

Scheme 2.1 Synthetic route to D-D-π-A type organic dyes (**CFTATn-A, n = 1-3**)(**Cont.**).

2.3.3 Optical properties

The absorption spectra of all the D-D-π-A type organic dyes in dilute CH_2Cl_2 solution are shown in Figure 2.22 (a) and listed in Table 2.1. Dyes **(CFTAn-A, n= 1-3)** exhibited broad absorption spectra ranging from 250 to 600 nm. The spectra exhibit two major absorption bands. The absorption band at around 294 nm can be attributed to the π-π^* transition of the carbazole moieties and the absorption bands at longer wavelength around 450 nm corresponding to the intramolecular charge transfer (ICT) transition between the donor and the acceptor. This indicates that the molecules have a D-D-π-A character. As the number of thiophene units in the molecules increase, the spetra are red shifted and the molar extinction coefficients (ε) increase. Thier ε values range from 17,400 to 27,800 $M^{-1}cm^{-1}$. The broad absorption spectra and high ε value are the key requirments for best sentisizer for efficient DSC.

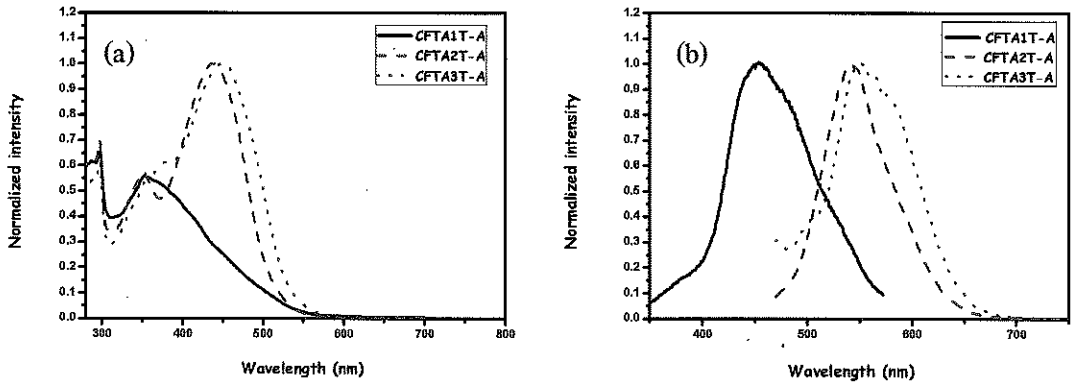

Figure 2.33 Absorption (a) spectra and PL spectra (b) of **CFTATn-A n=1-3** in dry CH_2Cl_2 solution.

The PL spectra of **CFTAn-A, n = 1-3** were located in the yellow to orange region, and their emission maxima were increasingly red-shifted with the increasing number of thiophene rings (Figure 2.33 (b)).

Table 2.1 The absorption and fluorescence data of **CFTATn-A n=1-3** in dry CH_2Cl_2 solution.

Compound	λmax of absorbance (nm) and ε(10^4 $M^{-1}cm^{-1}$)	λmax of emission (nm)
CFTA1T-A	298 (0.92), 354 (0.79)	456
CFTA2T-A	297 (5.58), 439 (8.04)	542
CFTA3T-A	297 (4.59), 450 (7.57)	548

2.3.4 Thermal properties

For optoelectronic applications, the thermal stability of organic materials is crucial for device stability and lifetime. The degradation of organic optoelectronic devices depends on morphological changes resulting from the thermal stability of the amorphous organic layer. Morphological change might be promoted by rapid molecular motion near the glass transition temperature (T_g).

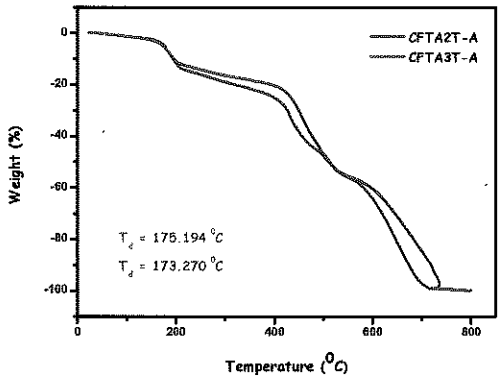

Figure 2.34 TGA curves of **CFTAn-A, n = 2-3** measured under nitrogen atmosphere at heating rate of 10 °C/min.

The thermal properties of **CFTAn-A, n=1-3** were measured by uising TGA analysis. A 5% weight loss temperature (T_{-5d}) of **CFTAn-A, n=1-3** were found to be 175 and 173 °C, respectively. Before and during evaporation no decomposition was detected indicating an excellent themal stability of **CFTAn-A, n=1-3**. This suggests that the presence of carbazole

dendron donor moieties to the thiophenes as π-conjugated linker is indeed beneficial to their thermal stabilities.

2.4 Conclusions

The designed dye compounds **CFTAn-A, n = 1-3** composed of three parts: (1) carbazole donating groups (D); (2) an oligothiophene and oligothiophene-phenylene (π); and (3) a cyanoacrylic acid anchoring group (A) were synthesized using a combination of alkylation, bromination, Ullmann coupling, Suzuki cross-coupling and Knoevenagel condensation reactions. The electronic, electrochemical, and thermal properties of these compounds can be tuned by varying the number of thiophene rings. These compounds exhibited a high molar absorptivity in the blue/green region of solar light. The number of thiophene increased the conjugation length of compounds resulting a red-shift and broad in absorption solution spectra. The dye **CFTA3-A** should be promising materials for DSCs devices.

CHAPTER 3

SYNTHESIS AND CHARACTERIZATION OF DICARBAZOLE DENDRIMERS AS EMITTING MATERIALS FOR OLEDs (C_2TnG1 = 0-2)

3.1 Introduction

The general structure of OLEDs consists of a light emissive layer sandwiched in between two metal electrodes, one of which is transparent conducting electrode. Additional layers between the cathode and the emissive layer (electrontransport layer, ETL) or between the anode and the emissive layer (hole transport layer, HTL) is used for high efficiency OLED devices. Recent studies revealed that organic multilayer structures typically enhance the performance of the devices by lowering the barrier for hole injection from the anode and by enabling control over the electron-hole recombination region, moving it from the organic/cathode interface, where the defect density is high, into the bulk. Hence, the layer deposited on the anode would generally be a good hole transport material (HTM), providing HTL. Similarly, the organic layer in contact with the cathode would be the optimized ETL [33, 48-50].

3.2 Aim of the Study

Carbazole molecules have been used as HTLs owing to their excellent hole-transporting capability, high charge carrier mobility, high thermal, morphological and photochemical stability.It can easily be functionalized at its 3,6-, 1,8- or *N* positions and then covalently linked into polymeric systems, both as building blocks in the main chain and pending groups in the side chain. The molecular structures of carbazole dendrimers compounds are shown in Figure 3.1 [51-53].

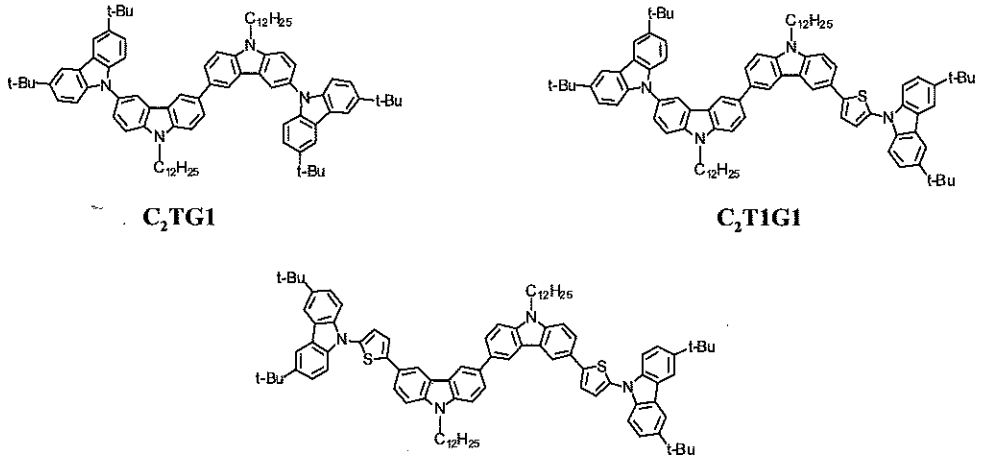

C_2TG1 C_2T1G1

C_2T2G1

Figure 3.1 Structure of di-carbazole dendrimers compounds (C_2TnG1 = 0-2).

3.3 Results and Discussion

3.3.1 Synthesis

Alkylation reaction of carbazole with 1-bromododecane using sodium hydride as base gave 9-dodecyl carbazole(**C**) in 95% yield, show in Figure 3.2.

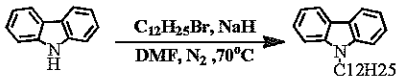

C

Figure 3.2 Alkylation reaction to form 9-dodecyl-9H-carbazole(**C**) compound.

The chemical structures of 9-dodecyl-9H-carbazole(**C**) compounds were confirmed by ^{1}H-NMR spectrum of 9-dodecyl-9H-carbazole(**C**) shows a doublet signal at chemical shift 8.09 ppm (2H, J = 2.4 Hz)(**a**) assigning as 4-H and 5-H position of carbazole ring, a multiplet signal at chemical shift 7.20-7.50 ppm (4H) assigning H of carbazole and a triplet signal at chemical shift 3.30 ppm (2H, J = 2.1 Hz)(**b**) assigning proton of dodecane, show in Figure 3.3.

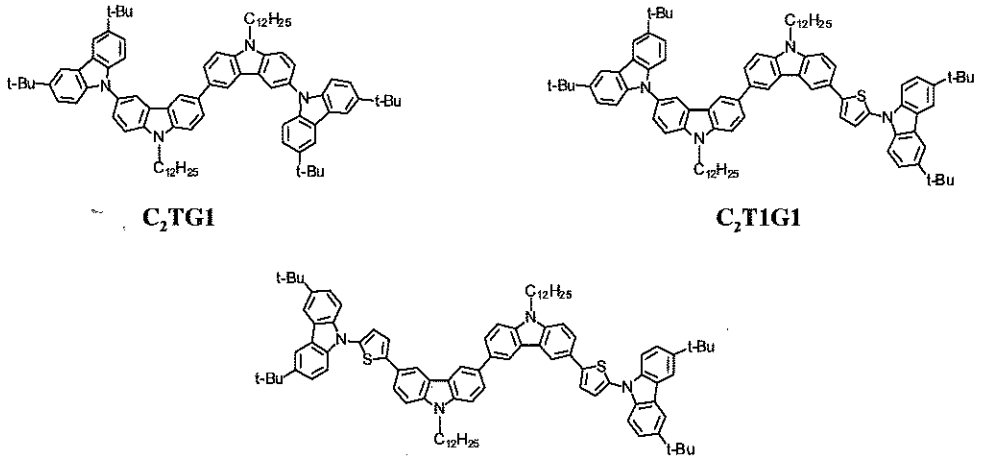

C_2TG1 C_2T1G1

C_2T2G1

Figure 3.1 Structure of di-carbazole dendrimers compounds (C_2TnG1 = 0-2).

3.3 Results and Discussion

3.3.1 Synthesis

Alkylation reaction of carbazole with 1-bromododecane using sodium hydride as base gave 9-dodecyl carbazole(**C**) in 95% yield, show in Figure 3.2.

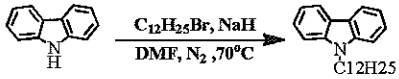

C

Figure 3.2 Alkylation reaction to form 9-dodecyl-9H-carbazole(**C**) compound.

The chemical structures of 9-dodecyl-9H-carbazole(**C**) compounds were confirmed by ^{1}H-NMR spectrum of 9-dodecyl-9H-carbazole(**C**) shows a doublet signal at chemical shift 8.09 ppm (2H, J = 2.4 Hz)(**a**) assigning as 4-H and 5-H position of carbazole ring, a multiplet signal at chemical shift 7.20-7.50 ppm (4H) assigning H of carbazole and a triplet signal at chemical shift 3.30 ppm (2H, J = 2.1 Hz)(**b**) assigning proton of dodecane, show in Figure 3.3.

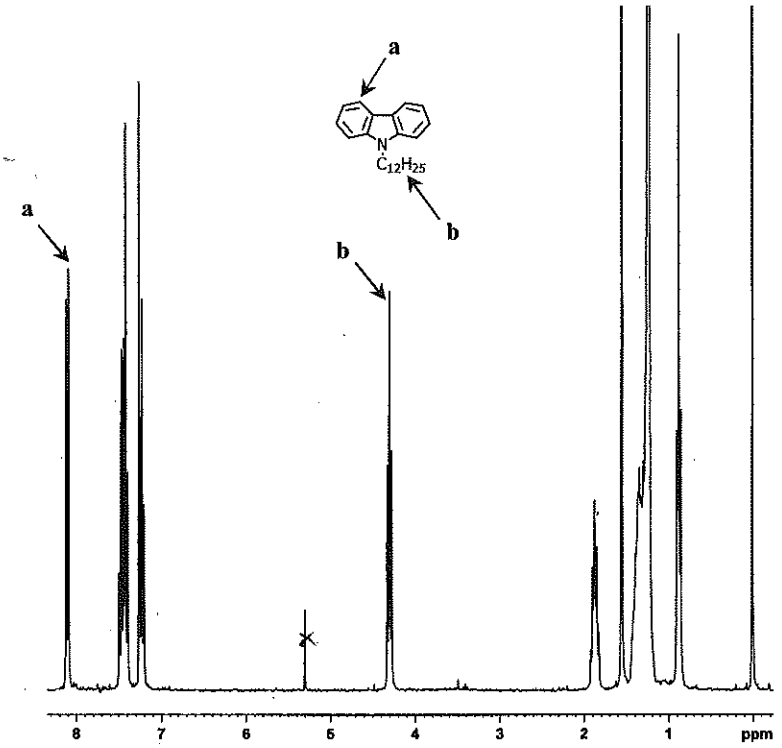

Figure 3.3 H^1-NMR spectrum of 9-dodecyl-9H-carbazole(**C**) in $CDCl_3$

The proposed mechanism of alkylation reaction. The mechanism pathway S_N2 reaction. This pathway is a concerted process (single step, single step reactions have no intermediates and a single transition state (TS)) as shown in Figure 3.4. The nucleophile attacks at the carbon with the partial positive charge as a result of the polar s bond to the electronegative atoms in the leaving group.

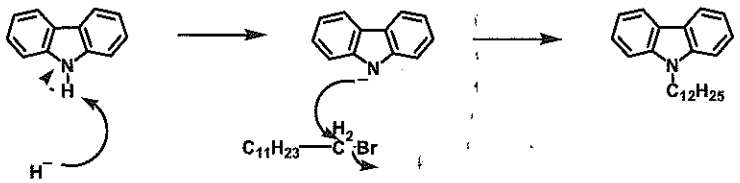

Figure 3.4 The proposed mechanism of nucleophilic substitution reaction.

Oxidative coupling reaction of 9-dodecyl carbazole(**C**) was carried out using $FeCl_3$ as a catalyst in $CHCl_3$ solvent resulting in Bis-9-dodecyl carbazole($\mathbf{C_2}$) in 86% yield, show in Figure 3.5.

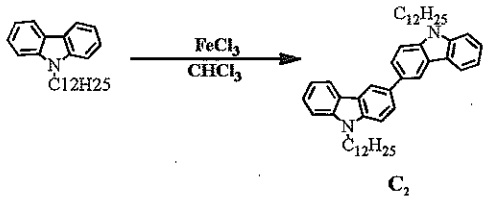

$\mathbf{C_2}$

Figure 3.5 Oxidative coupling reaction to form 9,9'-didodecyl-9*H*,9'*H*-3,3'-bicarbazole($\mathbf{C_2}$) compound.

The chemical structure of 9,9'-didodecyl-9H,9'H-3,3'-bicarbazole($\mathbf{C_2}$) was confirmed by ^{1}H-NMR analysis. The ^{1}H-NMR spectrum of 9,9'-didodecyl-9*H*,9'*H*-3,3'-bicarbazole($\mathbf{C_2}$) shows a doublet signal at chemical shift 8.41 ppm (2H, J = 1.2 Hz)(**a**) assigning as 4-H of carbazole, a doublet signal at chemical shift 8.19 ppm (2H, J = 7.8 Hz)(**b**) assigning as 2-H of *t*-Bu carbazole and a triplet signal at chemical shift 3.45 ppm (4H, J = 7.2 Hz)(**c**) assigning as proton of dodecane, show in Figure 3.6.

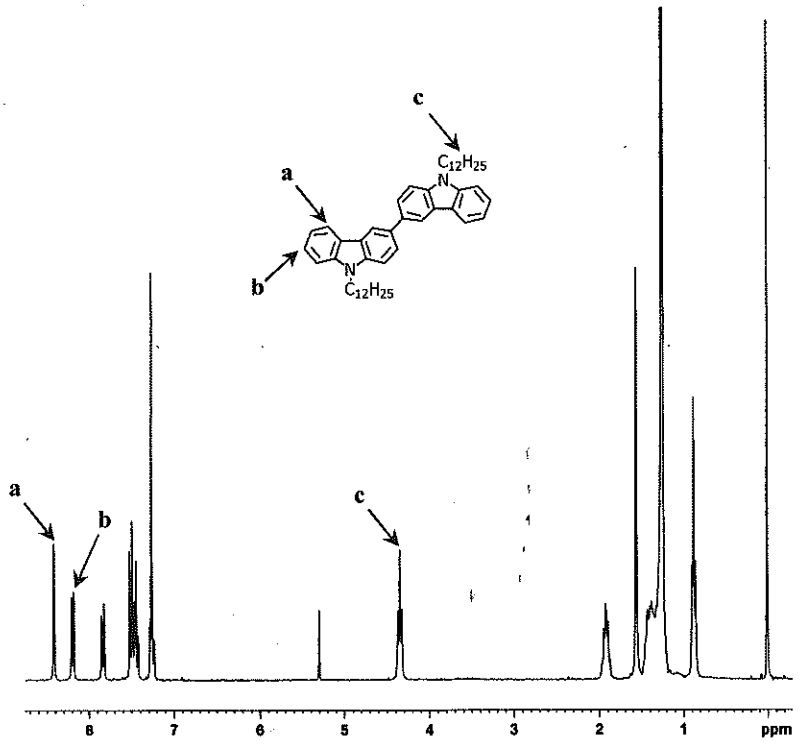

Figure 3.6 H^1-NMR spectrum of 9,9'-didodecyl-9*H*,9'*H*-3,3'-bicarbazole($\mathbf{C_2}$) in $CDCl_3$

Bromination reaction of Bis-9-dodecyl carbazole($\mathbf{C_2}$) with NBS in THF at room temperature gave 6,6'-dibromo-9,9'-didodecyl-9*H*,9'*H*-3,3'-bicarbazole (**$\mathbf{C_2}$-diBr**) in 50% yield, show in Figure 3.7.

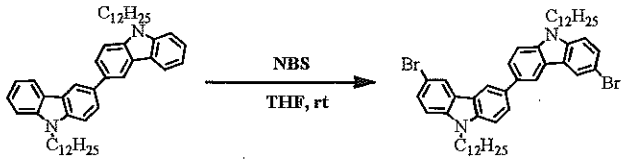

Figure 3.7 Bromination reaction to form 6,6'-dibromo-9,9'-didodecyl-9*H*,9'*H*-3,3'-bicarbazole (**$\mathbf{C_2}$-diBr**) compound.

The chemical structure of **$\mathbf{C_2}$-diBr** was confirmed by ^{1}H-NMR analysis. The ^{1}H-NMR spectrum of **$\mathbf{C_2}$-diBr** shows a triplet signal at chemical shift 8.30 ppm (2H, J = 6.0 Hz)(**a**) assigning as 4-H of *t*-Bu carbazole, a quartet signal at chemical shift 7.83 ppm (2H, J = 8.1 Hz)(**b**) assigning as 2-H of carbazole and a triplet signal at chemical shift 4.29 ppm (4H, J = 7.20 Hz)(**c**) assigning as proton of dodecane, show in Figure 3.8.

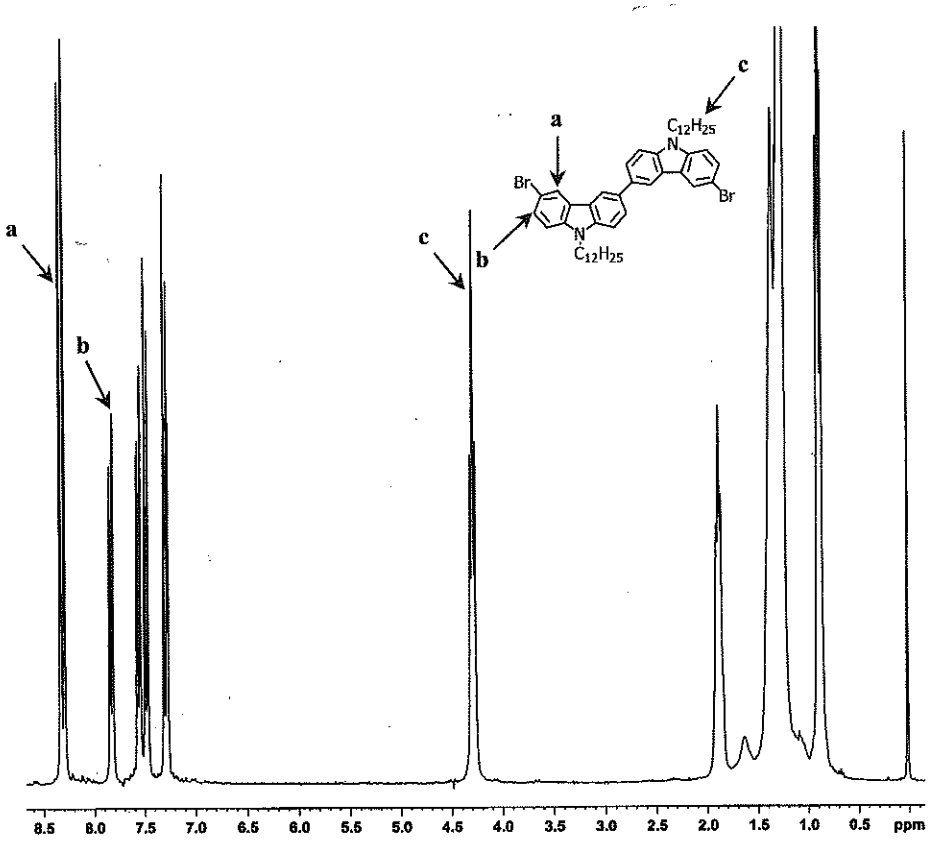

Figure 3.8 H^1-NMR spectrum of 6,6'-dibromo-9,9'-didodecyl-9*H*,9'*H*-3,3'-bicarbazole (**C_2-diBr**) in $CDCl_3$

Ullmann coupling reaction between **C_2-diBr** and *t*-Bu-carbazole(**G1**) were used copper(I) iodide as catalyst, potassium phosphate as base and (±)-*trans*-diaminocyclohexane as co-catalyst in toluene at 170°C under N_2 to give **C_2TG1** in 76% yield, show in Figure 3.9.

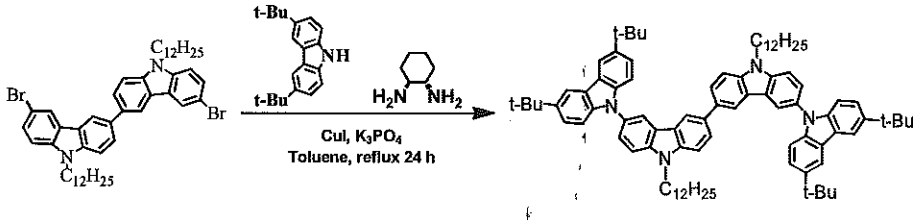

Figure 3.9 Ullmann coupling reaction to form 3,3''',6,6'''-tetra-tert-butyl-9',9''-didodecyl-9'*H*,9''*H*-9,3':6',3'':6'',9'''-quatercarbazole(**C_2TG1**) compound.

The chemical structure of **C_2TG1** was confirmed by ^{1}H-NMR analysis. The ^{1}H-NMR spectrum of **C_2TG1** shows a doublet signal at chemical shift 8.69 ppm (2H, J = 0.9 Hz)(**a**) assigning as 4-H of *t*-Bu-carbazole, a singlet signal at chemical shift 8.32 ppm (2H)(**b**) assigning as 2-H of carbazole and a triplet signal at chemical shift 8.17 ppm (6H, J = 3.0 Hz)(**c**) assigning as 4-H of carbazole and a triplet signal at chemical shift 4.36 ppm (4H, J = 7.2 Hz)(**d**) as proton of dodecane, show in Figure 3.10.

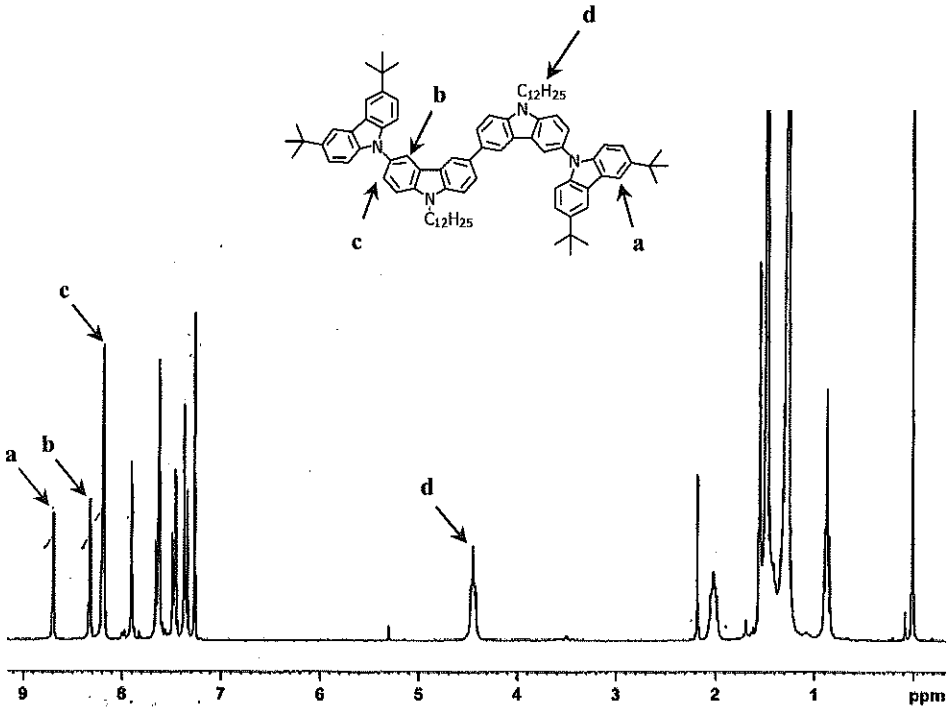

Figure 3.10 H^1-NMR spectrum of 3,3'",6,6'"-tetra-tert-butyl-9',9"-didodecyl-9'*H*,9"*H*-9,3':6',3":6",9'"-quatercarbazole(**C_2TG1**) in $CDCl_3$

Suzuki coupling reaction between dibromocarbazole(**C_2-diBr**) and 2-thiopheneboronic acid was carried out using $Pd(PPh_3)_4$ as catalyst, Na_2CO_3 as a base in THF as a solvent at reflux 24h resulting in bromothiophene (**C_2T1Br**) 38% yield, show in Figure 3.11.

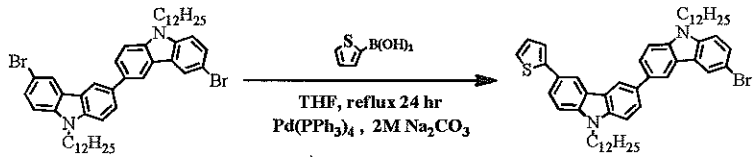

Figure 3.11 Suzuki cross-coupling reaction to form bromothiophene(**C_2T1Br**) compound.

The chemical structure of bromothiophene(**C_2T1Br**) was confirmed by ^{1}H-NMR analysis. The ^{1}H-NMR spectrum of bromothiophene(**C_2T1Br**) shows a singlet signal at chemical shift 8.45 ppm (2H)(**a**) assigning as 5-H position of carbazole ring, a singlet signal at chemical shift 8.39 ppm (1H)(**b**) assigning as 2-H of carbazole with thiophene, a singlet signal at chemical shift 8.34 ppm (1H) assigning as 2-H of carbazole and a doublet signal at chemical shift 4.25 ppm (4H, J = 7.2 Hz)(**c**) assigning as proton of dodecane, show in Figure 3.12.

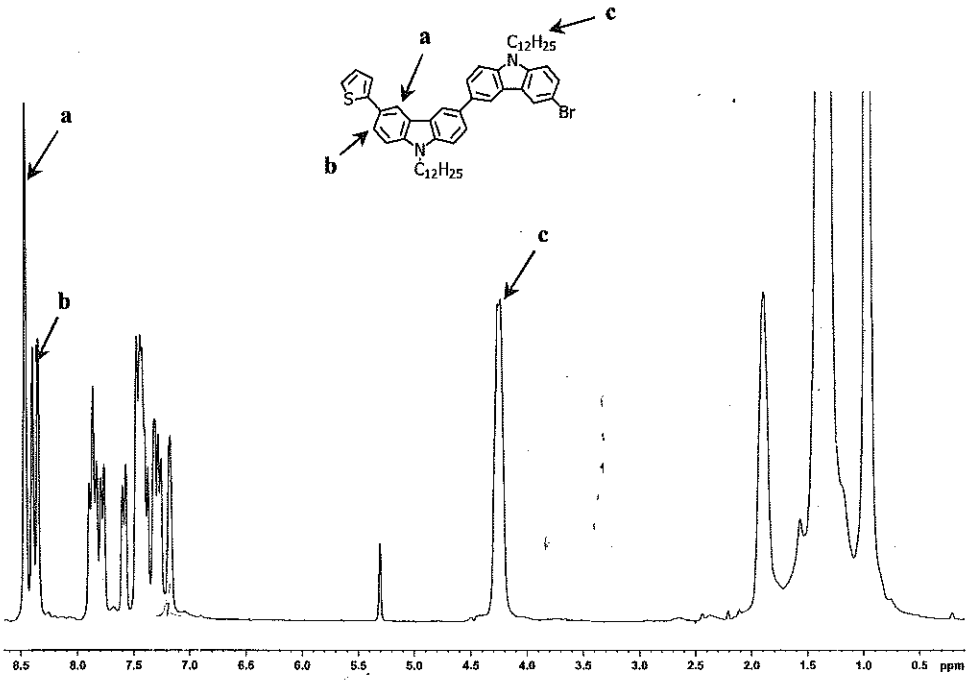

Figure 3.12 H^1-NMR spectrum of bromothiophene(**C_2T1Br**) in $CDCl_3$

Suzuki coupling reaction between dibromocarbazole(**C_2-diBr**) and 2-thiopheneboronic acid was carried out using $Pd(PPh_3)_4$ as catalyst, Na_2CO_3 as a base in THF as a solvent at reflux 24h resulting in dithiophene(**C_2T2**) 48% yield, show in Figure 3.13.

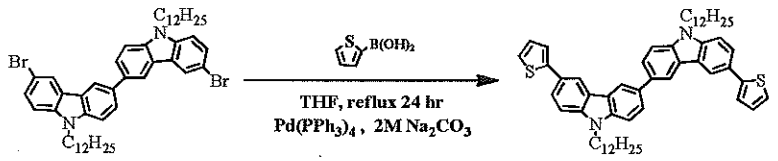

Figure 3.13 Suzuki cross-coupling reaction to form dithiophene(**C_2T2**) compound.

The chemical structure of dithiophene(**C_2T2**) was confirmed by ^{1}H-NMR analysis. The ^{1}H-NMR spectrum of dithiophene(**C_2T2**) shows a doublet signal at chemical shift 8.49 ppm (4H, J = 7.2 Hz)(**a**) assigning as 4-H and 5-H position of carbazole ring, a doublet signal at chemical shift 7.88 ppm(2H, J = 7.2 Hz)(**b**) assigning as 2-H of thiophene, a doublet signal at chemical shift 7.78 ppm(2H, J = 7.2Hz)(**c**) assigning as 3-H of thiophene and a triplet signal at chemical shift 4.34 ppm(4H, J = 7.2 Hz)(**d**) assigning as proton of dodecane, show in Figure 3.14.

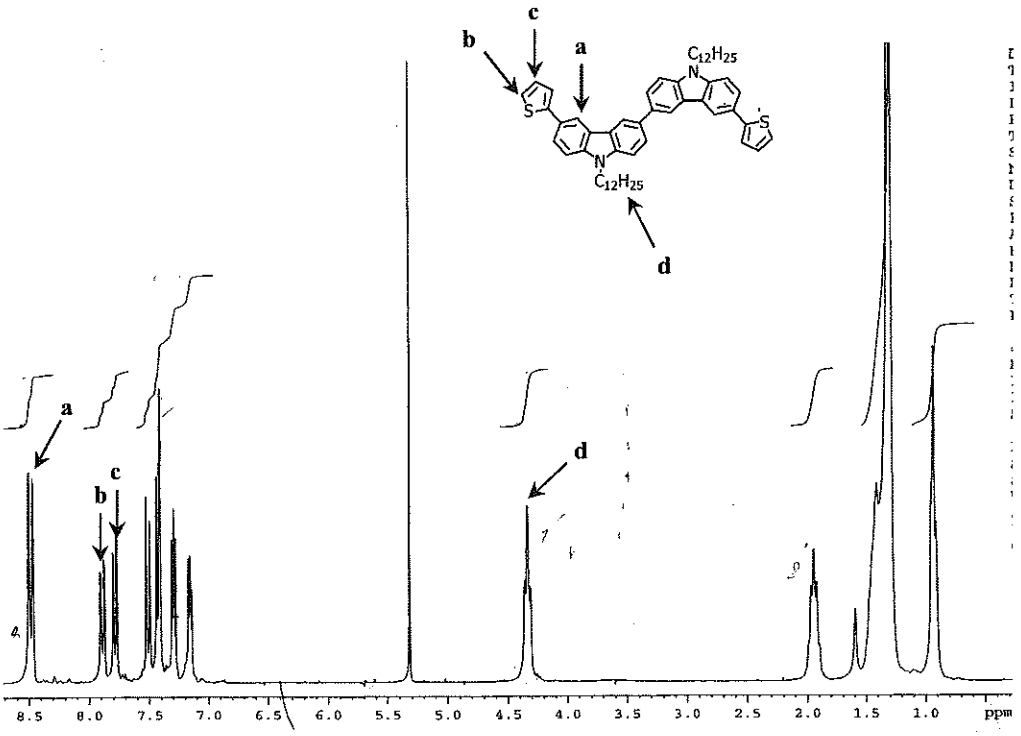

Figure 3.14 H^1-NMR spectrum of bromothiophene(C_2T2) in $CDCl_3$

Bromination reaction of bromothiophene (**C_2T1Br**) with NBS in THF at room temperature gave dibromo (**C_2T1-diBr**) compound in 37% yield, show in Figure 3.15.

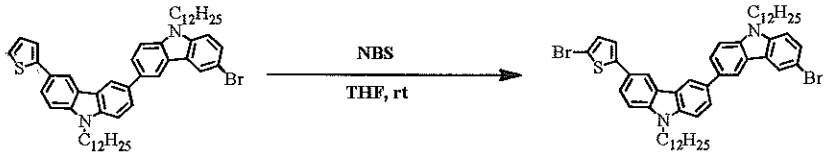

Figure 3.15 Bromination reaction to form dibromo(**C_2T1-diBr**) compound.

The chemical structure of dibromo(**C_2T1-diBr**) was confirmed by ^{1}H-NMR analysis. The ^{1}H-NMR spectrum of dibromo(**C_2T1-diBr**) shows a singlet signal at chemical shift 8.40 ppm (1H)(**a**) assigning as 5-H position of carbazole with thiophene, a singlet signal at chemical shift 8.35 ppm (1H) assigning as 2-H of carbazole with thiophene, a singlet signal at chemical shift 8.30 ppm (2H)(**b**) assigning as 2-H and 3-H of thiophene and a doublet signal at chemical shift 4.28 ppm (4H, J = 5.1 Hz)(**d**) assigning as proton of dodecane, show in Figure 3.16.

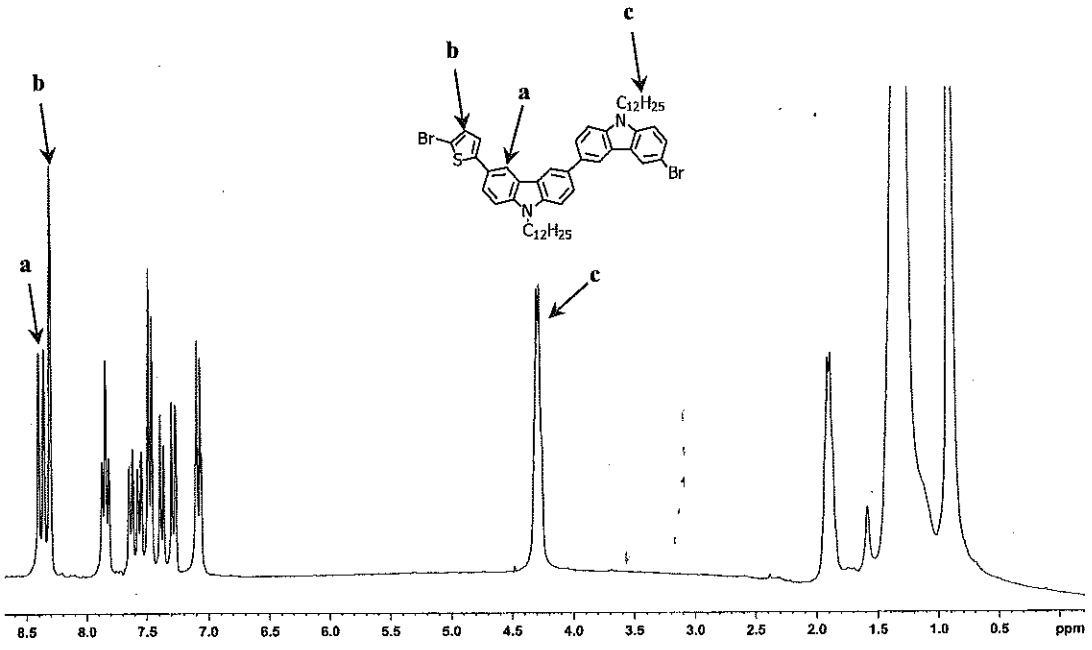

Figure 3.16 H^1-NMR spectrum of bromothiophene(**C_2T1-diBr**) in $CDCl_3$

Bromination reaction of bromothiophene (**C_2T2**) with NBS in THF at room temperature gave dibromo (**C_2T2-diBr**) compound in 61% yield, show in Figure 3.17.

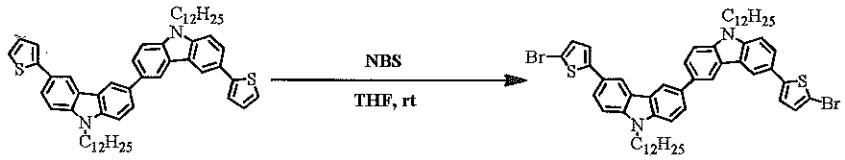

Figure 3.17 Bromination reaction to form dibromo(**C_2T2-diBr**) compound.

The chemical structure of dibromo(**C_2T2-diBr**) was confirmed by ^{1}H-NMR analysis. The ^{1}H-NMR spectrum of dibromo(**C_2T2-diBr**) shows a singlet signal at chemical shift 8.43 ppm (2H)(**a**) assigning as 4-H position of carbazole ring, a singlet signal at chemical shift 8.32 ppm (2H)(**b**) assigning as 2-H position of carbazole ring, a doublet signal at chemical shift 7.86 ppm (2H, J = 7.5 Hz) assigning as 2-H position of thiophene ring, and a triplet signal at chemical shift 4.34 ppm (4H, J = 6.9 Hz) assigning as proton of dodecane, show in Figure 3.18.

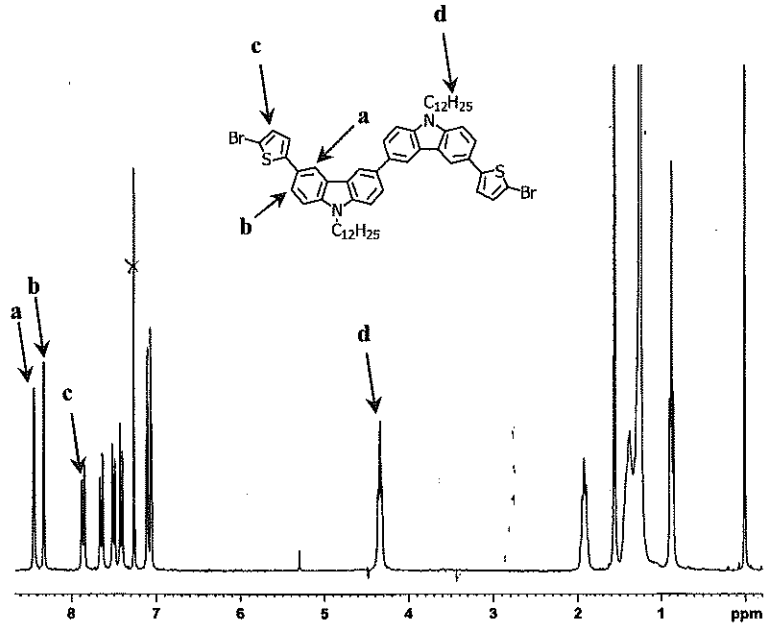

Figure 3.18 H^1-NMR spectrum of bromothiophene(**C_2T2-diBr**) in $CDCl_3$

Ullmann coupling reaction between dibromocarbazole(**C_2T1-diBr**) and *t*-Bu-carbazole(**G1**) were used copper(I) iodide as catalyst, potassium phosphate as base and (±)-*trans*-diaminocyclohexane as co-catalyst in toluene at 170°C under N_2 to give **C_2T1G1** in 26% yield, show in Figure 3.19.

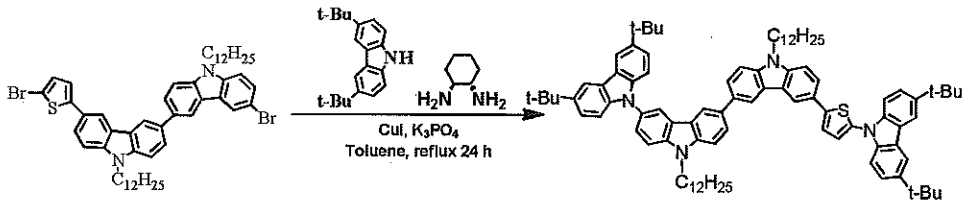

Figure 3.19 Ullmann coupling reaction to form **C_2T1G1** compound.

The chemical structure of dibromo(**C_2T1G1**) was confirmed by ^{1}H-NMR analysis. The ^{1}H-NMR spectrum of dibromo(**C_2T1G1**) shows a singlet signal at chemical shift 8.40 ppm (1H)(**a**) assigning as 5-H position of carbazole with thiophene, a singlet signal at chemical shift 8.35 ppm (1H) assigning as 2-H of carbazole with thiophene, a singlet signal at chemical shift 8.30 ppm (2H)(**b**) assigning as 2-H and 3-H of thiophene and a doublet signal at chemical shift 4.28 ppm (4H, J = 5.1 Hz)(**d**) assigning as proton of dodecane, show in Figure 3.19.

Ullmann coupling reaction between dibromocarbazole(**C_2T2-diBr**) and *t*-Bu-carbazole(**G1**) were used copper(I) iodide as catalyst, potassium phosphate as base and (±)-*trans*-diaminocyclohexane as co-catalyst in toluene at 170°C under N_2 to give **C_2T2G1** in 14% yield, show in Figure 3.20.

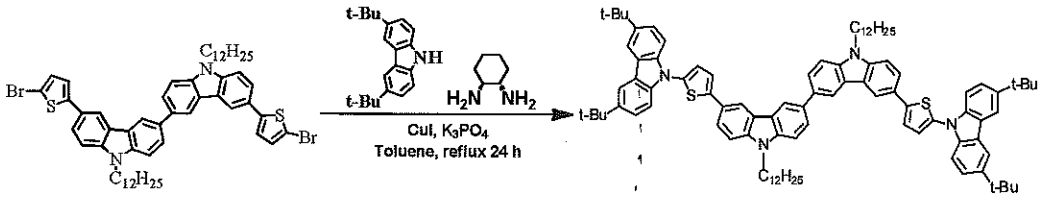

Figure 3.20 Ullmann coupling reaction to form **C_2T2G1** compound.

3.3.2 Synthetic Strategy

The synthetic routes of dicarbazole dendrimers compounds are shown in Schemes 3.1. The target molecules bearing biscarbazole donor, thiophene linker and cyanoacrylic acid or acceptor were synthesized as shown in Scheme 3.1. Alkylation reaction of carbazole with 1-bromododecane using sodium hydride as base gave 9-dodecyl carbazole(**C**) in 95% yield. Oxidative coupling reaction of 9-dodecyl carbazole(**C**) was carried out using $FeCl_3$ as a catalyst in $CHCl_3$ solvent resulting in Bis-9-dodecyl carbazole($\mathbf{C_2}$) in 86% yield. Bromination reaction of Bis-9-dodecyl carbazole($\mathbf{C_2}$) with NBS in THF gave dibromocarbazole(**C_2-diBr**) in 50% yield. Suzuki coupling reaction between dibromocarbazole(**C_2-diBr**) and 2-thiopheneboronic acid was carried out using $Pd(PPh_3)_4$ as catalyst, Na_2CO_3 as a base in THF as a solvent at reflux 24h resulting in the mixture products of dithiophene(**C_2T2**) and bromothiophene (**C_2T1Br**) in 48% and 38% yield, respectively. Treatment of the resulting product with NBS in THF gave dibromination product (**C_2T2-diBr**) and product (**C_2T1-diBr**) in 61%yield and 37%yield respectively. Ullmann coupling reaction between dibromocarbazole(**C_2-diBr**) and *t*-Bu-carbazole(**G1**) gave product **C_2TG1** in 76% yield. Ullmann coupling reaction between dibromocarbazole(**C_2T1-diBr**) and *t*-Bu-carbazole(**G1**) gave product **C_2T1G1** in 26% yield. Ullmann coupling reaction between dibromocarbazole(**C_2T2-diBr**) and *t*-Bu-carbazole(**G1**) gave product **C_2T2G1** in 14% yield.

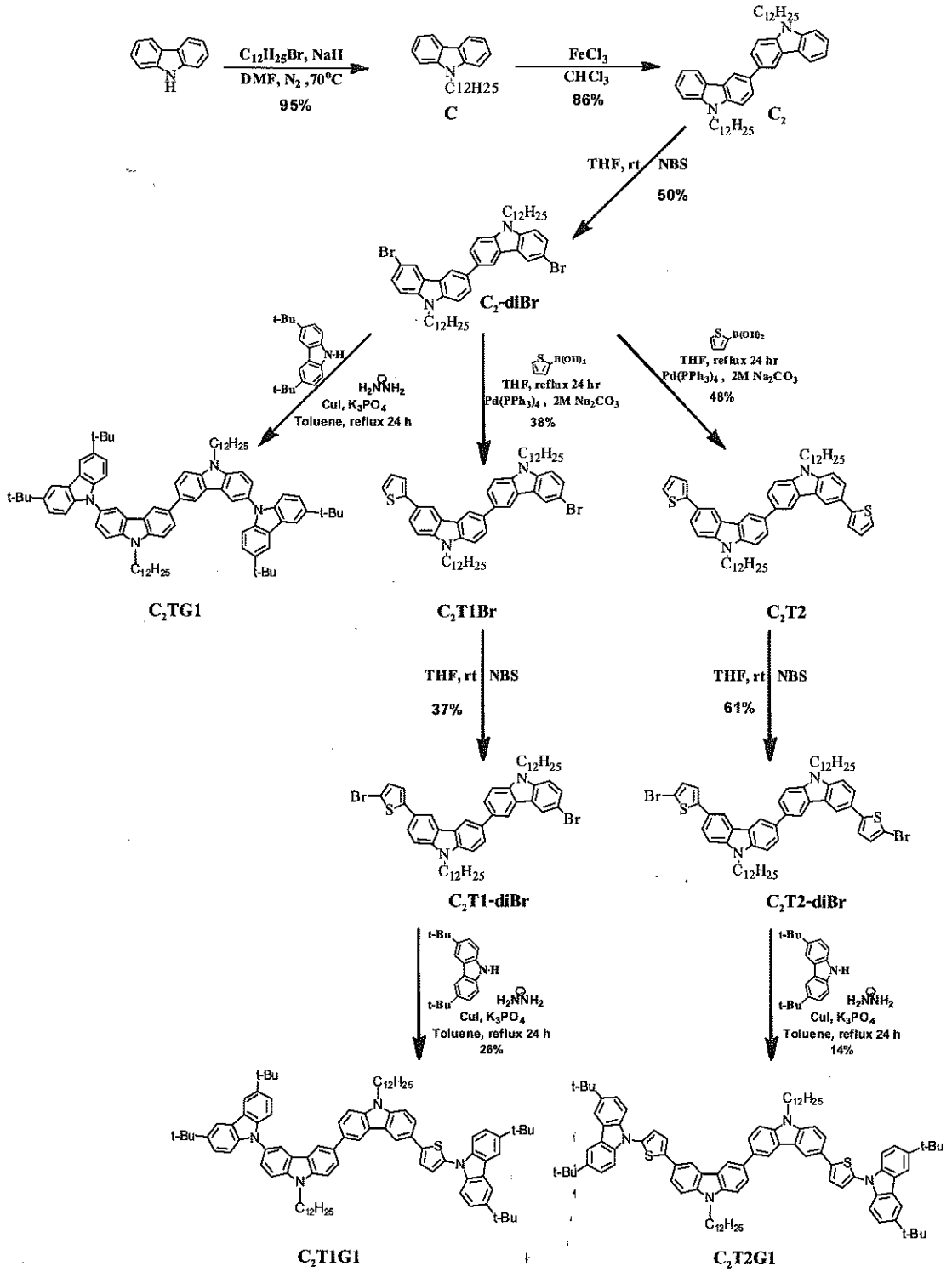

Scheme 3.1 Synthetic route to dicarbazole dendrimers compounds (**C_2TnG1 = 0-2**).

3.3.2 Optical properties

The optical properties of the **C_2TG1**, **C_2T1G1** and **C_2T2G1** dendrimers were investigated by UV-Vis spectroscopy in a dilute solution of CH_2Cl_2 and shown in Figure 3.2.

The absorption spectra of **C_2TG1**, **C_2T1G1** and **C_2T2G1** are dominated by strong absorption bands in the 250-300 nm region and by less intense absorption bands in the 340-450 nm region. The strong absorption band at about 300 nm could be assigned to the π-π^* local electron transition of a carbazole dendron at the terminal ends. While bands of low intensities at λ_{max} 350 nm corresponds to the π-π^* electron transfer of the entire conjugated backbone.

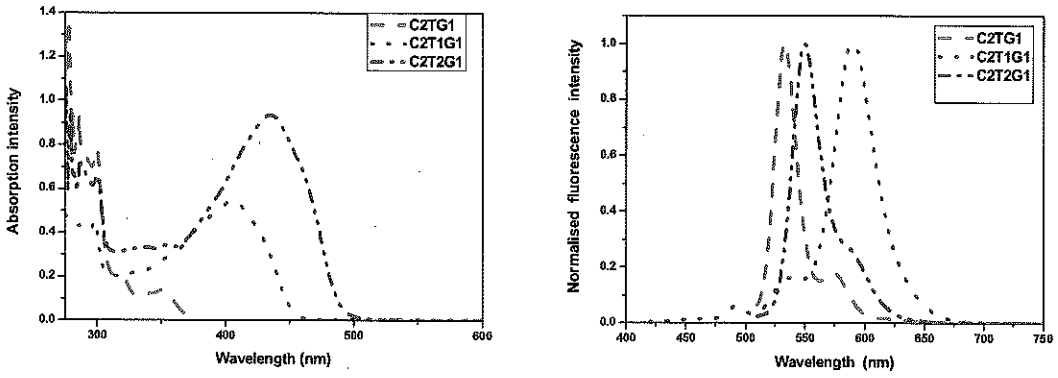

Figure 3.21 Absorption (a) spectra and PL spectra (b) of **C_2TG1**, **C_2T1G1** and **C_2T2G1** in dry CH_2Cl_2 solution.

Table 3.1 The absorption and fluorescence data of **C_2TnG1 (n=0-2)** in dry CH_2Cl_2 solution.

Compound	λmax of absorbance (nm) and ε(10^4 $M^{-1}cm^{-1}$)	λmax of emission (nm)
C_2TG1	298 (1.47), 349 (6.45)	530
C_2T1G1	298 (1.74), 411 (7.31)	548
C_2T2G1	298 (2.01), 438 (7.82)	597

3.4 Conclusions

We have synthesized amorphous hole-transporting dendrimers, **C_2TnG1 (n=0-2)** using a divergent route involving Alkylation reaction, Oxidative coupling reaction, Bromination reaction, Suzuki coupling reaction and Ullmann coupling reactions. The optical properties of the resulting can using materials.

CHAPTER 4

SYNTHESIS AND CHARACTERIZATION OF CARBAZOLE-FLUORENE AND PYRENE DERIVATIVES AS EMITTING MATERIALS FOR OLEDs (PFC, PFCdi-Py, PFCdi-CPy and CFP4)

4.1 Introduction

Since the breakthrough discovery by Tang and van Slyke in organic light emitting diodes (OLEDs), research into OLEDs has been pursued intensively because of their potential use in information displays such as TVs, computer monitors and cellular phones. Developing blue light emitters isessential for the development of full color displays. It is much more difficult to produce blue emission due to the intrinsic characteristic of having a wide bandgap irrespective of the type of materials. Because of their high solution and solid-state photoluminescence (PL) quantum yields, recently much research into blue-emitting materials has centered on fluorene conjugated derivatives. In order to block the interchain interaction and improve the thermal stability, two bulky aryl groups are introduced at C3,6 positions of cerbazole moiety [54]. However, the difference between ionization potential (IP) of conjugated fluorene derivatives (5.6-5.8 eV) and work-function of the indium tin oxide (ITO) (-4.7 eV) requires the use of hole-injection layers to obtain efficient hole-injection,nand the poly(3,4-ethylenedioxythiophene): poly(styrenesulfonate)(PEDOT:PSS) is commonly used as the hole injection materials. But it is not ideal because of its absorption in the visible region and the unstable interface between ITO and PEDOT:PSS. In order to avoid above disadvantages and simplify the OLEDs device, triarylamines was incorporated into the carbazole moiety to improve the hole-injection ability [55, 56].

4.2 Aim of the Study

Inspired by the results, we design and synthesize the following new triphenylamin and pyrene derivatives containing a carbazole core (**PFC, PFCdi-Py, PFCdi-CPy** and **CFP4**) (Figure 4.1). We found that substituents at the C-3, 6 positions of carbazole affect the thermal properties and optical properties, whereas those at the C-9 position mainly affect the thermal properties of the carbazole derivatives. Significantly, by suitable adjustment of the substitutent group in carbazoles, blue-emitting materials with a high thermal stability and high electroluminescence efficiency can be achieved. In this chapter, we report on the synthesis and investigation of a new series of carbazole derivatives and their blue light-emission and hole-transport with additional high thermal stability.

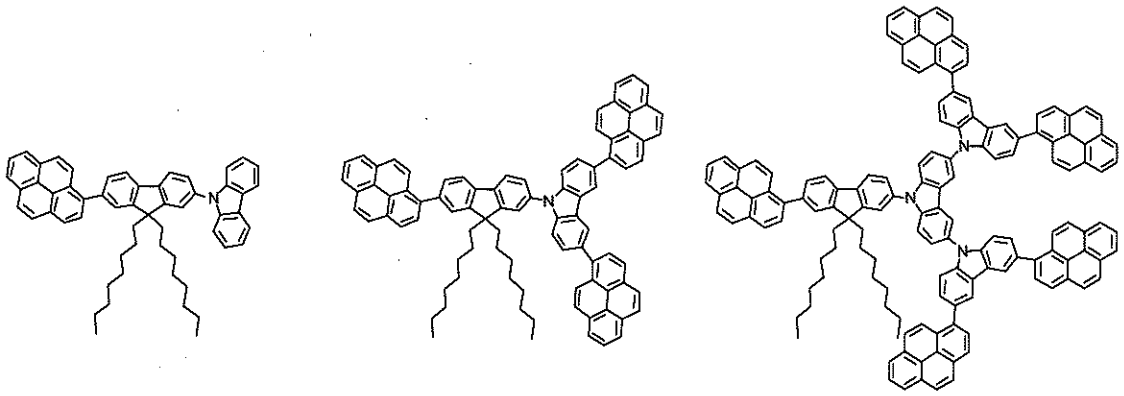

PFC **PFCdi-Py** **PFCdi-CPy**

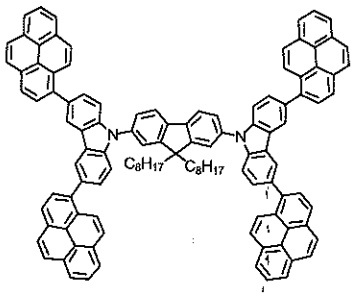

CFP4

Figure 4.1 The target molecules (**PFC, PFCdi-Py**, **PFCdi-CPy** and **CFP4**).

4.3 Results and Discussion

4.3.1 Synthesis

Fluorene was brominated with bromine in chloroform. The most nucleophilic C-7 position of fluorene ring was attacked by Br^+ to provide 2,7-dibromofluorene **(2BrF)** as white solid in 80% yield (Figure 4.2).

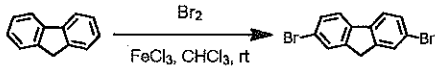

(2BrF)

Figure 4.2 Alkylation reaction to form 2,7-dibromo-9*H*-fluorene (**2BrF**) compound.

The reaction mechanism involved three-steps reaction as described in Figure 3.6. Step 1 bromine reacts with the Lewis acid to form a complex that makes the bromine more electrophillic. Step 2 the π electron of the aromatic C=C acting as a nucleophillic attacks the electrophillic Br following and displacing iron tribromine. This step destroys the aromaticity giving the cyclohexanedienyl cation intermediate. Step 3 removal of the proton from the sp^3-C bearing the bromo group reforms the C=C and the aromatic system, generates HBr and regenerates the active catalyst.

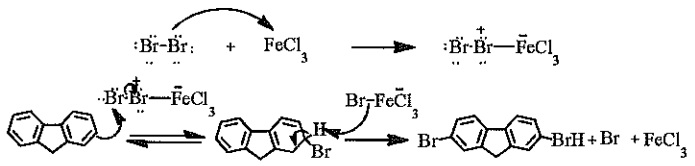

Figure 4.3 The propose mechanism of aromatic electrophilic bromination.

The chemical structure of **2BrF** was confirmed by ^{1}H-NMR analysis. The ^{1}H-NMR of the brominated product shows a singlet signal at chemical shift 7.75 ppm (2H) ppm assigning as 1-H and 8-H position of fluorene ring, doublet signal at chemical shift 7.65 ppm (2H, J = 9.0 Hz) assigning as 4-H and 5-H position of fluorene ring, doublet signal at chemical shift

7.55 ppm (2H, J = 9.0 Hz) assigning as 4-H and 5-H position of fluorene ring and a singlet signal at chemical shift 3.85 ppm (2H) ppm assigning as 9-H position of fluorene ring.

In order to improve a great solubility in organic solvent of final product long alkyl chain of C_8 was intensively attached to C-9 of fluorene ring, moreover with long alkyl chain on fluorene would allows the purification by chromatographic techniques of intermediate compounds formed in each synthetic steps be possible. Alkylation of **2BrF** with bromooctane by using tetrabutylammonium bromide as phase transfer catalyst and 50% sodium hydroxide as base in dimethylsulphoxide under this condition fluorene was formed cabanion by hydroxide ion abstracted the proton at acidic position (C-9 position) and the electrophilic position of alkyl bromide was attacked by nucleophile gave the dialkylated product 2,7-dibromo-9,9-dioctyl-9*H*-fluorene(**2BrAlkyl-F**) in 89% yield.

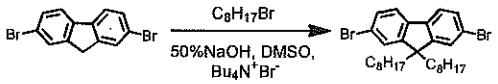

2BrAlkyl-F

Figure 4.4 Bromination reaction to form 2,7-dibromo-9,9-dioctyl-9*H*-fluorene(**2BrAlkyl-F**) compound.

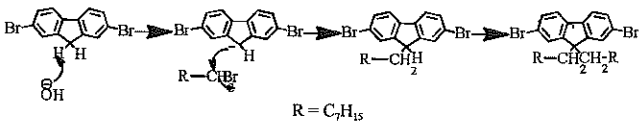

Figure 4.5 The propose mechanism of nucleophilic alkylation.

The chemical structure of **2BrAlkyl-F** was confirmed by ^{1}H-NMR analysis. The ^{1}H-NMR of the brominated product shows multiplet signal at chemical shift 7.50 ppm (6H) ppm assigning as proton of fluorene ring, triplet signal at chemical shift 1.95 ppm (2H, J = 8.4 Hz) assigning as proton of alkyl group.

Ullmann coupling reaction between **2BrAlkyl-F** and carbazole using K_3PO_4 as base, CuI catalyst and used *trans*-diaminocyclohexane as co-catalyst in toluene gave **BrFC** in 89%yield.

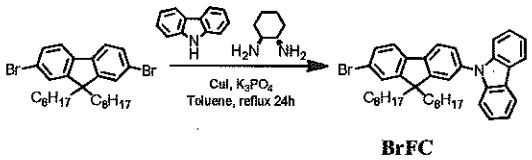

BrFC

Figure 4.6 Ullmann coupling reaction to form 9-(7-bromo-9,9-dioctyl-9*H*-fluoren-2-yl)-9*H*-carbazole**(BrFC)** compound.

The chemical structure of **BrFC** was confirmed by ^{1}H-NMR analysis. The ^{1}H-NMR spectrum of bromofluorene**(BrFC)** shows a doublet signal at chemical shift 8.21 ppm (2H) assigning as 4-H and 5-H position of carbazole ring, and a doublet signal at chemical shift 2.08 ppm (2H)(**b**) and chemical shift 2.02 ppm (2H)(**c**) assigning as methylene proton of fluorene, show in Figure 4.7.

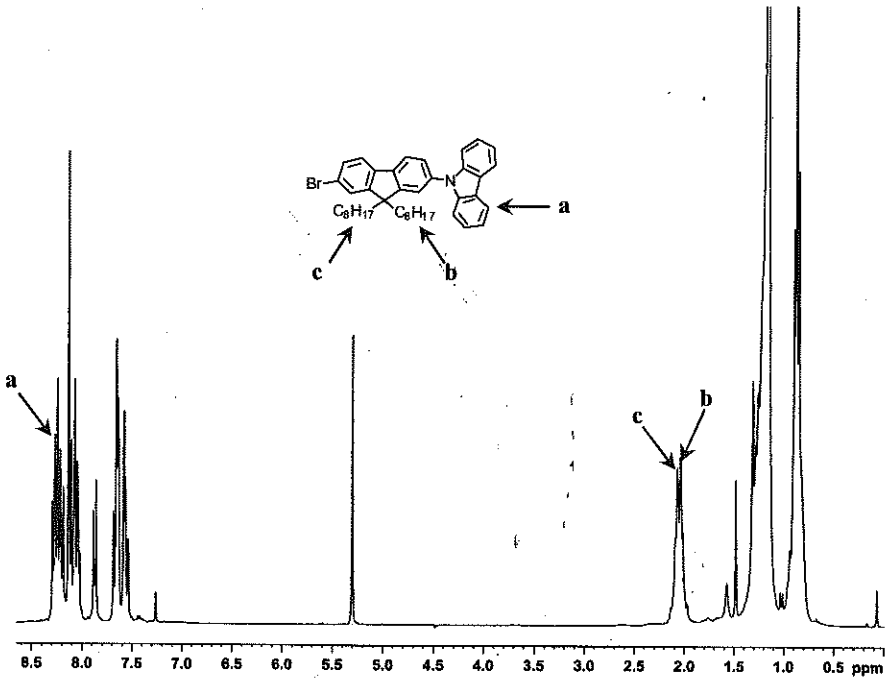

Figure 4.7 H^1-NMR spectrum of 9-(7-bromo-9,9-dioctyl-9*H*-fluoren-2-yl)-9*H*-carbazole**(BrFC)** in $CDCl_3$.

The proposed mechanism of Ullmann coupling reaction is shown in Figure 4.8. The active species is a copper(I)iodide which undergoes oxidative addition with the second equivalent of halide, followed by reductive elimination and the formation of the fluorene-carbazole carbon bond.

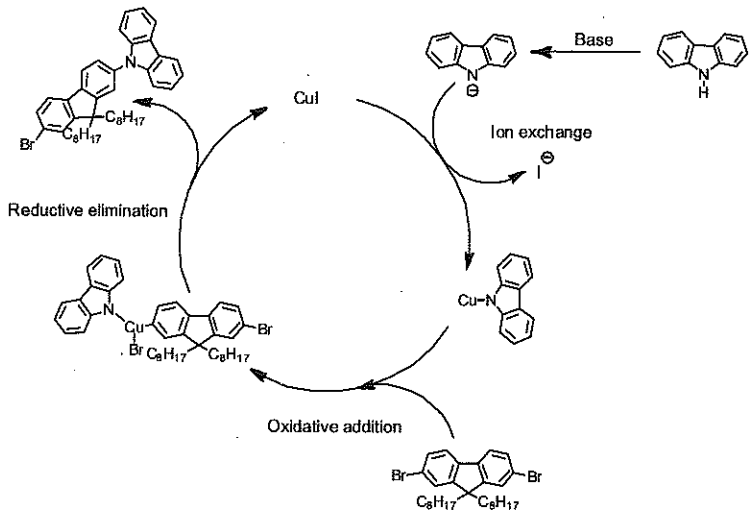

Figure 4.8 The proposed mechanism of Ullmann coupling reaction.

Suzuki coupling reaction of **BrFC** and pyrene broronic acid with $Pd(PPh_3)_4$ as catalyst and Na_2CO_3 as base in THF/H_2O as solvent at reflux for 24 h to gave a green solid of **PFC** in 90%yields.

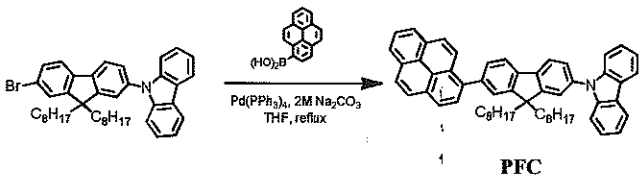

PFC

Figure 4.9 Suzuki cross-coupling reaction to form 9-(9,9-dioctyl-7-(pyren-1-yl)-9*H*-fluoren-2-yl)-9*H*-carbazole(**PFC**) compound.

The chemical structure of **PFC** was confirmed by ^{1}H-NMR analysis. The ^{1}H-NMR spectrum of PFC shows a multiple signal at chemical shift 7.97-8.15 ppm (9H) assigning as H position of fluorene ring and a doublet signal at chemical shift 2.08 ppm (2H)(**b**) and chemical shift 2.02 ppm (2H)(**c**) assigning as methylene proton of fluorene.

The proposed mechanism of Suzuki cross-coupling reaction is shown in Figure 4.10. The Suzuki reaction is the coupling of pyrene boronic acid with fluorene halide using a palladium catalyst to form C-C bond. Thus, base activation of organoboron reagents as boronate intermediates facilitated the transfer of the organic group from boron to palladium (transmetallation). The reaction has later been extended to also include couplings with alkyl groups [57].

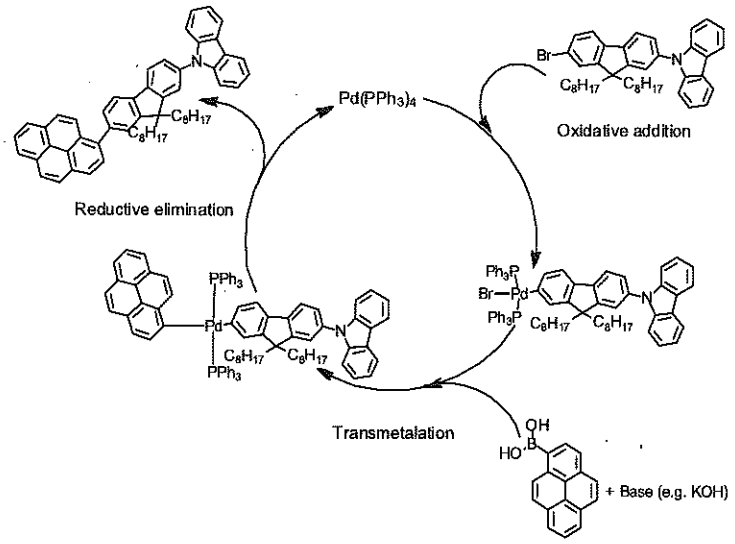

Figure 4.10 The proposed mechanism of Suzuki cross-coupling.

Bromination reaction of **PFC** with NBS in distill tetrahydrofuran as solvent at reflux for 3 h to give a **PFC-2Br** in 90%yield.

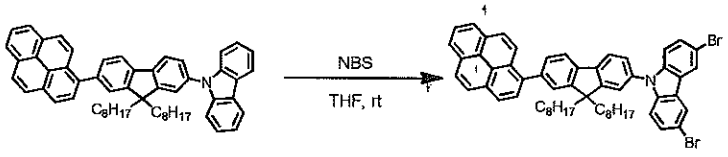

Figure 4.11 Bromination reaction to form 3,6-dibromo-9-(9,9-dioctyl-7-(pyren-1-yl)-9*H*-fluoren -2-yl)-9*H*-carbazole**(PFC-2Br)** compound.

The chemical structure of **PFC-2Br** was confirmed by ^{1}H-NMR analysis. The ^{1}H-NMR spectrum of **PFC-2Br** shows a doublet signal at chemical shift 8.50 ppm (2H, J = 9.5 Hz)(**a**) assigning as 4-H and 5-H position of *t*-Bu carbazole ring, a multiplet signal at chemical shift 7.96-8.14 ppm (9H)(**b**) assigning as proton position of pyrene, a multiple signal at chemical shift 7.31-7.66 ppm (10H) assigning as proton position of fluorene and carbazoe and a doublet signal at chemical shift 2.06 ppm (2H, J = 3.5 Hz)(**c**) assigning as methylene proton of fluorene, show in Figure 4.12.

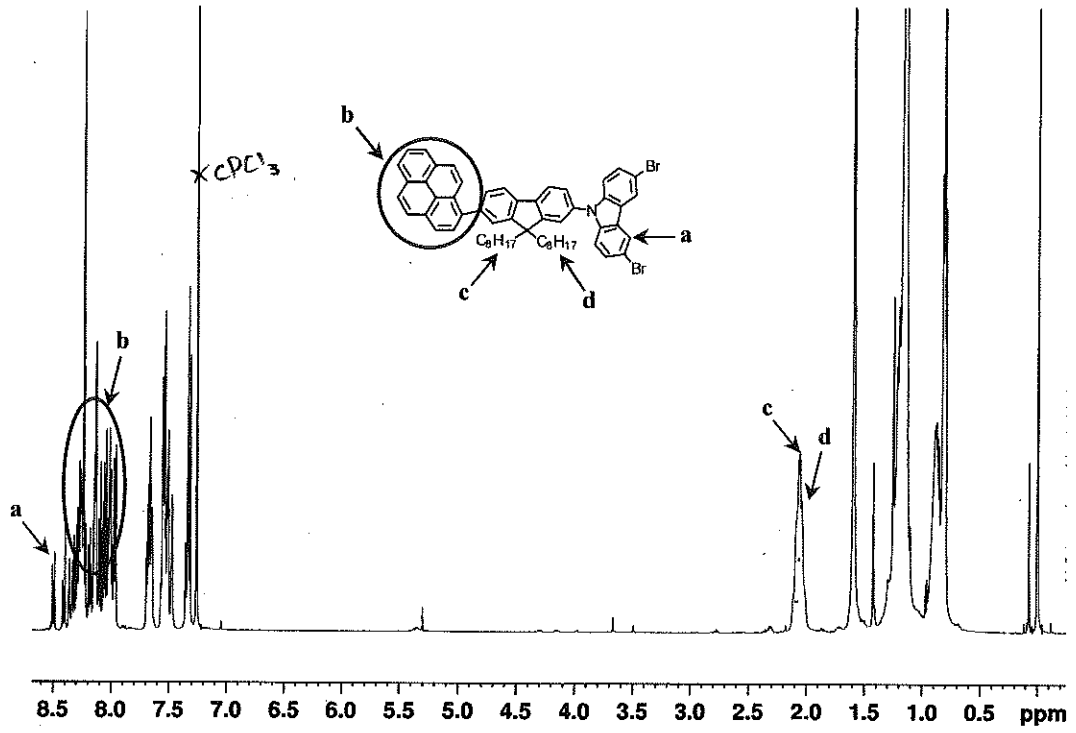

Figure 4.12 H^1-NMR spectrum of 3,6-dibromo-9-(9,9-dioctyl-7-(pyren-1-yl)-9*H*-fluoren-2-yl)-9*H*-carbazole (**PFC-2Br**) in $CDCl_3$.

Suzuki coupling reaction of **PFC-2Br** and pyrene broronic acid with $Pd(PPh_3)_4$ as catalyst and Na_2CO_3 as base in THF/H_2O as solvent at reflux for 24 h to give **PFCdi-Py** in 23% yield.

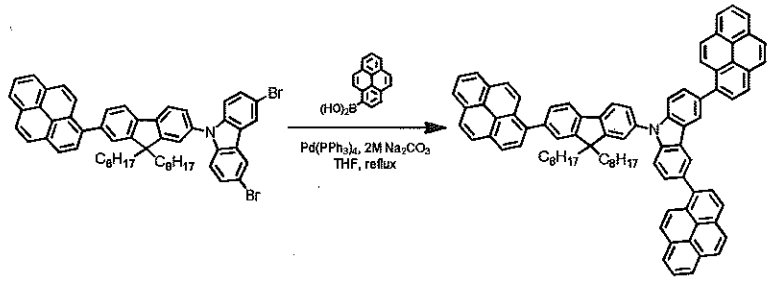

Figure 4.13 Suzuki cross-coupling reaction to form 9-(9,9-dioctyl-7-(pyren-1-yl)-9*H*-fluoren-2-yl)-3,6-di(pyren-1-yl)-9*H*-carbazole **(PFCdi-Py)** compound.

The chemical structure of **PFCdi-Py** was confirmed by ^{1}H-NMR analysis. The ^{1}H-NMR spectrum of **PFCdi-Py** shows a singlet signal at chemical shift 8.51 ppm (2H)(**a**) assigning as 4-H and 5-H position of *t*-Bu carbazole ring, a multiplet signal at chemical shift 7.97-8.25 ppm (27H)(**b**) assigning as proton position of pyrene, a multiple signal at chemical shift 7.23-7.75 ppm (10H) assigning as proton position of fluorene and carbazole and a singlet signal at chemical shift 2.06 ppm (2H)(**c**) and a singlet signal at chemical shift 2.17 ppm (2H)(**d**) assigning as methylene proton of fluorene.

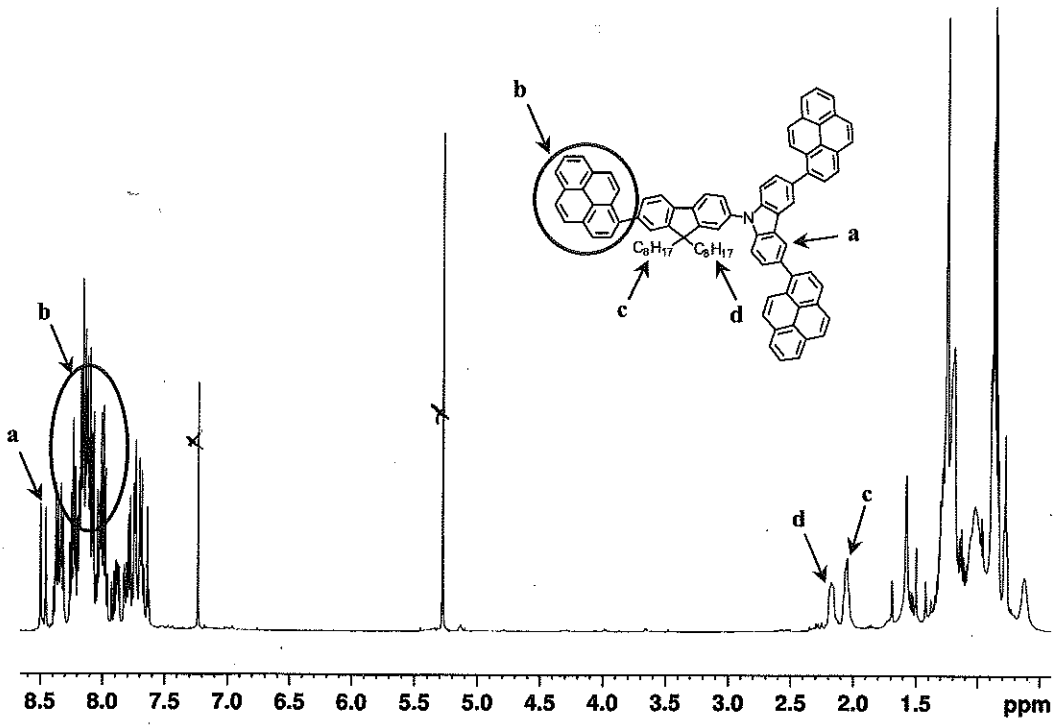

Figure 4.14 H^1-NMR spectrum of 9-(9,9-dioctyl-7-(pyren-1-yl)-9*H*-fluoren-2-yl)-3,6-di(pyren-1-yl)-9*H*-carbazole**(PFCdi-Py)** in $CDCl_3$.

Ullmann coupling reaction between **PFC-2Br** and carbazole(dipyrene) using K_3PO_4 as base, CuI catalyst and used *trans*-diaminocyclohexane as co-catalyst in toluene gave **PFCdi-CPy** in 14% yield.

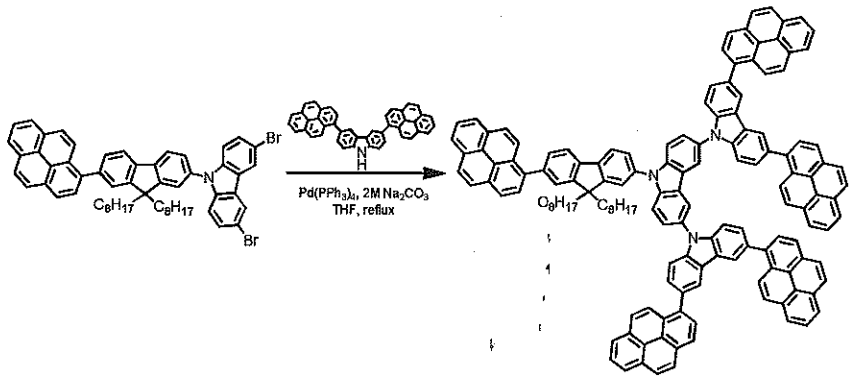

Figure 4.15 Ullmann coupling reaction to form 9'-(9,9-dioctyl-7-(pyren-1-yl)-9*H*-fluoren-2-yl)-3,3",6,6"-tetra(pyren-1-yl)-9'*H*-9,3':6',9"-terbenzo[b]indole **(PFCdi-CPy)** compound.

The chemical structure of **PFCdi-CPy** was confirmed by ^{1}H-NMR analysis. The ^{1}H-NMR spectrum of **PFCdi-CPy** shows a singlet signal at chemical shift 7.7 ppm (2H) assigning as 1-H and 8-H position of fluorene ring, a doublet signal at chemical shift 7.65 ppm (2H, J = 7.45 Hz) assigning as 3-H and 4-H of fluorene adduct and a singlet signal at chemical shift 3.9 ppm (2H) assigning as methylene proton of fluorene.

Ullmann coupling reaction between **2BrAlkyl-F** and carbazole using K_3PO_4 as base, CuI catalyst and used *trans*-diaminocyclohexane as co-catalyst in toluene gave **2CF** in 67%yield.

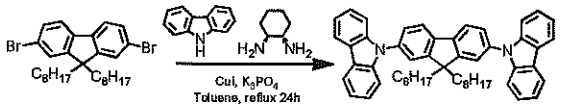

Figure 4.16 Ullmann coupling reaction to form 9,9'-(9,9-dioctyl-9*H*-fluorene-2,7-diyl)bis(9*H*-carbazole)**(2CF)** compound.

The chemical structure of **2CF** was confirmed by ^{1}H-NMR analysis. The ^{1}H-NMR spectrum of **2**CF shows a doublet signal at chemical shift 8.24 ppm (4H d, J = 7.6 Hz) assigning as 4-H and 5-H position of carbazole ring, a singlet signal at chemical shift 8.00 ppm (2H, J = 8.1 Hz) assigning as 3-H and 4-H of fluorene adduct and a multiplet signal at chemical shift 2.02-2.08 ppm (4H) assigning as methylene proton of fluorene.

Bromination of **2CF** with NBS in distill tetrahydrofuran as solvent at reflux for 3 h to give a **4BrCF** in 99%yield.

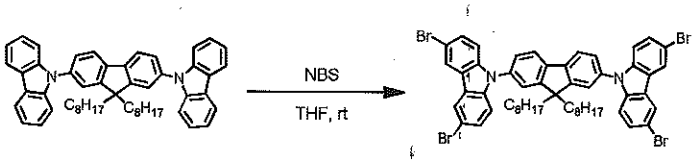

Figure 4.17 Bromination reaction to form 9,9'-(9,9-dioctyl-9*H*-fluorene-2,7-diyl)bis(3,6-dibromo-9*H*-carbazole)**(4BrCF)** compound.

The chemical structure of **4BrCF** was confirmed by ^{1}H-NMR analysis. The ^{1}H-NMR spectrum of product **4BrCF** shows a singlet signal at chemical shift 7.7 ppm (2H) assigning as 1-H and 8-H position of fluorene ring, a doublet signal at chemical shift 7.65 ppm (2H, J = 7.45 Hz) assigning as 3-H and 4-H of fluorene adduct and a triplet signal at chemical shift 2.04 ppm (4H, t, J = 8.1 Hz) assigning as methylene proton of fluorene.

Suzuki coupling reaction of **4BrCF** and pyrene broronic acid with $Pd(PPh_3)_4$ as catalyst and Na_2CO_3 as base in THF as solvent at reflux for 24 h o gave **CFP4** in 11%yield

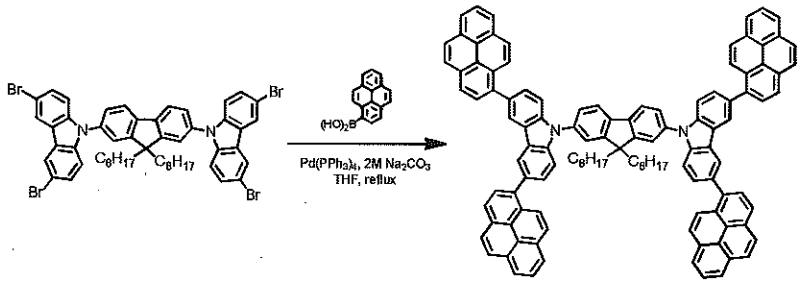

Figure 4.18 Suzuki cross-coupling reaction to form 2,7-Bis[3,6-dipyrenecarbazol-9-yl]-9,9-bis-n-Octylfluorene (**CFP4**) compound.

The chemical structure of **CFP4** was confirmed by ^{1}H-NMR analysis. The ^{1}H-NMR spectrum of product **CFP4** shows a singlet signal at chemical shift 8.52 ppm (4H) assigning as 4-H and 5-H position of carbazole, a multiple signal at chemical shift 8.00-8.23 ppm (36H) assigning as H position of pyrene ring and a singlet signal at chemical shift 2.25 ppm (4H) assigning as methylene proton of fluorene.

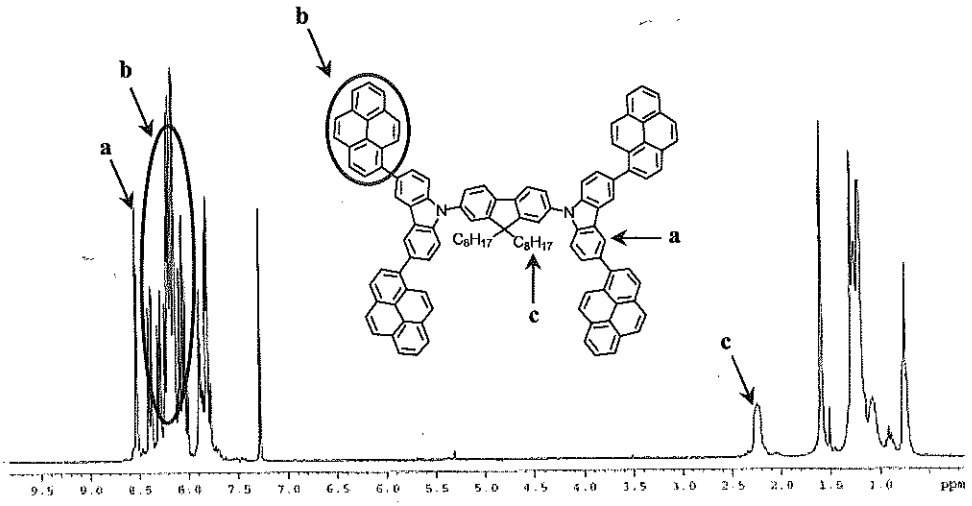

Figure 4.19 ^{1}H-NMR Spectrum of 2,7-Bis[3,6-dipyrenecarbazol-9-yl]-9,9-bis-n-Octylfluorene (**CFP4**).

4.3.2 Synthetic Strategy

The synthetic routes of the pyrene-fluorene-carbazole(**PFC**), dipyrene-substituted carbazole derivatives (**PFCdi-Py**), di(carbazole-dipyrene)-substituted carbazole derivatives (**PFCdi-Py**) and tetrapyrene-substituted carbazole derivatives **CFP4** compound.

The compounds **PFC, PFCdi-Py, PFCdi-CPy** and **CFP4** were synthesized stalic via a divergent approach involving Alkylation, Suzuki coupling, Bromination and Ullmann cross coupling reactions as illustrated in Scheme 4.1. Alkylation of fluorene with 1-bromooctane sodium hydride as base in DMF solvent at roomtemperature for 3 h to give a white solid of **Alkyl-F** in 87% yield. Bromination of **Alkyl-F** with NBS in distill tetrahydrofuran as solvent at reflux for 24 h to give **2BrAlkyl-F** in 95% yield. Ullmann coupling reaction between **2BrAlkyl-F** and carbazole using K_3PO_4 as base, CuI catalyst and used *trans*-diaminocyclohexane as co-catalyst in toluene gave **BrFC** in 89%yield. Suzuki coupling reaction of **BrFC** and pyrene broronic acid with $Pd(PPh_3)_4$ as catalyst and Na_2CO_3 as base in THF/H_2O as solvent at reflux for 24 h to gave a green solid of **PFC** in 90%yields. Bromination of **PFC** with NBS in distill tetrahydrofuran as solvent at reflux for 3 h to give a **PFC-2Br** in 90%yield. Suzuki coupling reaction of **PFC-2Br** and pyrene broronic acid with $Pd(PPh_3)_4$ as catalyst and Na_2CO_3 as base in THF/H_2O as solvent at reflux for 24 h to gave **PFCdi-Py** in 23% yield. Ullmann coupling reaction between **PFC-2Br** and carbazole(dipyrene) using K_3PO_4 as base, CuI catalyst and used *trans*-diaminocyclohexane as co-catalyst in toluene

gave **PFCdi-CPy** in 14% yield. Ullmann coupling reaction between **2BrFAlkyl** and carbazole using K_3PO_4 as base, CuI catalyst and used *trans*-diaminocyclohexane as co-catalyst in toluene gave **2CF** in 67%yield. Bromination of **2CF** with NBS in distill tetrahydrofuran as solvent at reflux for 3 h to give a **2BrCF** in 99%yield. Suzuki coupling reaction of **2BrCF** and pyrene broronic acid with $Pd(PPh_3)_4$ as catalyst and Na_2CO_3 as base in THF/H_2O as solvent at reflux for 24 h to gave **CFP4** in 11%yield, as show in scheme 4.1.

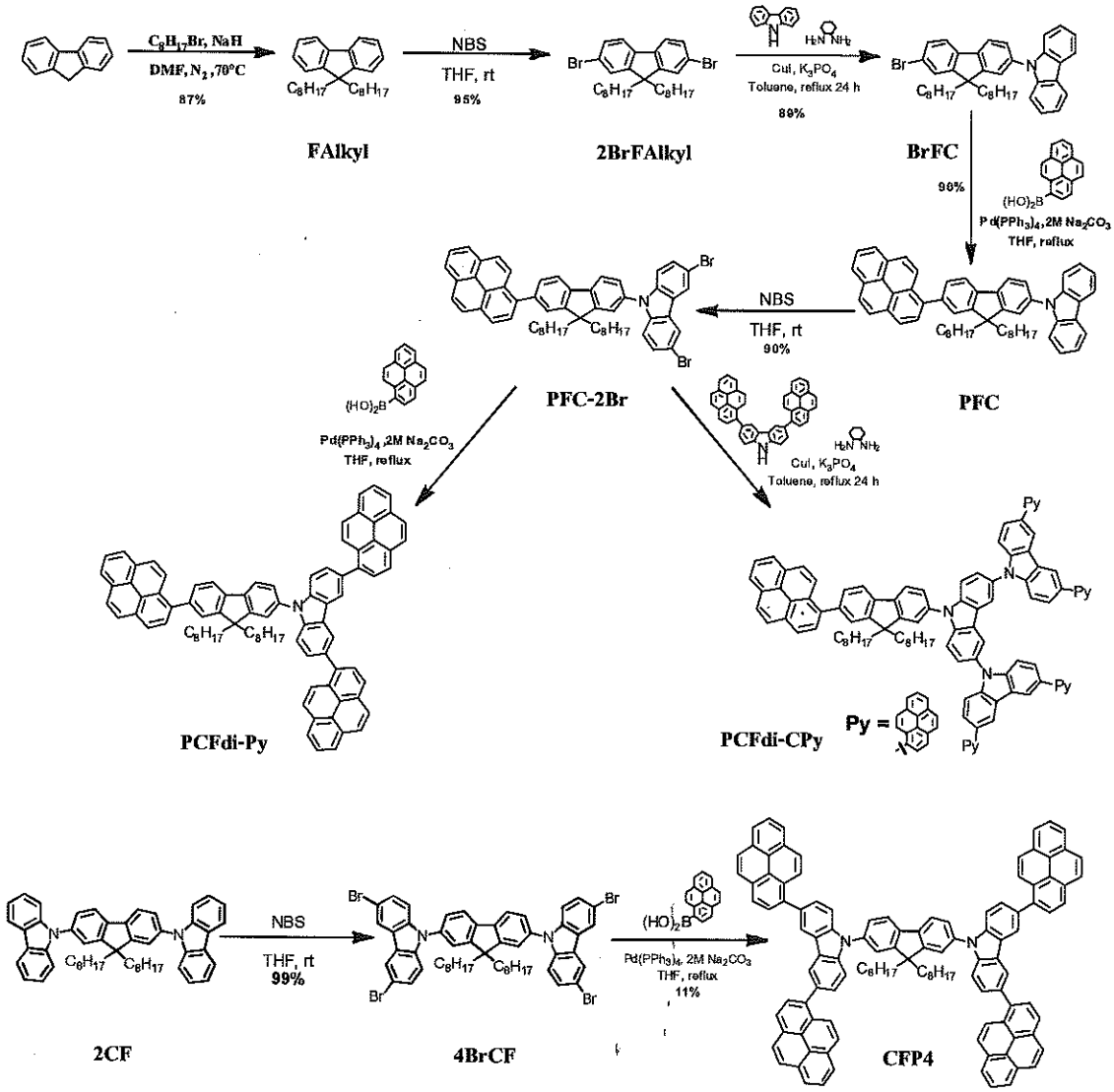

Scheme 4.1 Synthetic route to target molecules (**PFC, PFCdi-Py, PFCdi-CPy** and **CFP4**).

4.3.2 Optical properties

The spectroscopic properties of the four materials were measured in dichloromethane (CH_2Cl_2) solution and the corresponding data were summarized in Table 4.1. In solution absorption spectra. The absorption bands at around 225-275 nm can be attributed to the π-π^* transition of the carbazole moieties and the absorption bands at longer wavelength around 325-400 nm corresponding to the intramolecular charge transfer (ICT) transition between the carbazole and conjugated substituted pyrene backbone (Figure 4.20 (a)).

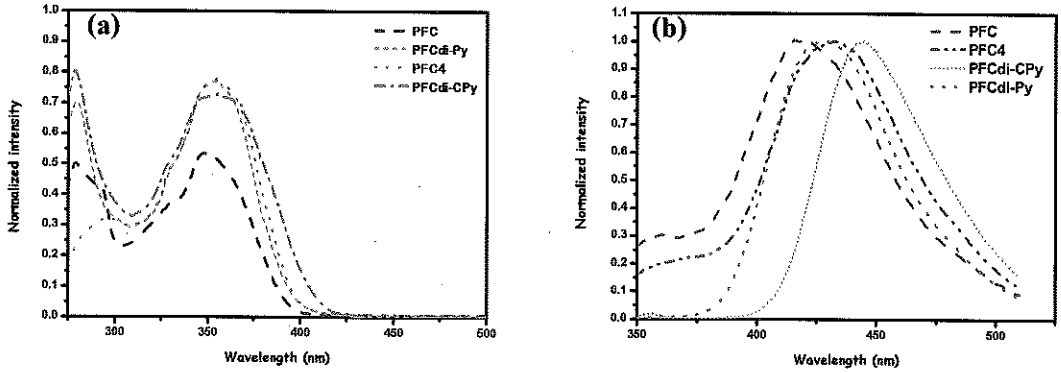

Figure 4.20 (a) Absorption spectra of **PFC, PFCdi-Py, PFCdi-CPy** and **CFP4** and (b) PL spectrum of **PFC, PFCdi-Py, PFCdi-CPy** and **CFP4** in CH_2Cl_2 solution.

The emission spectra display maxima at 420, 427, - and 432 nm, for **PFC, PFCdi-Py, PFCdi-CPy** and **CFP4** respectively. From the substituted pyrene and carbazole(pyrene) to substituted fluorene, the PL spectra also show a gradual red-shift, concomitant with the increasing conjugation length (Figure 4.20 (b)).

Table 4.1 The absorption and fluorescence data of **PFC, PFCdi-Py, PFCdi-CPy** and **CFP4**

Compound	λmax of absorbance (nm) and ε($M^{-1}cm^{-1}$)	λmax of emission (nm)	E_g (eV)
PFC	293 (7.26), 348 (7.34)	420	3.16
PFCdi-Py	297 (7.13), 356 (7.21)	427	3.13
PFCdi-CPy	299 (7.09), 355 (7.17)	444	3.09
CFP4	279 (5.18), 353 (5.22)	432	2.92

4.4 Conclusions

We have synthesized amorphous hole-transporting dendrimers, **PFC, PFCdi-Py, PFCdi-CPy** and **CFP4** using a divergent route involving Bromination, Alkylation, Ullmann and Suzuki coupling reactions. The optical properties of the resulting new materials could be readily controlled by an increased number of pyrene, carbazole(pyrene) dendron units.

CHAPTER 5

SUMMARY

The designed D-D-π-A type organic dyes **CFTAn-A n = 1-3**, **C_2TnG1 = 0-2** and **PFC, PFCdi-Py** and **PFCdi-CPy** composed of three parts: (1) cabarzole donating groups (D); (2) an oligothiophene and oligothiophene-phenylene (π); and (3) an cyanoacrylamide and cyanoacrylic acid anchoring groups (A). They were synthesized using a combination of alkylation, bromination, Ullmann coupling, Suzuki cross-coupling and Knoevenagel condensation reactions. The electronic, electrochemical, and thermal properties of these compounds can be tuned by varying the number of thiophene rings and anchoring group. The electron distribution before the light irradiation (HOMO) is delocalized mainly over carbazole-carbazole donor and oligothiophene; whereas after light irradiation (LUMO) it moves to the acceptor units close to the anchoring groups. These compounds exhibited a high molar absorptivity in the blue/green region of solar light. The number of thiophene increased the conjugation length of compounds resulting a red-shift and broad in absorption solution spectra. The dye **CFTA3-A** should be promising materials for DSCs devices. The target emitting materilals **C_2TnG1 = 0-2** and **PFC, PFCdi-Py** and **PFCdi-CPy** for using as emitting molecules in OLEDs devices were successfully synthesized from bromination, Ullmann coupling and Suzuki cross-coupling condensation reactions. The electronic, electrochemical, and thermal properties of these compounds can be tuned by varying the number of thiophene rings and dendron moieties. The number of thiophene and dendron units increased the conjugation length of compounds resulting a red-shift and broad in absorption solution spectra. All compounds in this study are fluorescent with the color ranging from blue to green. All targets have good electrochemical and thermal stabilities and could be used as emissive layers in OLEDs. The performance of OLEDs using these materials as light-emitting layer is under investigation and will be reported in the future.

CHAPTER 6

EXPERIMENT

6.1 General procedures and instruments

^{1}H-NMR spectra were recorded on Brüker AVANCE (300 MHz) spectrometer. ^{13}C NMR spectra were recorded on Brüker AVANCE (75 MHz) spectrometer and were fully decoupled. Chemical shifts (δ) are reported relative to the residual solvent peak in part per million (ppm). Coupling constants (*J*) are given in Hertz (Hz). Multiplicities are quoted as singlet (s), broad (br), doublet (d), triplet (t), quartet (q), AA′BB′ quartet system (AA′BB′), AB quartet (ABq) and multiplet (m).

The UV-visible spectra were measured in spectrometric grade dichloromethane on a Perkin-Elmer UV Lambda 25 spectrometer. The absorption peaks are reported as in wavelength (nm) (log ε /dm^{3}mol^{-1}cm^{-1}) and sh refers to shoulder. Fluorescence spectra were recorded as a dilute solution in spectroscopic grade dichloromethane on a Perkin-Elmer LS 50B Luminescence Spectrometer.

Dichloromethane was washed with conc. H_2SO_4 and distilled twice from calcium hydride. Tetrahydrofuran (THF) was heated at reflux under nitrogen over sodium wire and benzophenone until the solution became blue and freshly distilled before use. All reagents and solvents were purchased from Aldrich, Acros, Fluka or Thai Supplies and received unless otherwise stated.

Analytical thin-layer chromatography (TLC) was performed with Merck aluminium plates coated with silica gel 60 F_{254}. Column chromatography was carried out using gravity feed chromatography with Merck silica gel mesh, 60 Å. Where solvent mixtures are used, the portions are given by volume.

The electrochemistry was performed using a AUTOLAB spectrometer.
All measurements were made at room temperature on sample dissolved in freshly distilled dichloromethane, 0.1 M tetra-*n*-butylammonium hexafluorophosphate as electrolyte. The solutions were degassed by bubbling with argon. Dichloromethane was washed with concentrated

sulfuric acid and distilled from calcium hydride. A glassy carbon working electrode, platinum wire counter electrode, and a Ag/AgCl/NaCl (Sat.) reference electrode were used.
The ferrocenium/ferrocene couple was used as standard, and the ferrocene was purified by recrystallisation from ethanol and then dried under high vacuum and stored over P_2O_5.

Differential scanning carolimetry (DSC) analysis was performed on a METTLER DSC823e thermal analyzer using a heating rate of 10 °C/min and a cooling rate of 50 °C/min under a nitrogen flow. Samples were scanned from 25 to 350 °C and then rapidly cooled to 25 °C and scanned for the second time at the same heating rate to 350 °C.

Thermogravimetric measurements were carried out using a thermoanalysis apparatus TGA/SDTA851 from Mettler Toledo. Samples for the measurements were prepared by filling alox crucibles. Measurements were performed at a heating rate of 10 °C /min under a nitrogen flow rate of 75 cm^3/min in the temperature range from 25 to 800 °C.

Melting points was measured by BIBBY Stuart Scientific melting point apparatus SMP3 in open capillary method and are uncorrected and reported in degree celsius.

6.2 Synthesis and characterization

Chapter 2

2,7-dibromo-9*H*-fluorene(BrF2)

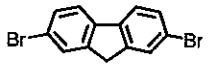

To a solution of fluorine (15 g, 90.24 mmol) in chloroform (100 ml), was cooled to 0 °C then added $FeCl_3$ (80 mg, 0.694 mmol) with stirring Br_2 in chloroform was slowly added the mixture and stirred at room temperature for 3 h. The reaction mixture was poured into water and washed with aqueous sodium thiosulfate solution until red color of bromine disappeared. The organic layer was dried over sodium sulfate anhydrous, filtered and evaporate to dryness. The residue was purified by crystallization by dichloromethane gave **BrF2** as white solid (23 g, 80%); ^{1}H-NMR (300 MHz, $CDCl_3$) δ 7.75 (2H, s), 7.65 (2H, d, J = 9.0 Hz), 7.55 (2H, d, J = 9.0 Hz) and 3.85 (2H, s) ppm.

2,7-dibromo-9,9-dihexyl-9*H*-fluorene(Alkyl-BrF(3))

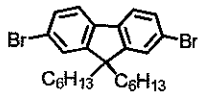

To a mixture of 2,7-dibromofluorene (10g, 30.86 mmol) and tetrabutyl ammonium bromide (1 g, 3 mmol) in DMSO (100 ml) was added an aqueous NaOH solution (50% wt/V, 6 ml) follow by 1-brromohexane (15 ml). After being stirred at room temperature for 3 h, the reaction mixture was extracted with ethyl acetate (100 mlx3). The combined organic phase was washed with water (100 ml), HCl solution (1 M, 50 ml), brine solution (100 ml), dried over sodium sulfate anhydrous, filtered and the organic phase was removed in vacuum. Purification by column chromatography using silica gel eluent with hexane gave **Alkyl-BrF(3)** solid colorless viscous (12.7 g, 86%); ^{1}H-NMR (300 MHz, $CDCl_3$) δ 7.50 (6H, m), 1.95 (4H, t, J = 8.4 Hz), 1.00-1.40 (16H, m) and 0.95 (6H, m) ppm.

3,6-Di-*tert*-butylcarbazole

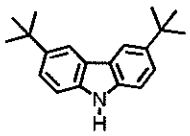

Carbazole (10 g, 59.80 mmol) and $ZnCl_2$ (24.45 g, 179.41 mmol) were dissolved in nitromethane (150 ml), then *tert*–butyl chloride was slowly added to the mixture. The reaction mixture was stirred at room temperature under N_2 for 5 h. The reaction mixture was poured into water and extracted with dichloromethane (100 ml x 3). The combined organic phase was washed with water (100 ml), brine solution (100 ml), dried over sodium sulfate anhydrous, filtered and the solvent was remove in vacuum. The residue was purified by recrystallization with hexane, gave 3,6-di-*tert*-butylcarbazole as white powder (15.370 g, 92%); m.p. 222-224 °C; ^{1}H-NMR (300 MHz, $CDCl_3$) δ 8.09 (2H, s), 7.85 (1H, s), 7.48 (2H, dd, J = 8.5 Hz, J = 1.6 Hz), 7.34 (2H, d, J = 8.5 Hz), and 1.47 (18H, s) ppm; FT-IR (KBr) 3411, 3059, 2959, 2903, 2864, 1628, 1577, 1492, 1466, 880, and 815 cm^{-1}.

9-(7-bromo-9,9-dihexyl-9*H*-fluoren-2-yl)-3,6-di-*tert*-butyl-9*H*-carbazole(CFBr(4))

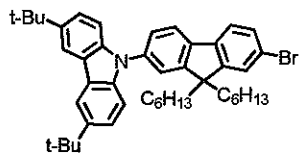

A stirred mixture of 2,7-dibromo-9,9-dihexyl-*9H*-fluorene (21.1294 g, 42.9640 mmol), 3,6-di-*tert*-butyl-*9H*-carbazole (3 g, 10.7365 mmol), copper iodide (1.0224 g, 5.3683 mmol), potassium phosphate (5.6976 g, 26.8413 mmol) and *trans*-diaminocyclohexane (0.6120 g, 5.3683 mmol) in toluene (130 ml) was refluxed for 24 h under N_2 atmosphere. After cooling, the reaction mixture was extracted with dichloromethane (100 ml x 3). The combined organic phase was washed with water (150 ml), brine solution (150 ml), dried over sodium sulfate anhydrous, filtered and the solvent was removed in vacuum. The product was purified by silica gel chromatography to give **CFBr(4)** as yellow viscous (2.0984 g, 72% yield); ^{1}H-NMR (300 MHz, $CDCl_3$) δ 8.36 (2H, s), 8.10 (1H, d, J = 8.1 Hz), 7.88 (2H, d, J = 6.0 Hz), 7.49-7.71 (9H, m) and 2.15 (4H, s) ppm.

3,6-di-*tert*-butyl-9-(9,9-dihexyl-7-(thiophen-2-yl)-9*H*-fluoren-2-yl)-9*H*-carbazole (CFT(5))

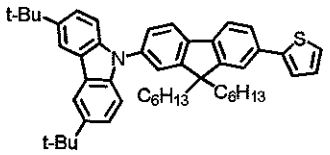

A mixture of 9-(7-bromo-9,9-dihexyl-*9H*-fluoren-2-yl)-3,6-di-*tert*-butyl-*9H*-carbazole (6.0767 g, 8.7962 mmol), $Pd(PPh_3)_4$ (0.3050 g, 0.2639 mmol) and an aqueous Na_2CO_3 solution (2 M, 90 ml) in freshly distilled tetrahydrofuran (100 ml) were added 2-thiophene-broronic acid (1.1256 g, 8.7962 mmol). The mixture was heated at reflux under N_2 atmosphere for 24 h. After the mixture cooled to room temperature water (50 ml) was added. The mixture was extracted with dichloromethane (50 ml x 3). The combined organic layer as washed with water (50 ml), brine solution (50 ml) dried over anhydrous sodium sulfate, filtered and the organic solvent was

removed in vacuum. Purification by column chromatography using silica gel eluting with hexane gave **CFT(5)** as light green viscous (2.220 g, 77%yield; ^{1}H-NMR (300 MHz, $CDCl_3$) δ 8.18 (2H, d, J = 8.7 Hz), 7.91 (2H, d, J = 8.7 Hz), 7.12-7.67 (11H, m) and 2.03 (4H, *t*, J = 5.7 Hz) ppm.

3,6-di-*tert*-butyl-9-(9,9-dihexyl-7-(5-iodothiophen-2-yl)-9*H*-fluoren-2-yl)-9*H*-carbazole(CFTIodo(6))

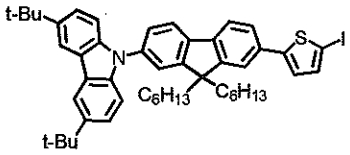

3,6-di-*tert*-butyl-9-(9,9-dihexyl-7-(thiophen-2-yl)-*9H*-fluoren-2-yl)-*9H*-carbazole (4.1915 g, 6.0390 mmol) was added in small portions to a stirred solution of chloroform : acetic acid (1:1) 50 ml, then added *N*-Iodosuccinimide (1.4268 g, 6.3409 mmol) was slowly. After being stirred at room temperature for 60 min, water was added. The mixture was extracted with dichloromethane (50 ml x 3). The combined organic layer was washed with water (50 ml), brine solution (50 ml), dried over anhydrous sodium sulfate, filtered and the solvent was removed in vacuum. Purification by short column chromatography using silica gel eluting with dichloromethane : hexane, 5:95 gave **CFTIodo(6)** as light green solid (0.650 g, 90%yield); ^{1}H-NMR (300 MHz, $CDCl_3$) δ 8.33 (2H, s), 7.94 (1H, *t*, J = 7.8 Hz), 7.14-7.82 (11H, m) and 2.14 (4H, d, J = 4.5 Hz) ppm.

***N*-(4-bromophenyl)-5-(7-(3,6-di-*tert*-butyl-9*H*-carbazol-9-yl)-9,9-dihexyl-9*H*-fluoren-2-yl)-*N*-(5-(7-(3,6-di-*tert*-butyl-9*H*-carbazol-9-yl)-9,9-dihexyl-9*H*-fluoren-2-yl)thiophen-2-yl)thiophen-2-amine(CFTA(7))**

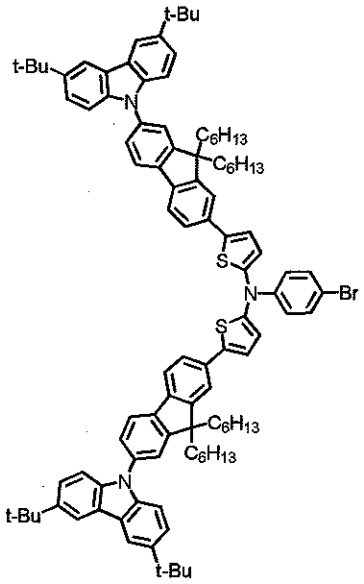

A mixture of 3,6-di-*tert*-butyl-9-(9,9-dihexyl-7-(5-iodothiophen-2-yl)-9*H*-fluoren-2-yl)-9*H*-carbazole (3.8253 g, 4.6652 mmol), 4-bromoaniline (0.3230 g, 1.8781 mmol), *tran*-diaminocyclohaxane(0.2144 g, 1.8781 mmol), K_3PO_4 (1.9935 g, 9.3905 mmol) and CuI (0.3577 g, 1.8781 mmol) in toluene (180 ml). The reaction mixture was stirred at reflux under N_2 atmosphere for 24 h. Water (100 ml) was added and the mixture was extracted with dichloromethane (50 ml x 3). The organic layer was separated and dried in Na_2SO_4. The solvent was removed in vacuum. The pure product was purified by column chromatography over silica gel eluting with hexane and dichloromethane ratio 9 : 1 gave **CFTA(7)** as a green solid (1.7214g, 45% yield); ^{1}H-NMR (300 MHz, $CDCl_3$) δ 8.20 (4H, s), 7.15-7.90 (28H, m) and 2.05 (8H, *t*, *J* = 7.9 Hz) ppm.

5-(4-(bis(5-(7-(3,6-di-*tert*-butyl-9*H*-carbazol-9-yl)-9,9-dihexyl-9*H*-fluoren-2-yl)thiophen-2-yl)amino)phenyl)thiophene-2-carbaldehyde(CFTA-T-aldehyde(7a))

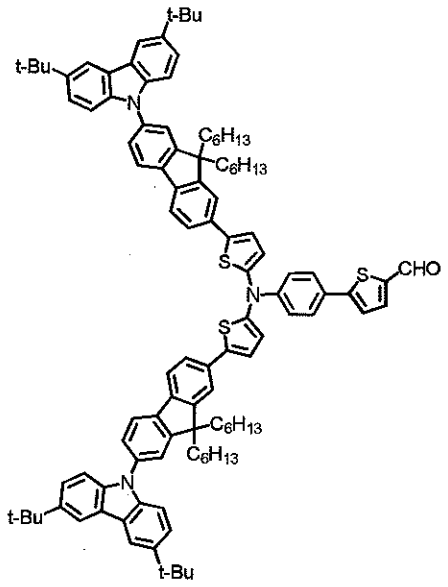

To a stirred solution of *N*-(4-bromophenyl)-5-(7-(3,6-di-*tert*-butyl-9*H*-carbazol-9-yl)-9,9-dihexyl-9*H*-fluoren-2-yl)-*N*-(5-(7-(3,6-di-*tert*-butyl-9*H*-carbazol-9-yl)-9,9-dihexyl-9*H*-fluoren-2-yl)thiophen-2-yl)thiophen-2-amine (0.5000 g, 0.3213 mmol) and $Pd(PPh_3)_4$ (0.0111 g, 0.0096 mmol) in freshly distilled tetrahydrofuran (40 ml) were added 5-formylthiophene-boronic acid (0.0500 g, 0.3213 mmol), and an aqueous Na_2CO_3 solution (2 M, 29 ml). The mixture was stirred at reflux under N_2 atmosphere for 24 h. After cooling the solution, water (50 ml x 3) was added to the solution and extracted by dichloromethane (50 ml x 3). The organic layer was separated and dried in Na_2SO_4. The solvent was removed in vacuum. The pure product was purified by silica gel chromatography using a mixture of hexane and dichloromethane (8:2) to give **CFTA-T-aldehyde(7a)** as orange solids (0.3400 g, 68% yield); m.p. 150-151 °C; ^{1}H-NMR (300 MHz, $CDCl_3$) δ 9.89 (1H, s), 8.17 (4H, d, J = 1.2 Hz), 7.26-7.91 (31H, m) and 2.03 (8H, dd, J = 10.0 Hz) ppm; FT-IR (KBr) 3053, 2952, 2926, 2862, 2364, 1737, 1665, 1610, 1492, 1451, 1364, 1325, 1295, 1263, 1228, 1049, 875, and 808 cm^{-1}.

(*E*)-3-(5-(4-(bis(5-(7-(3,6-di-*tert*-butyl-9*H*-carbazol-9-yl)-9,9-dihexyl-9*H*-fluoren-2-yl)thiophen-2-yl)amino)phenyl)thiophen-2-yl)-2-cyanoacrylic acid(CFTAT1-A)

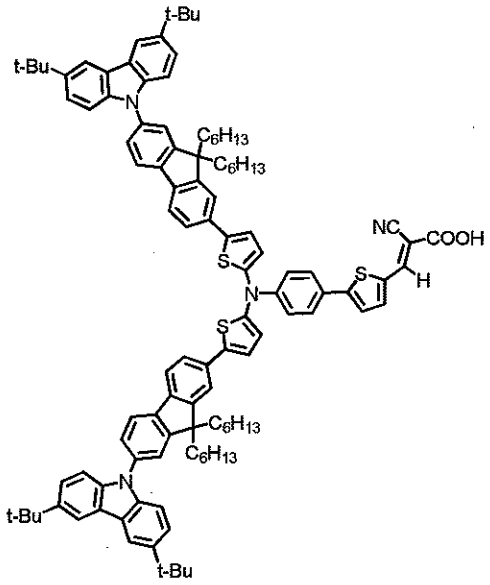

A mixture of 5-(4-(bis(5-(7-(3,6-di-*tert*-butyl-9*H*-carbazol-9-yl)-9,9-dihexyl-9*H*-fluoren-2-yl)thiophen-2-yl)amino)phenyl)thiophene-2-carbaldehyde (0.1629 g, 0.1026 mmol) and cyanoacetic acid (0.0873 g, 1.0263 mmol) and piperidine (0.0131 g, 0.1539 mmol) in chloroform (25 ml). The solution was refluxed 24h. After cooling the solution, water (50 ml x 3) was added to the solution and extracted by dichloromethane (50 ml x 3). The organic layer was separated and dried in Na_2SO_4. The solvent was removed in vacuum. The pure product was purified by silica gel chromatography using a mixture of hexane and dichloromethane (1:2) gave **CFTAT1-A** as a red solids (0.1414 g, 97% yield); m.p. 153-154 ^{o}C; ^{1}H-NMR (300 MHz, $CDCl_3$) δ 8.19 (6H, *t*, *J* = 6.0 Hz), 7.24-7.90 (32H, m) and 3.24 (8H, s) ppm; FT-IR (KBr) 3333, 3064, 2952, 2925, 2854, 2359, 1736, 1727, 1658, 1641, 1461, 1451, 1366, 1261, 1114, 1020, 951, 809, 760 and 668 cm^{-1}.

5-(7-(3,6-di-*tert*-butyl-9*H*-carbazol-9-yl)-9,9-dihexyl-9*H*-fluoren-2-yl)-*N*-(5-(7-(3,6-di-*tert*-butyl-9*H*-carbazol-9-yl)-9,9-dihexyl-9*H*-fluoren-2-yl)thiophen-2-yl)-*N*-(4-(thiophen-2-yl)phenyl)thiophen-2-amine(CFTAT(8a))

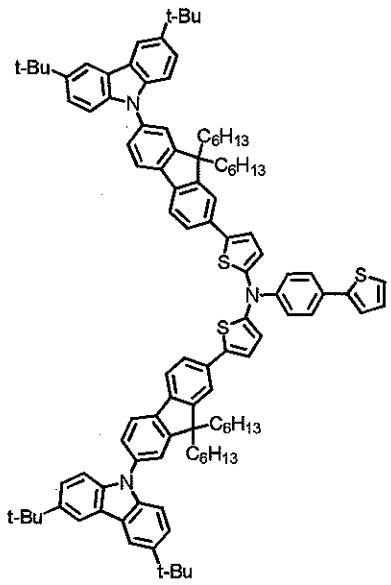

To a stirred solution of *N*-(4-bromophenyl)-5-(7-(3,6-di-*tert*-butyl-9*H*-carbazol-9-yl)-9,9-dihexyl-9*H*-fluoren-2-yl)-*N*-(5-(7-(3,6-di-*tert*-butyl-9*H*-carbazol-9-yl)-9,9-dihexyl-9*H*-fluoren-2-yl)thiophen-2-yl)thiophen-2-amine (1.1040 g, 0.6617 mmol) and $Pd(PPh_3)_4$ (0.0229 g, 0.0198 mmol) in freshly distilled tetrahydrofuran (25 ml) were added 2-thiophene-broronic acid (0.0931 g, 0.7279 mmol), and an aqueous Na_2CO_3 solution (2 M, 14 ml). The mixture was stirred at reflux under N_2 atmosphere for 24 h. After cooling the solution, water (50 ml x 3) was added to the solution and extracted by dichloromethane (50 ml x 3). The organic layer was separated and dried in Na_2SO_4. The solvent was removed in vacuum. The pure product was purified by silica gel chromatography using a mixture of hexane and dichloromethane (8:2) gave **CFTAT(8a)** as green solids (0.7400 g, 67% yield); m.p. 149.5-150 °C; ^{1}H-NMR (300 MHz, $CDCl_3$) δ 8.21 (4H, s), 7.05-7.91 (35H, m) and 2.06 (8H, m) ppm; FT-IR (KBr) 3042, 2956, 2924, 2857, 2360, 1611, 1491, 1365, 1324, 1295, 1263, 1034 and 810 cm^{-1}.

_N_-(4-(5-bromothiophen-2-yl)phenyl)-5-(7-(3,6-di-*tert*-butyl-9*H*-carbazol-9-yl)-9,9-dihexyl-9*H*-fluoren-2-yl)-_N_-(5-(7-(3,6-di-*tert*-butyl-9*H*-carbazol-9-yl)-9,9-dihexyl-9*H*-fluoren-2-yl)thiophen-2-yl)thiophen-2-amine(CFTATBr(9a))

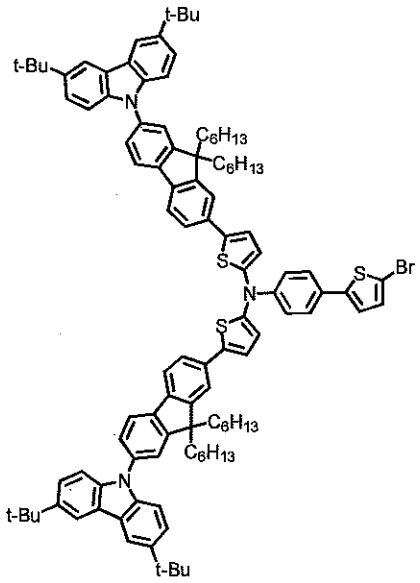

To a stirred solution of 5-(7-(3,6-di-*tert*-butyl-9*H*-carbazol-9-yl)-9,9-dihexyl-9*H*-fluoren-2-yl)-*N*-(5-(7-(3,6-di-*tert*-butyl-9*H*-carbazol-9-yl)-9,9-dihexyl-9*H*-fluoren-2-yl)thiophen-2-yl)-*N*-(4-(thiophen-2-yl)phenyl)thiophen-2-amine (0.7400 g, 0.4427 mmol) was added in small portions in distilled tetrahydrofuran solution (15ml) at room temperature. After that, *N*-Bromosuccinimide (0.0867 g, 0.4870 mmol) was slowly added in mixture solution. After being stirred for 3 h, water (50 ml) was added and the mixture was extracted with dichloromethane (50 ml x 3). The organic layer was separated, dried over anhydrous sodium sulphate, filtered and dried to remove the solvents in vacuum. Purification by column chromatographyl over silica gel eluting with a mixture of hexane and dichloromethane (8:2) followed by recrystallization with a mixture of dichloromethane and methanol afforded green solid (0.6414 g, 86% yield); ^{1}H-NMR (300 MHz, $CDCl_3$) δ 9.89 (1H, s), 8.17 (4H, d, J = 1.20 Hz), 7.26-7.91 (31H, m) and 2.03 (8H, dd, J = 10.05 Hz) ppm; FT-IR (KBr) 3044, 2956, 2927, 2858, 2361, 1611, 1584, 1475, 1365, 1325, 1295, 1263, 1235, 1034, 878, and 810 cm^{-1}.

5'-(4-(bis(5-(7-(3,6-di-*tert*-butyl-9*H*-carbazol-9-yl)-9,9-dihexyl-9*H*-fluoren-2-yl) thiophen-2-yl)amino)phenyl)-[2,2'-bithiophene]-5-carbaldehyde(CFTAT2-aldehyde(10a))

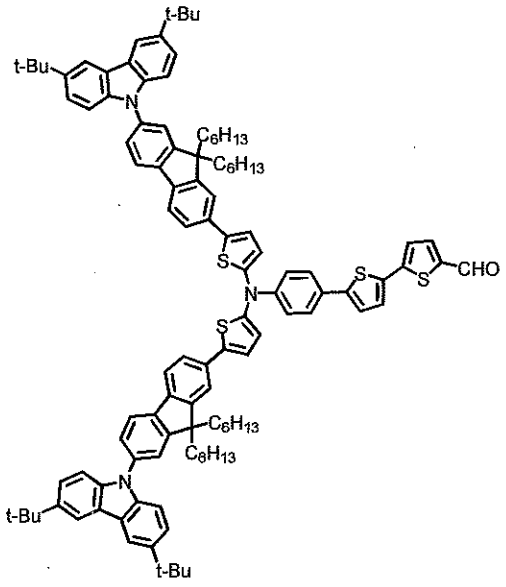

A mixture of 4-bromo thiophen-2-amine compound (0.6289 g, 0.3839 mmol), $Pd(PPh_3)_4$ (0.0133 g, 0.0115 mmol), 5-formylthiophene-boronic acid (0.0599 g, 0.3839 mmol), an aqueous Na_2CO_3 solution (2 M, 15 ml) in freshly distilled tetrahydrofuran (20 ml) was stirred at reflux under N_2 atmosphere for 24 h. After cooling the solution, water (50 ml) was added to the mixture and extracted by dichloromethane (50 ml x 3). The organic layer was separated and dried in Na_2SO_4. The solvent was removed in vacuum. The pure product was purified by column chromatography over silica gel eluting with hexane and dichloromethane ratio 6 : 4 to give **CFTAT2-aldehyde(10a)** as an eluent a orange solids (0.6163g, 98% yield); m.p. 162-162.5 °C; ^{1}H-NMR (300 MHz, $CDCl_3$) δ 9.89 (1H, s), 8.17 (4H, d, J = 1.2 Hz), 7.26-7.91 (31H, m) and 2.03 (8H, dd, J = 10.0 Hz) ppm.

(*E*)-3-(5'-(4-(bis(5-(7-(3,6-di-*tert*-butyl-9*H*-carbazol-9-yl)-9,9-dihexyl-9*H*-fluoren-2-yl)thiophen-2-yl)amino)phenyl)-[2,2'-bithiophen]-5-yl)-2-cyanoacrylic acid(CFTAT2-A)

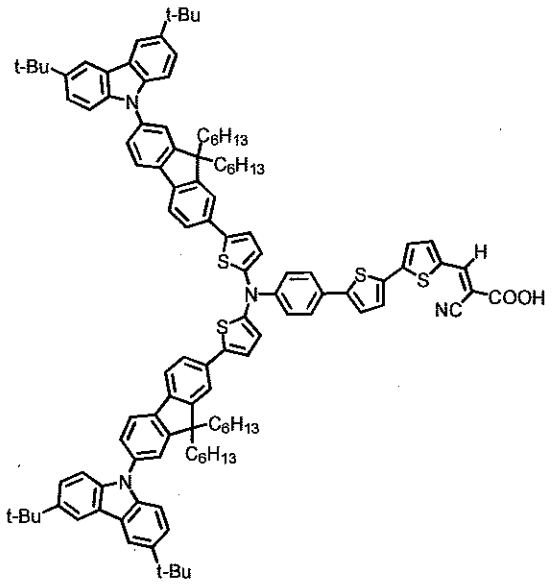

A mixture of 5'-(4-(bis(5-(7-(3,6-di-*tert*-butyl-9*H*-carbazol-9-yl)-9,9-dihexyl-9*H*-fluoren-2-yl)thiophen-2-yl)amino)phenyl)-[2,2'-bithiophene]-5-carbaldehyde (0.2021 g, 0.1211 mmol) and cyanoacetic acid (0.1030 g, 1.2110 mmol) and piperidine (0.0516 g, 0.6055 mmol) in chloroform (15 ml). The solution was refluxed 24h. After cooling the solution, water (50 ml x 3) was added to the solution and extracted by dichloromethane (50 ml x 3). The organic layer was separated and dried in Na_2SO_4. The solvent was removed in vacuum. The pure product was purified by silica gel chromatography using a mixture of hexane and dichloromethane (1:1) to give **CFTAT2-A** as a red solids (0.1960g, 97% yield); m.p. 160-161 °C; ^{1}H-NMR (300 MHz, $CDCl_3$) δ 8.19 (6H, *t*, *J* = 6.0 Hz), 7.24-7.90 (32H, m) and 3.24 (8H, s) ppm. ^{13}C NMR (300 MHz, $CDCl_3$): 152.71, 151.99, 146.05, 144.25, 142.86, 140.65, 139.31, 139.21, 137.18, 136.35, 135.22, 132.59, 126.55, 125.44, 124.92, 124.06, 123.80, 123.58, 123.40, 121.40, 120.87, 120.33, 120.00, 116.32, 109.22, 55.53, 44.43, 40.35, 34.75, 32.03, 31.54, 29.70, 29.65, 23.91, 22.75, 22.59 and 14.03. FT-IR (KBr) 3411, 3042, 2956, 2928, 2857, 2364, 2208, 1726, 1613, 1584, 1477, 1453, 1348, 1295, 1263, 1237, 1079, 878, 809, 741 and 615 cm^{-1}.

***N*-(4-([2,2'-bithiophen]-5-yl)phenyl)-5-(7-(3,6-di-*tert*-butyl-9*H*-carbazol-9-yl)-9,9-dihexyl-9*H*-fluoren-2-yl)-*N*-(5-(7-(3,6-di-*tert*-butyl-9*H*-carbazol-9-yl)-9,9-dihexyl-9*H*-fluoren-2-yl)thiophen-2-yl)thiophen-2-amine(CFTAT2 (8b))**

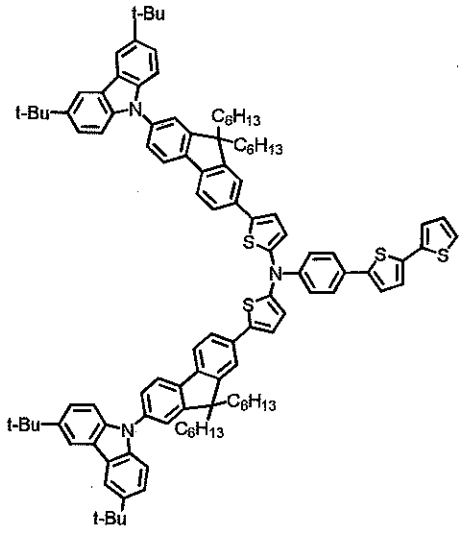

To a stirred solution of *N*-(4-(5-bromothiophen-2-yl)phenyl)-5-(7-(3,6-di-*tert*-butyl-9*H*-carbazol-9-yl)-9,9-dihexyl-9*H*-fluoren-2-yl)-*N*-(5-(7-(3,6-di-*tert*-butyl-9*H*-carbazol-9-yl)-9,9-dihexyl-9*H*-fluoren-2-yl)thiophen-2-yl)thiophen-2-amine (0.6414 g, 0.3915 mmol) and $Pd(PPh_3)_4$ (0.0136 g, 0.03 mmol) in freshly distilled tetrahydrofuran (35 ml) were added 2-thiophene-broronic acid (0.0551 g, 0.4307 mmol) and an aqueous Na_2CO_3 solution (2M, 30 mmol).

The mixture was refluxed for 24 h. After cooling the solution, water (50 ml x 3) was added to the solution and extracted by dichloromethane (50 ml x 3). The organic layer was separated and dried in Na_2SO_4. The solvent was removed in vacuum. The pure product was purified by silica gel chromatography using a mixture of hexane and dichloromethane (8:2) to give **CFTAT2 (8b)** as a dark green solids (0.5773g, 90% yield). ^{1}H-NMR (300 MHz, $CDCl_3$) δ 9.89 (1H, s), 8.17 (4H, d, J = 1.20 Hz), 7.26-7.91 (31H, m) and 2.03 (8H, dd, J = 10.05 Hz) ppm. ^{13}C NMR (300 MHz, $CDCl_3$): 152.68, 151.91, 143.81, 142.86, 140.16, 139.41, 139.39, 137.04, 136.57, 133.12, 127.2, 125.45, 124.81, 124.70, 124.40, 123.67, 123.62, 123.43, 121.44, 120.78, 120.28, 119.90, 116.35, 109.28, 55.53, 40.40, 34.79, 32.08, 31.58, 29.70, 23.94, 22.63 and 14.08. FT-IR (KBr) 3068, 2956, 2928, 2903, 2857, 2361, 1610, 1584, 1478, 1454, 1364, 1325, 1295, 1263, 1235, 1034, 878 and 810 cm^{-1}.

_N_-(4-(5'-bromo-[2,2'-bithiophen]-5-yl)phenyl)-5-(7-(3,6-di-*tert*-butyl-9*H*-carbazol-9-yl)-9,9-dihexyl-9*H*-fluoren-2-yl)-_N_-(5-(7-(3,6-di-*tert*-butyl-9*H*-carbazol-9-yl)-9,9-dihexyl-9*H*-fluoren-2-yl)thiophen-2-yl)thiophen-2-amine(CFTAdi-TBr(9b))

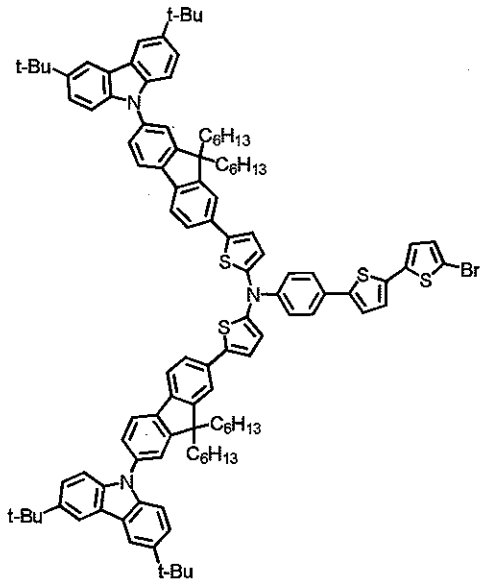

_N_-Bromosuccinimide (0.0678 g, 0.3812 mmol) was added in small portions to a solution of _N_-(4-([2,2'-bithiophen]-5-yl)phenyl)-5-(7-(3,6-di-*tert*-butyl-9*H*-carbazol-9-yl)-9,9-dihexyl-9*H*-fluoren-2-yl)-_N_-(5-(7-(3,6-di-*tert*-butyl-9*H*-carbazol-9-yl)-9,9-dihexyl-9*H*-fluoren-2-yl)thiophen-2-yl) thiophen-2-amine (0.5688 g, 0.3465 mmol) in distilled tetrahydrofuran (15ml) at room temperature. After being stirred for 3 h, water (50 ml) was added and the mixture was extracted with dichloromethane (50 ml x 3). The organic layer was separated, dried over anhydrous sodium sulphate, filtered and dried to remove the solvents in vacuum. Purification by column chromatographyl over silica gel eluting with a mixture of hexane and dichloromethane (8:2) followed by recrystallization with a mixture of dichloromethane and methanol afforded green solid (0.5631g, 99% yield); ^{1}H-NMR (300 MHz, $CDCl_3$) δ 9.89 (1H, s), 8.17 (4H, d, J = 1.20 Hz), 7.26-7.91 (31H, m) and 2.03 (8H, dd, J = 10.05 Hz) ppm. FT-IR (KBr) 3042, 2955, 2927, 2857, 2360, 1611, 1584, 1478, 1452, 1365, 1324, 1294, 1263, 1235, 1033, 969, 877, 809 and 614 cm^{-1}.

5''-(4-(bis(5-(7-(3,6-di-*tert*-butyl-9*H*-carbazol-9-yl)-9,9-dihexyl-9*H*-fluoren-2-yl)thiophen-2-yl)amino)phenyl)-[2,2':5',2''-terthiophene]-5-carbaldehyde(CFTAT3-aldehyde(10b))

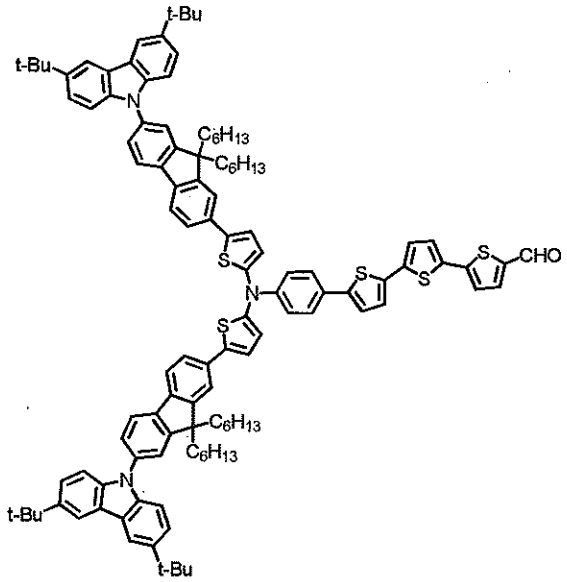

To a solution of *N*-(4-(5'-bromo-[2,2'-bithiophen]-5-yl)phenyl)-5-(7-(3,6-di-*tert*-butyl-9*H*-carbazol-9-yl)-9,9-dihexyl-9*H*-fluoren-2-yl)-*N*-(5-(7-(3,6-di-*tert*-butyl-9*H*-carbazol-9-yl)-9,9-dihexyl-9*H*-fluoren-2-yl)thiophen-2-yl)thiophen-2-amine (0.3000 g, 0.1744 mmol), 5-formylthiophenboronic acid (0.0272 g, 0.1744 mmol), $Pd(PPh_3)_4$(0.0060 g, 0.0052 mmol), and aqueous Na_2CO_3 solution (2 M, 20 mmol) in freshly distilled tetrahydrofuran (20 ml) was degas with nitrogen for 5 min. The reaction mixture was stirred at reflux under nitrogen for 24 h. After being cooled to room temperature, water (50 ml) was added and extracted with dichloromethane (50 ml x 3). The combined organic layer were washed with water (50 ml) and brine solution (50 ml), dried over anhydrous Na_2SO_4, filtered, and the solvents were removed to dryness. Purification by column chromatography over silica gel eluting with a mixture of 50% dichloromethane and hexane follow by recrystallization with a mixture of dichloromethane and methanol afforded **CFTAT3-aldehyde(10b)** as pale a orange solid (0.2660 g, 88% yield); m.p. 174-175.5 °C; ^{1}H-NMR (300 MHz, $CDCl_3$) δ 9.88 (1H, s), 8.18 (4H, s), 7.19-7.91 (33H, m) and 2.03 (8H, *t*, *J* = 3.9 Hz) ppm. ^{13}C NMR (300 MHz, $CDCl_3$): 182.38, 152.67, 151.96, 146.82, 144.98, 142.87, 141.65, 140.48, 139.32, 139.28, 139.24, 137.35, 137.15, 135.39, 134.42, 132.73, 127.04, 125.47, 124.88, 124.46, 124.04, 123.87, 123.58,

123.41, 121.40, 120.83, 120.31, 119.93, 116.33, 109.22, 55.52, 40.36, 34.76, 32.04, 31.54, 29.66, 23.91, 22.59 and 14.04. FT-IR (KBr) 3474, 3067, 2956, 2928, 2857, 2369, 1725, 1610, 1584, 1491, 1477, 1455, 1364, 1325, 1295, 1263, 1228, 1048, 878, 810, 794, 740 and 615 cm^{-1}.

(*E*)-3-(5"-(4-(bis(5-(7-(3,6-di-*tert*-butyl-9*H*-carbazol-9-yl)-9,9-dihexyl-9*H*-fluoren-2-yl)thiophen-2-yl)amino)phenyl)-[2,2':5',2"-terthiophen]-5-yl)-2-cyanoacrylic acid(CFTAT3-A)

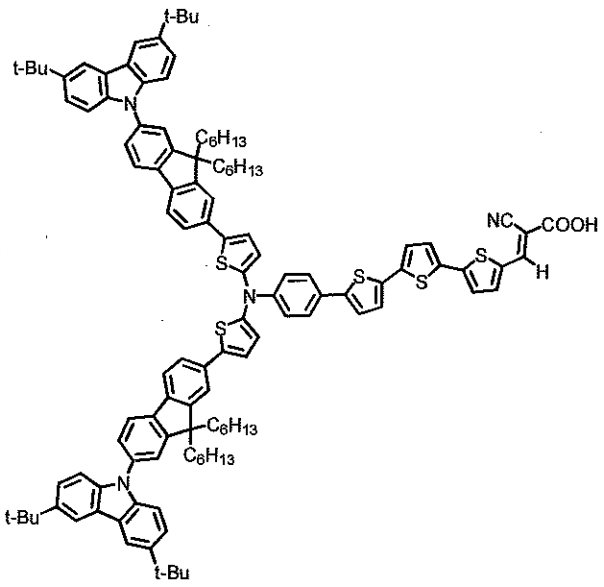

A mixture of 5"-(4-(bis(5-(7-(3,6-di-*tert*-butyl-9*H*-carbazol-9-yl)-9,9-dihexyl-9*H*-fluoren-2-yl)thiophen-2-yl)amino)phenyl)-[2,2':5',2"-terthiophene]-5-carbaldehyde (0.2400 g, 0.1370 mmol) and cyanoacetic acid (0.1165 g, 1.3701 mmol) was vacuum-dried and chloroform (20ml) and piperidine (0.0583g, 0.6851 mmol)were added. The solution was refluxed for overnight. After cooling the solution, water (50 ml x 3) was added to the solution and extracted by dichloromethane (50 ml x 3). The organic layer was separated and dried in Na_2SO_4. The solvent was removed in vacuum. The pure product was purified by silica gel chromatography using a mixture of hexane and dichloromethane (1:1) to give **CFTAT3-A** as a red solids (0.2375g, 99% yield); m.p. 180-180.5 °C; ^{1}H-NMR (300 MHz, $CDCl_3$) δ 8.18 (5H, s), 7.16-7.89 (33H, m) and 3.22 (8H, s) ppm. ^{13}C NMR (300 MHz, $CDCl_3$): 152.67, 151.94, 144.67, 143.79, 142.85, 140.39, 139.32, 139.28, 138.48, 137.11, 136.22, 135.66, 135.60, 134.83, 132.81, 126.36, 125.43, 125.22, 124.85, 124.45, 123.93, 123.86, 123.57, 123.40, 121.40, 120.81, 120.30, 119.91, 116.32, 109.22,

55.51, 44.42, 40.35, 34.75, 32.03, 31.54, 29.66, 23.91, 22.73, 22.58 and 14.03. FT-IR (KBr) 3400, 3059, 2957, 2925, 2857, 2353, 2207, 1727, 1658, 1613 1479, 1453, 1348, 1295, 1263, 1033, 877, 795, 741 and 615 cm^{-1}.

Chapter 3

9-Dodecylcarbazole(C)

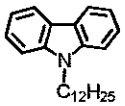

To a solution of carbazole (10.00 g, 59.80 mmol) in DMF (93 ml) was added followed by NaH (2.15 g). 1-Bromododecane (15.00 g, 89.70 mmol) was added slowly. The reaction mixture was stirred at 70 °C for 20 h. Water (100 ml) was added and the mixture was extracted with methylene chloride (50 ml x 3). The combined organic phases were washed with a dilute HCl solution (50 ml x 2), water (100 ml), and brine solution (50 ml), dried over anhydrous Na_2SO_4, filtered and the solvents were removed to dryness. Purification by column chromatography over silica gel eluting with hexane gave a pale yellow viscous oil (9.50g, 95% yield) ^{1}H NMR (300 MHz, $CDCl_3$): δ 8.09 (2H, J = 2.4 Hz, d), 7.44 (4H, m), 7.25 (d, J = 2.4 Hz), 3.30 (2H, J = 2.1 Hz, t), 1.88 (t, J = 2.1 Hz, 2H), 1.33 (m, 18H) and 0.89 (t, J = 2.1, 3H). ^{13}C NMR (300 MHz, $CDCl_3$): 140.57, 125.67, 122.98, 120.45, 118.82, 108.77, 43.15, 32.09, 29.77, 29.66, 29.56, 29.51, 29.09, 27.45, 22.86 and 14.19 MS (TOF MS ES+) *m/z*: 336.2691 $[M + H]^+$.

9,9'-didodecyl-9*H*,9'*H*-3,3'-bicarbazole(C_2)

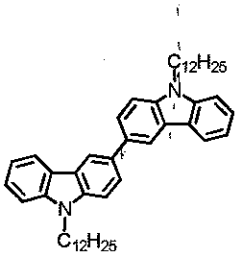

To a stirred solution of $FeCl_3$ (22.612g, 139.4 mmol) in freshly distilled tetrahydrofuran (250 ml) was added slowly a solution of carbazole (9.7372g, 34.85 mmol) in freshly distilled

tetrahydrofuran (50ml) After initiative stirred at room temperature for 24 h, water (100 ml) was added. The mixture was extracted with CH_2Cl_2 (50 ml x 3). The combined organic phase was washed with water (100 ml), brine solution (50 ml), dried over anhydrous Na_2SO_4, sodium thiosulphate, filtered and the solvent was removed to dryness. Purification by column chromatography using silica gel eluting with hexane gave pale yellow viscous oil. (9.1145g, 93% yield); ^{1}H-NMR (300 MHz, $CDCl_3$) δ 8.41 (2H, d, J = 1.2 Hz), 8.19 (2H, d, J = 7.8 Hz) and 3.45 (4H, *t*, J = 7.8 Hz) ppm. ^{13}C NMR (300 MHz, $CDCl_3$): 140.92, 139.55, 133.38, 125.63, 125.53, 123.41, 123.07, 120.44, 118.94, 118.72, 108.86, 108.77, 43.24, 31.91, 29.60, 29.52, 29.45, 29.33, 29.05, 27.36, 22.68 and 14.11. FT-IR (KBr) 3051, 2957, 2923, 2852, 1629, 1600, 1462, 1347, 1330, 878, 796, 744 and 726 cm^{-1}.

6,6'-dibromo-9,9'-didodecyl-9*H*,9'*H*-3,3'-bicarbazole(C_2-diBr)

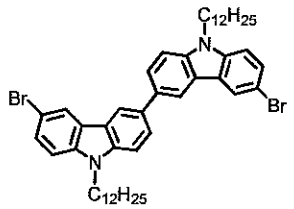

N-Bromosuccinimide (3.7104 g, 20.8460 mmol) was added slowly in small portions to a stirred solution of 9,9'-didodecyl-9*H*,9'*H*-3,3'-bicarbazole (6.8034 g, 10.1688 mmol) in distilled tetrahydrofuran (25 ml). After initiative stirred at room temperature for 3 h, water (50 ml) was added. The mixture was extracted with CH_2Cl_2 (50 ml x 3). The combined organic phase was washed with water (50 ml), brine solution (50 ml), dried over anhydrous Na_2SO_4, sodium thiosulphate, filtered and the solvent was removed to dryness. Purification by column chromatography using silica gel eluting with a mixture of CH_2Cl_2 and hexane gave yellow viscous oil. (3.4017 g, 50% yield); ^{1}H-NMR (300 MHz, $CDCl_3$) δ 8.30 (2H, *t*, J = 6.0 Hz), 7.83 (2H, q, J = 8.1 Hz) and 4.29 (4H, *t*, J = 7.2 Hz) ppm; FT-IR (KBr) 3047, 2957, 2923, 2853, 1629, 1597, 1470, 1453, 1378, 1348, 1149, 1055, 869, and 797 cm^{-1}.

6-bromo-9,9'-didodecyl-6'-(thiophen-2-yl)-9*H*,9'*H*-3,3'-bicarbazole(C_2T1Br)

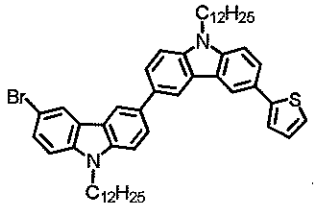

To a stirred solution of 6,6'-dibromo-9,9'-didodecyl-9*H*,9'*H*-3,3'-bicarbazole (1.3690 g, 1.6557 mmol) and $Pd(PPh_3)_4$ (0.0574 g, 0.0417 mmol) in freshly distilled tetrahydrofuran (35 ml) were added 2-thiophene-broronic acid (0.2128 g, 1.6557 mmol) and an aqueous Na_2CO_3 solution (2M, 30 mmol). The mixture was refluxed for 24 h. After cooling the solution, water (50 ml x 3) was added to the solution and extracted by dichloromethane (50 ml x 3). The organic layer was separated and dried in Na_2SO_4. The solvent was removed in vacuum. The product was purified by silica gel chromatography using a mixture of hexane and dichloromethane (8:2) as an eluent a green solids (0.5202g, 38% yield); ^{1}H-NMR (300 MHz, $CDCl_3$) δ 8.45 (2H, s), 8.39 (1H, s), 8.34 (1H, s) and 4.25 (4H, d, J = 7.2 Hz) ppm.

6-bromo-6'-(5-bromothiophen-2-yl)-9,9'-didodecyl-9*H*,9'*H*-3,3'-bicarbazole (C_2T1-diBr)

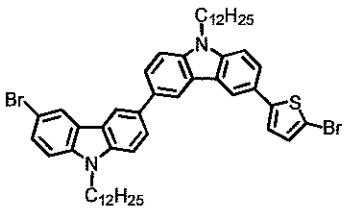

N-Bromosuccinimide (0.2960 g, 1.6632 mmol) was added slowly in small portions to a stirred solution of 6-bromo-9,9'-didodecyl-6'-(thiophen-2-yl)-9*H*,9'*H*-3,3'-bicarbazole (1.3148 g, 1.5840 mmol) in distilled tetrahydrofuran (15 ml). After initiative stirred at room temperature for 3 h, water (50 ml) was added. The mixture was extracted with CH_2Cl_2 (50 ml x 3). The combined organic phase was washed with water (50 ml), brine solution (50 ml), dried over anhydrous Na_2SO_4, sodium thiosulphate, filtered and the solvent was removed to dryness. Purification by

column chromatography using silica gel eluting with a mixture of CH_2Cl_2 and hexane gave white solids. (0.4865 g, 37% yield); ^{1}H-NMR (300 MHz, $CDCl_3$) δ 8.40 (1H, s), 8.35 (1H, s), 8.30 (2H, s) and 4.28 (4H, d, J = 5.1 Hz) ppm.

9,9'-didodecyl-6,6'-di(thiophen-2-yl)-9*H*,9'*H*-3,3'-bicarbazole(C_2T2)

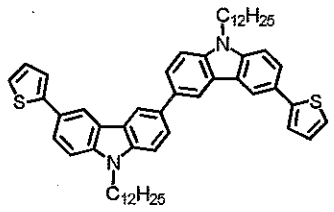

To a stirred solution of 6,6'-dibromo-9,9'-didodecyl-9*H*,9'*H*-3,3'-bicarbazole (2.2803 g, 2.7578 mmol) and $Pd(PPh_3)_4$ (0.0956 g, 0.0827 mmol) in freshly distilled tetrahydrofuran (35 ml) were added 2-thiophene-broronic acid (0.7058 g, 5.5156 mmol) and an aqueous Na_2CO_3 solution (2M, 30 mmol). The mixture was refluxed for 24 h. After cooling the solution, water (50 ml x 3) was added to the solution and extracted by dichloromethane (50 ml x 3). The organic layer was separated and dried in Na_2SO_4. The solvent was removed in vacuum. The pure product was obtained by silica gel chromatography using a mixture of hexane and dichloromethane (8:2) as an eluent a green solids (1.0945g, 48% yield); ^{1}H-NMR (300 MHz, $CDCl_3$) δ 8.49 (4H, J = 7.2 Hz, d), 7.88 (2H, J = 7.2 Hz, d), 7.78 (4H, J = 7.2 Hz, d) and 4.34 (4H, J = 7.2 Hz, t) ppm. ^{13}C NMR (300 MHz, $CDCl_3$): 147.40, 140.63, 140.09, 133.52, 130.80, 125.95, 124.93, 123.97, 123.53, 123.31, 122.09, 119.03, 117.77, 109.78, 109.22, 43.39, 31.91, 29.60, 29.50, 29.42, 29.33, 29.06, 27.32, 22.68 and 14.11

6,6'-bis(5-bromothiophen-2-yl)-9,9'-didodecyl-9*H*,9'*H*-3,3'-bicarbazole

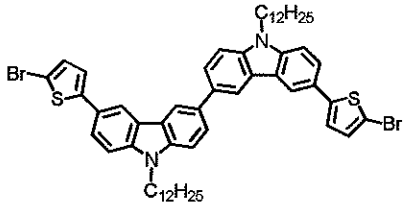

N-Bromosuccinimide (0.1815 g, 1.0200 mmol) was added slowly in small portions to a stirred solution of 6-bromo-9,9'-didodecyl-6'-(thiophen-2-yl)-9*H*,9'*H*-3,3'-bicarbazole (0.4137 g, 0.4976 mmol) in distilled tetrahydrofuran (25 ml). After initiative stirred at room temperature for 3 h, water (50 ml) was added. The mixture was extracted with CH_2Cl_2 (50 ml x 3). The combined organic phase was washed with water (50 ml), brine solution (50 ml), dried over anhydrous Na_2SO_4, sodium thiosulphate, filtered and the solvent was removed to dryness. Purification by column chromatography using silica gel eluting with a mixture of CH_2Cl_2 and hexane gave white solids. (0.2534 g, 61% yield); ^{1}H-NMR (300 MHz, $CDCl_3$) δ 8.43 (2H, s), 8.32 (2H, s), 7.86 (2H, J = 7.5 Hz, d) and 4.34 (4H, J = 6.9 Hz, t) ppm.

3,3''',6,6'''-tetra-tert-butyl-9',9''-didodecyl-9'*H*,9''*H*-9,3':6',3'':6'',9'''-quatercarbazole(C_2TG1)

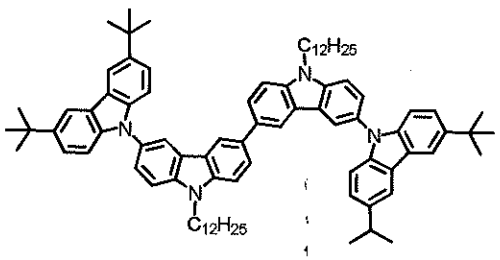

A stirred mixture of 6,6'-dibromo-9,9'-didodecyl-9*H*,9'*H*-3,3'-bicarbazole (0.4603 g, 0.65 mmol), 3,6-di-*tert*-butyl-*9H*-carbazole (0.5449 g, 1.95 mmol), copper iodide (0.1238 g, 0.65 mmol), potassium phosphate (0.6899 g, 3.25 mmol) and *trans*-diaminocyclohexane (0.0371 g, 0.32 mmol) in toluene (130 ml) was refluxed for 24 h under N_2 atmosphere. After cooling, the reaction mixture was extracted with dichloromethane (50 ml x 3). The combined organic phase

was washed with water (15 ml), brine solution (50 ml), dried over sodium sulfate anhydrous, filtered and the solvent was removed in vacuum. The product was purified by silica gel chromatography to afforded **C_2TG1** as white solid (0.2416 g, 76 % yield); m.p. 134 °C; ^{1}H-NMR; δ 8.69 (2H, d, J = 0.9 Hz), 8.32 (2H, s), 8.17 (6H, s), 7.64-7.55 (6H, m), 7.46 (4H, J = 8.7 Hz, d), 7.36-7.30 (6H, m), 7.26 (2H, s), 4.36 (4H, J = 7.2 Hz, t), 1.94 (4H, J = 7.2 Hz, t), 1.48-1.26 (72H, m) ppm; ^{13}C-NMR (300 MHz, $CDCl_3$): 142.51, 140.21, 139.71, 139.57, 129.83, 128.89, 125.73, 124.22, 123.52, 123.33, 123.07, 122.63, 119.30, 116.20, 111.89, 110.48, 109.85, 109.12, 43,54, 34.74, 32.06, 31.91, 29.61, 29.58, 29.52, 29.40, 29.34, 29.02, 27.33, 22.69 and 14.11.

3'',6''-di-*tert*-butyl-6-(5-(3,6-di-*tert*-butyl-9*H*-carbazol-9-yl)thiophen-2-yl)-9,9'-didodecyl-9*H*,9'*H*-3,3':6',9''-tercarbazole(C_2T1G1)

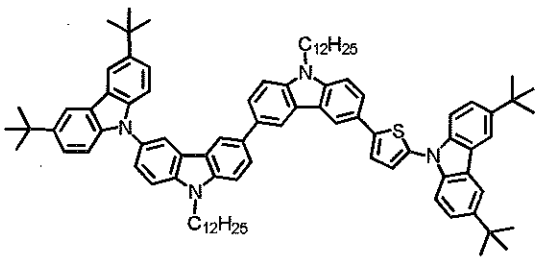

A stirred mixture of 6-bromo-6'-(5-bromothiophen-2-yl)-9,9'-didodecyl-9*H*,9'*H*-3,3'-bicarbazole (0.4152 g, 0.4568 mmol), 3,6-di-*tert*-butyl-*9H*-carbazole (0.3829 g, 1.3704 mmol), copper iodide (0.0870 g, 0.4568 mmol), potassium phosphate (0.4848 g, 2.2840 mmol) and *trans*-diaminocyclohexane (0.0261 g, 0.284 mmol) in toluene (30 ml) was refluxed for 24 h under N_2 atmosphere. After cooling, the reaction mixture was extracted with dichloromethane (50 ml x 3). The combined organic phase was washed with water (50 ml), brine solution (50 ml), dried over sodium sulfate anhydrous, filtered and the solvent was removed in vacuum. The product was obtain by silica gel chromatography to afforded **(C_2T1G1)** as light green solid (0.1188 g, 26% yield); ^{1}H-NMR; δ 8.69 (2H, d, J = 0.9 Hz), 8.32 (2H, s), 8.17 (6H, s), 7.64-7.55 (6H, m), 7.46 (4H, J = 8.7 Hz, d), 7.36-7.30 (8H, m), 7.25 (2H, s), 4.36 (4H, J = 7.2 Hz, t), 1.92 (4H, J = 7.2 Hz, t), 1.48-1.26 (72H, m) ppm

6,6'-bis(5-(3,6-di-*tert*-butyl-9*H*-carbazol-9-yl)thiophen-2-yl)-9,9'-didodecyl-9*H*,9'*H*-3,3'-bicarbazole(C_2T2G1)

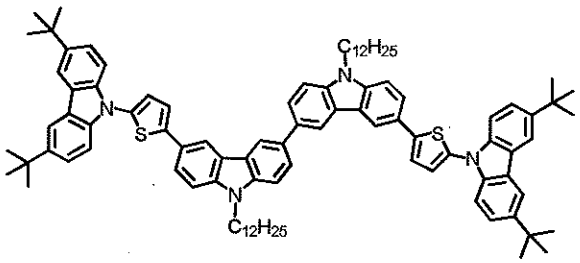

A stirred mixture of 6,6'-bis(5-bromothiophen-2-yl)-9,9'-didodecyl-9*H*,9'*H*-3,3'-bicarbazole (0.1926 g, 0.1943 mmol), 3,6-di-*tert*-butyl-*9H*-carbazole (0.420 g, 0.5858 mmol), copper iodide (0.0370 g, 0.1943 mmol), potassium phosphate (0.2062 g, 0.9715 mmol) and *trans*-diaminocyclohexane (0.0111 g, 0.0972 mmol) in toluene (30 ml) was refluxed for 24 h under N_2 atmosphere. After cooling, the reaction mixture was extracted with dichloromethane (50 ml x 3). The combined organic phase was washed with water (50 ml), brine solution (50 ml), dried over sodium sulfate anhydrous, filtered and the solvent was removed in vacuum. The product was obtain by silica gel chromatography to afforded **C_2T2G1** as light green solid (0.0270 g, 14% yield); ^{1}H-NMR; δ 8.69 (2H, d, J = 0.9 Hz), 8.37 (2H, s), 8.19 (6H, s), 7.64-7.55 (6H, m), 7.46 (4H, J = 8.7 Hz, d), 7.36-7.30 (10H, m), 7.23 (2H, s), 4.33 (4H, J = 7.2 Hz, t), 1.91 (4H, J = 7.2 Hz, t), 1.48-1.24 (72H, m) ppm.

Chapter 4

2,7-dibromo-9*H*-fluorene (2BrFlu)

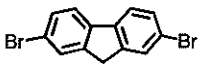

Fluorene (17 g, 102.27 mmol) and $FeCl_3$ (0.1281g ,0.7875 mmol) were added to the stirred in $CHCl_3$ (100 ml). Then, a mixture of bromime solution (10.48 ml) and Chloroform (50 ml) were added to the reaction. The reaction mixture was continue stirred under N_2 atmosphere at room temperature for 3 h. After the mixture was cooled to room temperature water (100 ml) was added. The mixture was extracted with CH_2Cl_2 (50 ml x 3) and sodium thiosulphate, dry over anhydrous Na_2SO_4, filtered and the solvent was removed to dryness. Purification by column chromatography using silica gel eluting with a mixture of CH_2Cl_2 and hexane gave white solids. (14.807 g, 87% yield). ^{1}H-NMR (300 MHz, $CDCl_3$) δ 7.75(2H, s), 7.65 (2H, d, J = 9.0 Hz), 7.55 (2H, d, J = 9.0 Hz), and 3.85 (2H, s) ppm.

2,7-dibromo-9,9-dioctyl-9*H*-fluorene (2BrFAlkyl)

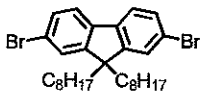

A mixture of 2BrFlu (14.804 g, 46.29 mmol), 1-bromooctane (13.66 ml g, 97.21 mmol), aqueous NaOH solution (50% (w/v), 16.6 ml) and tetrabutyl ammonium bromide (~ 2 g) in DMSO (80 ml). The reaction mixture was continue stirred at room temperature for 3 h, the reaction mixture was extracted with ethyl acetate (100 ml x 2). The combined organic phase was washed with water (100 ml x 2), HCl solution (1 M, 50 ml), water (100 ml), brine solution (50 ml), dried over anhydrous Na_2SO_4, filtered and the solvent was removed to dryness. Purification by column chromatography using silica gel eluting with hexane gave a colorless viscous. (14.06 g, 95% yield). ^{1}H-NMR (300 MHz, $CDCl_3$) δ 7.50(6H, m), 1.95 (4H, t, J = 8.4 Hz), 1.00-1.40 (24H, m) and 0.95 (6H, m) ppm.

9-(7-bromo-9,9-dioctyl-9*H*-fluoren-2-yl)-9*H*-carbazole (BrFC)

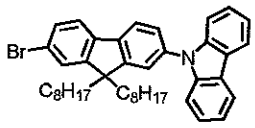

To a mixture of 2BrFAlkyl (1.0620 g, 1.9364 mmol), carbazole (0.1542 g, 0.9221 mmol), copper(I) iodide (0.1756g, 0.9221 mmol), potassium phosphate (0.5173g, 4.6105mmol) and trans-diaminocyclohexane (0.1053 ml, 0.9221 mmol) in toluene (20 ml) was degassed with N_2 for 5 min. The mixture was heated at reflux under N_2 atmosphere for 24 h. After the mixture was cooled to room temperature water (50 ml) was added. The mixture was extracted with CH_2Cl_2 (50 ml x 2). The combined organic phase was washed with water (50 ml), brine solution (50 ml), dried over anhydrous Na_2SO_4, filtered, and the solvents were removed to dryness. Purification by column chromatography using silica gel eluting with a mixture of CH_2Cl_2 and hexane afforded a colorless viscous. (0.9468 g, 89% yield) ; ^{1}H-NMR δH (300 MHz, $CDCl_3$) 0.78-0.88(10H, m), 1.15-1.30 (20H, m), 1.99-2.04 (4H, m), 7.32-7.43 (2H, m), 7.47 (4H, d, J = 3.9 Hz), 7.56 (4H, t, J = 6.0 Hz), 7.67 (1H, d, J = 8.7 Hz), 7.91 (1H, d, J = 7.8 Hz), 8.21 (2H, d, J = 7.8 Hz) ppm.

9-(9,9-dioctyl-7-(pyren-1-yl)-9*H*-fluoren-2-yl)-9*H*-carbazole (PFC)

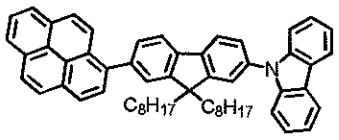

A mixture of BrFC (0.9468 g, 1.4917 mmol), 1-pyrene boronic acid (0.2169 g, 0.4972 mmol), $Pd(PPh_3)_4$ (34.3 mg, 0.0447 mmol) and an aqueous Na_2CO_3 solution (2 M, 10 ml) in freshly distilled tetrahydrofuran (20 ml) was degassed with N_2 for 5 min. The mixture was heated at reflux under N_2 atmosphere for 24 h. After the mixture was cooled to room temperature water (50 ml) was added. The mixture was extracted with CH_2Cl_2 (50 ml x 2). The combined organic phase was washed with water (50 ml), brine solution (50 ml), dried over anhydrous Na_2SO_4, filtered, and the solvents were removed to dryness. Purification by column chromatography using

silica gel eluting with a mixture of CH_2Cl_2 and hexane gave white solids. (0.8517 g, 90% yield);^{1}H-NMR δH (300 MHz, $CDCl_3$) 0.82-0.86 (6H, m), 0.94-0.96 (4H, m), 1.19-1.28 (20H, m), 2.07-2.11 (4H, m), 7.35 (2H, J = 7.5 Hz, t), 7.45-7.53 (4H, m), 7.62 (2H, J = 5.7 Hz, d), 7.70 (2H, J = 7.8 Hz, d),7.97-8.15 (7H, m), 8.21-8.31 (6H, m) ppm.

3,6-dibromo-9-(9,9-dioctyl-7-(pyren-1-yl)-9*H*-fluoren-2-yl)-9*H*-carbazole (PFC-2Br)

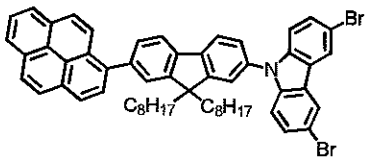

N-Bromosuccinimide (0.4209 g, 2.3655 mmol) was added slowly in small portions to a stirred solution of PFC (0.8517 g, 1.1264 mmol) in distilled tetrahydrofuran (25 ml). After initiative stirred at room temperature for 3 h, water (50 ml) was added. The mixture was extracted with CH_2Cl_2 (50 ml x 3). The combined organic phase was washed with water (50 ml), brine solution (50 ml), dried over anhydrous Na_2SO_4, sodium thiosulphate, filtered and the solvent was removed to dryness. Purification by column chromatography using silica gel eluting with a mixture of CH_2Cl_2 and hexane gave white solids. (0.8517 g, 90% yield) ;^{1}H-NMR δH (500 MHz, $CDCl_3$) 8.50 (2H, d, J = 9.5 Hz), 7.96-8.14 (9H, m), 7.31-66 (10H, m), 2.06 (4H, d, J = 3.5 Hz) ppm.

9-(9,9-dioctyl-7-(pyren-1-yl)-9*H*-fluoren-2-yl)-3,6-di(pyren-1-yl)-9*H*-carbazole (PFCdi-Py)

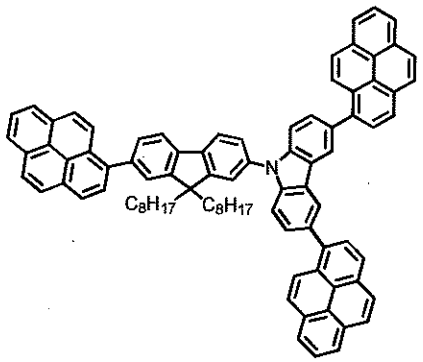

A mixture of PFC-2Br (0.95 g, 2.03 mmol), 1-pyrene boronic acid (1.23 g, 4.26 mmol), $Pd(PPh_3)_4$ (47 mg, 0.041 mmol) and an aqueous Na_2CO_3 solution (2 M, 10 ml) in freshly distilled tetrahydrofuran (15 ml) was degassed with N_2 for 5 min. The mixture was heated at reflux under N_2 atmosphere for 24 h. After the mixture was cooled to room temperature water (50 ml) was added. The mixture was extracted with CH_2Cl_2 (50 ml x 2). The combined organic phase was washed with water (50 ml), brine solution (50 ml), dried over anhydrous Na_2SO_4, filtered, and the solvents were removed to dryness. Purification by column chromatography using silica gel eluting with a mixture of CH_2Cl_2 and hexane gave light green solids. (1.36 g, 82% yield) ^{1}H-NMR δH (500 MHz, $CDCl_3$) 8.51 (2H, s), 7.97-8.25 (27H, m), 7.23-7.75 (10H, m), 2.17 (2H, s), 2.06 (2H, s) ppm.

2,7-Bis[3,6-dipyrenecarbazol-9-yl]-9,9-bis-n-octylfluorene (CFP4)

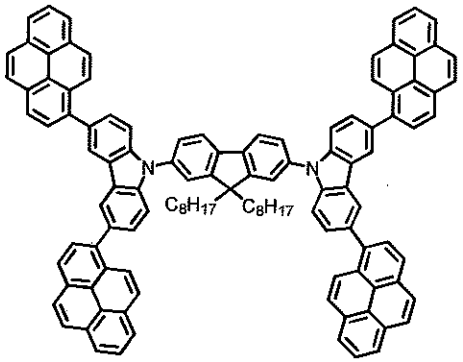

To a mixture of 4BrCF (0.50 g, 0.48 mmol), pyrene-1-boronic acid (0.53 g, 2.17 mmol), tetrakis (triphenylphosphine)palladium(0)(0.01g, 0.009 mmol), in freshly distilled tetrahydrofuran (20 ml) and 2M Na_2CO_3 4.8 mL was degassed with N_2 for 5 min. The mixture was heated at reflux under N_2 atmosphere for 24 h. After the mixture was cooled to room temperature water (50 ml) was added. The mixture was extracted with CH_2Cl_2 (50 mlx 2). The combined organic phase was washed with water (50 ml), brine solution (50 ml), dried over anhydrous Na_2SO_4, filtered, and the solvents were removed to dryness. Purification by column chromatography using silica gel eluting with a mixture of CH_2Cl_2 and hexane to give yellow solids. (0.085 g, 11% yield). ^{1}H-NMR δ_H (ppm) (300 MHz, $CDCl_3$) 0.73-0.75 (10H,m), 1.07-1.28 (20H, m), 2.23 (4H, s), 7.77-7.88 (6H, m), 8.00-8.23 (36H, m), 8.29 (4H, d, J = 7.8 Hz), 8.38 (4H, d, J = 9.3 Hz), 8.52 (4H, s) ppm.

REFERENCES

REFERENCES

[1] P. F. Baude and et al. (2003). "A lithographic process for integrated organic field-effect transistors", Appl. Phys. Lett. 82: 3964-3966.

[2] V. Sunder and et al. (2004). "Elastomeric Transistor Stamps: Reversible Probing of Charge Transport in Organic Crystals", Science. 303: 1644-1646.

[3] Y. Li, Y. Wu, S. Gardnera and B. S. Ong. (2005). "Novel peripherally substituted indolo [3, 2-b]carbazoles for high-mobility organic thin-film transistors", Adv. Mater. 17: 849-853.

[4] Y. Wu and et al. (2005). "High-Performance, Stable Organic Thin-Film Field-Effect Transistors Based on Bis-5'-alkylthiophen-2'-yl-2,6-anthracene Semiconductors", J. Am. Chem. Soc. 127: 614-618.

[5] D. Adam and et al (1994). "Fast photoconduction in the highly ordered columnar phase of a discotic liquid crystal", Nature. 371: 141-143.

[6] A. M. Van De Craats and et al. (1999). "Record Charge Carrier Mobility in a Room-Temperature Discotic Liquid-Crystalline Derivative of Hexabenzocoronene", Adv. Mater. 11: 1469-1472.

[7] A. Fechtenkotter and et al. (1999). "Highly Ordered Columnar Structures from Hexa-*peri*-hexabenzocoronenes-Synthesis, X-ray Diffraction, and Solid-State Heteronuclear Multiple-Quantum NMR Investigations", Angew Chem Int. Ed. 38: 3039-3042.

[8] M. Funahashi and J. Hanna. (2000). "High ambipolar carrier mobility in self-organizing terthiophene derivative", Appl. Phys. Lett. 76: 2574-2576.

[9] H. Sirringhaus and et al. (2000). "Mobility enhancement in conjugated polymer field-effect transistors through chain alignment in a liquid-crystalline phase", Appl. Phys. Lett. 77: 406.

[10] I. McCulloch and et al (2006). "Liquid-crystalline semiconducting polymers with high charge carrier mobility", Nature Materials. 5: 328-333.

[11] A. Fujishima and et al. (1972). "Electrochemical photolysis of water at a semiconductor electrode", Nature. 238: 37-38.

[12] H. Gerischer and et al. (1976). "Photo current measurements under illumination by monochromatic light using a jarrel ash grating", Current Chemistry. 61: 31-40.

REFERENCES (CONTINUED)

[13] H. Tsubomura and et al. (1976). "Dye sensitized zinc oxide: aqueous electrolyte: platinum photocell", Nature. 261: 402-403.

[14] J. Desilvestro and et al. (1985). "Photo cell and method of manufacturing such cell by co-valent growth of phase theron", American Chemical Society. 107: 2988-2990.

[15] B. Oregan and et al. (1991). "A low-cost, high-efficiency solar cell based on dye- sensitized colloidal titanium dioxide films", Nature. 353: 737-740.

[16] M. Grätzel and et al. (2005)."Solar energy conversion by dye-sensitized photovoltaic cells", Inorganica Chimica Acta. 44: 6841-6851.

[17] M. Grätzel and et al. (2006). "Molecular engineering of organic sensitizers for solar cell application", American Chemical Society. 128: 16701-16707.

[18] M. Gratzel and et al. (2003). "Dye-sensitized solar cells", Photochem. Photobiol. C. 4 : 145-153.

[19] K. Hara and et al. (2003). "Dye-sensitized nanocrystalline TiO_2 solar cells based on novel coumarin dyes", Solar Energy Mat. Sol. Cells. 77: 89–103.

[20] K. Hara and et al. (2005). "Oligothiophene-Containing Coumarin Dyes for Efficient Dye-Sensitized Solar Cells", J. Phys. Chem. B. 109: 15476-15482.

[21] S. Ito and et al. (2006). "High-Efficiency Organic-Dye- Sensitized Solar Cells Controlled by Nanocrystalline-TiO_2 Electrode Thickness", Adv. Mater. 18: 1202-1205.

[22] S. Kim and et al. (2007). "Novel conjugated organic dyes containing bis-dimethylfluorenyl amino phenyl thiophene for efficient solar cell", Tetrahedron. 63: 9206–9212.

[23] A. J. Lovinger and et al. (1996). "Electrically active organic and polymeric materials for thin-film-transistor technologies", Materials Research. 12: 3174-3186.

[24] K. Hara and et al. (2008). "Hexylthiophene-functionalized carbazoled for efficient molecular photovoltaics: tuning of solar-cell performance by structural modification", Chem Mater. 20: 3993-4003.

[25] J. Ko and et al. (2007). "Molecular engineering of organic dyes containing N-aryl carbazole moiety for solar cell", Tetrahedron. 63: 1913-1922.

REFERENCES (CONTINUED)

[26] L. Sun and et al. (2009). "Two novel carbazole dyes for dye-sensitized solar cells with open-circuit voltages up to 1 V basedon Br /Br_3 Electrolytes", Organic Letters. 11: 5542-5545.

[27] E. Galoppini (2004). "Linker for anchoring to semiconductor nanoparticle", Coord. Chem. Rev. 248 : 1283-1297.

[28] W. M. Capbell and et al. (2004). "Porphyrins as light harvesters in the dye-sensitised TiO_2 solar cell", Coor. Chem. Rev. 248: 1363-1379.

[29] Wikipedia the free encyclopedia. "Organic light-emitting diode", http://en.wikipedia.org/wiki/Organic light-emitting diode, April, 2010.

[30] A. J. Lovinger and et al. (1996). "Electrically active organic and polymeric materials for thin-film-transistor technologies", Materials Research. 12: 3174-3186.

[31] J. R. Sheats and et al. (1996). "Organic electroluminescent devices", Science. 273:884-888.

[32] D. D. C. Bradley and et al. (1992). "Electroluminescence: a bright future for conjugated polymers". Advanced Materials. 4: 756-758.

[33] S. A. VanSlyke and et al. (1987). "Organic electroluminescent diodes", Applied Physics Letters. 51: 913-915.

[34] K. Müllen and et al. (2001). "Contribution from the theoretical division and center for nonlinear", Synthetic Metals. 125: 73-80.

[35] A. B. Holmes and et al. (1990). "First polymer LED in the world - ITO glass/PPV/Aluminium", Nature. 347: 539-541.

[36] A . Heeger and et al. (1991). "Photonic devices made with semiconducting conjugated polymers: New developments", Applied Physics Letters. 58:1982-1984.

[37] W. Huang and et al. (2006). "Fluorene-substituted pyrenes-Novel pyrene derivatives as emitters in nondoped blue OLEDs", Organic Electronics. 7: 155-162.

[38] Y. S. Han and et al. (2009). "Synthesis and electro-optical properties of carbazole derivatives with high band gap energy", Thin Solid Films. 518: 284-289.

[39] N. Q. Li and et al. (2000). "Photoelectric conversion properties of nanocrystalline TiO_2 electrodes sensitized with hemicyanine derivatives", Phys. Chem.B. 104: 9676-9682.

REFERENCES (CONTINUED)

[40] H. Arakawa and et al. (2003). "Design of new coumarin dyes having thiophene moieties for highly efficient", New Journal of Chemistry. 27: 783-785.

[41] T. J. Chow and et al. (2009). "Dye-sensitized solar cell utilizing organic dyads containing triarylene conjugates", Tetrahedron. 65: 4726-4734.

[42] E. Galoppini and et al. (2007). " Tetrachelate porphyrin chromophores for metal oxide semiconductor sensitization: effect of the spacer length and anchoring group position", American Chemical Society. 129: 4655-4665.

[43] S. Uchida and et al. (2003). "Highly-effcient metal-free organic dyes for dye-sensitized solar cells", Chem. Commun. 24: 3036-3037.

[44] F. Matsui and et al. (2004). "Multi-colored dye-sensitized solar cells", Photochem. Photobio. A. 164: 67-73.

[45] J. Bäckvall. (2010) . "Paladium-catalyzed cross couplings in organic synthesis". The Royal Swedish Academy of Sciences. 1-13.

[46] K. Maruoka and T. Oo. (2007). "Recent Advances in Asymmetric Phase-Transfer Catalysis" Angew. Chem. Int. Ed. 46: 4222 – 4266.

[47] I. Tsutomu and K. Hiroyuki (2005) "*E*- or *Z*-Selective Knoevenagel Condensation of Acetoacetic Derivatives: Effect of Acylated Substituent, that is, TEMPO and Amines, as an Auxiliary, and New Accesses to Trisubstituted *E*- and *Z*-2-Alkenals and Furans", J. Org.Chem. 71: 947-953.

[48] S. Saito and et al. (1988). "Organic electroluminescent device having a hole conductor as an emitting layer", Applied Physics Letters. 55: 1489-1491.

[49] S. R. Forrest and et al. (1999). "White-light-emitting organic electroluminescent devices based on interlayer sequential energy transfer", Applied Physics Letters. 7(75): 888-890.

[50] Y. Chen and et al. (2009). "Synthesis, characterization, and electroluminescent properties of star shaped donor-acceptor dendrimers with carbazole dendrons as peripheral branches and heterotriangulene as central core", Tetrahedron. 23(65): 4455-4463.

REFERENCES (CONTINUED)

[51] B.C. Wang and et al. (2005). "Theoretical investigation of carbazole derivatives as hole-transporting materials in OLEDs", Journal of Molecular Structure. 725: 89-95.

[52] K. Takanashi and et al. (2008). "Synthesis and functionality of dendrimer with finely controlled metal assembly", Polymer. 49: 4033-4041.

[53] J. I. Jin and et al. (2004). "Electroluminescence of LEDs consisting two layers of Alq_3 and high t_g blue-light emitting branched compounds", Synthetic Metals. 1(143): 97-101.

[54] C. He and et al. (2010). "Highly fluorescent intramolecular dimmers of two pyrenyl-substituted fluorenes bridged by 1,6-hexanyl: synthesis, spectroscopic, and self-organized properties", Tetrahedron Letters. 9(51): 1317-1321.

[55] N. Periasamy and et al. (2011). "Tuning of HOMO levels of carbazole derivatives: New molecules for blue OLED", Synthetic Metals. 161: 466-473.

[56] C. S. Lee and et al. (2011). "Carbazole-pyrene derivatives for undoped organic light-emitting devices", Organic Electronics. 12: 541-546.

[57] K. Maruoka and T. Oo. (2007). "Recent Advances in Asymmetric Phase-Transfer Catalysis", Angew. Chem. Int. Ed. 46: 4222 – 4266.

APPENDIX

THE 6th PURE AND APPLIED CHEMISTRY INTERNATIONAL CONFERENCE 2012

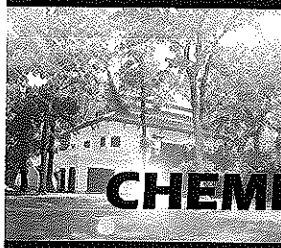

PACCON 2012- CHEMISTRY BEYOND BOUNDARIES

11 - 13 JANUARY 2012, THE EMPRESS CONVENTION CENTER
CHIANG MAI , THAILAND

PROCEEDINGS

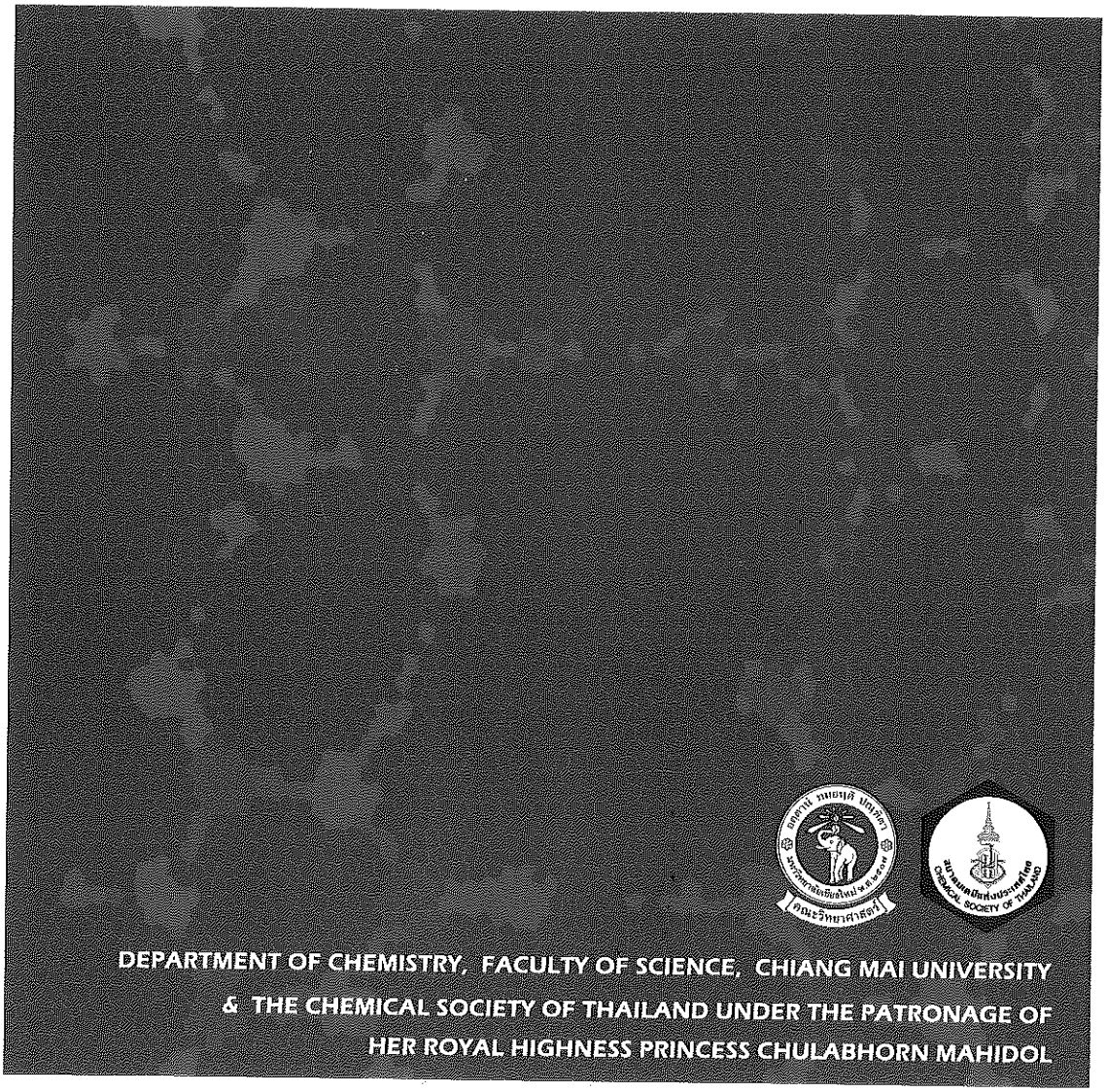

DEPARTMENT OF CHEMISTRY, FACULTY OF SCIENCE, CHIANG MAI UNIVERSITY
& THE CHEMICAL SOCIETY OF THAILAND UNDER THE PATRONAGE OF
HER ROYAL HIGHNESS PRINCESS CHULABHORN MAHIDOL

PACCON
PURE AND APPLIED CHEMISTRY INTERNATIONAL CONFERENCE 2012

"Chemistry Beyond Boundaries"

Content

PACCON 2012 proceedings are published in electronic form only. There is no index page but reader can search for interested keywords in this content by using pdf program searching tool. The full articles in the proceedings are grouped into various sessions and have been in separated files in order to reduce file size for convenient downloading. The sessions and associated files are listed below:

MNT-P-010

SYNTHESIS AND CHARACTERIZATION 2-PYRENE-7-(*N*-CARBAZOLE)FLUORENES AS BLUE LIGHT-EMITTING MATERIALS FOR ORGANIC LIGHT-EMITTING DIODE (OLED)

Teadkait Kaewpuang, Siriporn Jungsuttiwong, Taweesak Sudyoadsuk, Tinnagon Keawin, Vinich Promarak*

Center for Organic Electronic and Alternative Energy, Department of Chemistry and Center of Excellence for Innovation in Chemistry, Faculty of Science, Ubon Ratchathani University, Warinchumrap, Ubon Ratchathani, Thailand
**Corresponding Author : Teadkaitkaewpuang@gmail.com*

ABSTRACT

In this work, a series of novel fluorescent organic materials based on carbazole, fluorene and pyrene derivatives were synthesized and characterized for use as blue light-emitting materials for organic light-emitting diode (OLED). The key intermediate 1-(7-bromo-9,9-dioctyl-9*H*-fluoren-2-yl)pyrene was obtained by bromination of fluorene, alkylation of 2,7-dibromo-9*H*-fluorene with 1-bromooctain then Suzuki cross coupling of the resultant with pyrene-1-boronic acid. Target molecule PFC was synthezied by Ullmann coupling of 1-(7-bromo-9,9-dioctyl-9*H*-fluoren-2-yl)pyrene with carbazole. PFCdi-P was obtained from bromination of PFC using NBS and then Suzuki cross coupling reaction with pyrene-1-boronic acid. Ullmann coupling of 3,6-dibromo-9-(9,9-dioctyl-7-(pyren-1-yl)-9*H*-fluoren-2-yl)-9*H*-carbazole with 3,6-di(pyren-1-yl)-9*H*-carbazole to give PFCdi-CP. These 2-pyrene-7-(*N*-carbazole)fluorene derivatives were characterized by ^{1}H, ^{13}C NMR, FTIR, UV-Vis and fluorescence spectroscopy. The target molecules were expected to use as high efficient blue emitters with amorphous and high thermal stability for OLEDs.

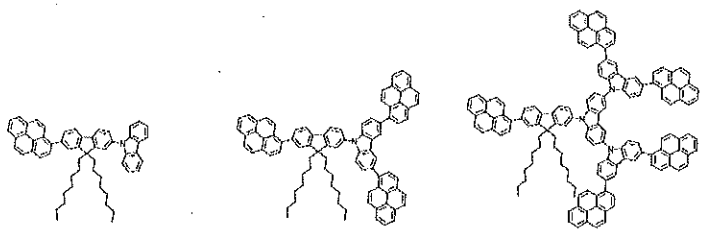

PFC PFCdi-P PFCdi-CP

Molecular structures of the target molecules

Keywords Carbazole; Fluorene; Pyrene; OLED; Blue light-emitting material

SYNTHESIS AND CHARACTERIZATION 2-PYRENE-7-(*N*-CARBAZOLE)FLUORENES AS BLUE LIGHT-EMITTING MATERIALS FOR ORGANIC LIGHT-EMITTING DIODES (OLEDs)

Teadkait Kaewpuang[1], Siriporn Jungsuttiwong[1], Taweesak sudyoadsuk[1], Tinnagon Keawin[1] and Vinich Promarak[1]*

[1] Center for Organic Electronic and Alternative Energy, Department of Chemistry and Center of Excellence for Innovation in Chemistry, Faculty of Science, Ubon Ratchathani University, Warinchumrap, Ubon Ratchathani, Thailand.

E-mail: Teadkaitkanwpuang@gmail.com

Abstract: In this work, a series of novel fluorescent organic materials based on carbazole, fluorene and pyrene derivatives were synthesized and characterized for use as blue light-emitting materials in organic light-emitting diodes (OLEDs). The key intermediate 1-(7-bromo-9,9-dioctyl-9*H*-fluoren-2-yl)pyrene was obtained by bromination of fluorene, alkylation of 2,7-dibromo-9*H*-fluorene with 1-bromooctaine then Suzuki cross coupling of the resultant with pyrene-1-boronic acid. Target molecule PFC was synthezied by Ullmann coupling of 1-(7-bromo-9,9-dioctyl-9*H*-fluoren-2-yl)pyrene with carbazole. PFCdi-P was obtained from brominationof PFC using *N*-Bromosucciniimide and then Suzuki cross coupling reaction with pyrene-1-boronic acid. Ullmann coupling of 2,7-Bis(3,6-dibromocarbazol-9-yl)-9,9-bis-n-octylfluorene with pyrene-1-boronic acid resulted in CPF4. These 2-pyrene-7-(*N*-carbazole)fluorene derivatives were characterized by ^{1}H and ^{13}C NMR, UV-Vis and fluorescence spectroscopy. The target molecules were expected to use as high efficient blue-light emitters with amorphous and high thermal stability for OLEDs.

1. Introduction

The normal structure of OLEDs includes of a light emissive layer sandwiched in between two metal electrodes, one of which is transparent conducting electrode. Additional layers between the cathode and the emissive layer (electrontransport layer, ETL) or between the anode and the emissive layer (hole transport layer, HTL) is used for high efficiency OLED devices. Recent studies revealed that organic multilayer structures typically increase the performance of the devices by decreasing the barrier for hole injection from the anode and by enabling control over the electron-hole recombination region, moving it from the organic/cathode interface, where the demerit density is high, into the bulk. Therefore, the layer deposited on the anode would generally be a good hole transport material (HTM), providing HTL. Similarly, the organic layer in contact with the cathode would be the optimized ETL [1-4].

In this work,we describe the synthesis and characterizationof blue light-emitting materials that conveniently prepared using bromination, alkylation , Ullmann coupling and Suzuki coupling reaction for use in organic light-emitting diodes (OLEDs)

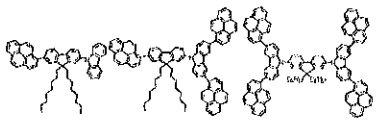

PFC PFCdi-P CPF4

Figure 1.Structures of PFC, PFCdi-P and CPF4 for use as organic light-emitting material.

2. Experimental

2.1. Materials and Instruments

Tetrahydrofuran (THF) was refluxed with sodium and benzophenone, and distilled. CH_2Cl_2 for DSC and TGA experimentswere washed with conc. H_2SO_4 and distilled twice from CaH_2. All reagents and solvents were purchased from Aldrich, Acros, Fluka or Thai Suppliers and used asreceived unless otherwise stated.

^{1}H-NMR spectra were recorded on Brüker AVANCE (300 MHz) spectrometer. ^{13}C-NMR spectra were recorded on Brüker AVANCE (75 MHz) spectrometer and were fully decoupled. Chemical shifts are reported relative to residual solvent peak in part per million (ppm). Coupling constants (*J*) are given in Hertz (Hz). UV-Visible spectra were measured in CH_2Cl_2 on Perkin-Elmer UV Lambda 25 spectrometer. Analytical thin-layer chromatography (TLC) was performed with Merck aluminium plates coated with silica gel 60 F_{254}. Column chromatography was carried out using gravity feed chromatography with Merck siliga gel mesh, 60 ^{0}A.

2.1.1 2,7-dibromo-9H-fluorene (2)

A solution of fluorene (17 g, 102.27 mmol) and FeCl3 (0.1281g ,0.7875 mmol) in CHCl3 (100 ml) were firstly prepared . Then, a mixture of bromine solution (10.48 ml) and CHCl3 (50 ml) was added to

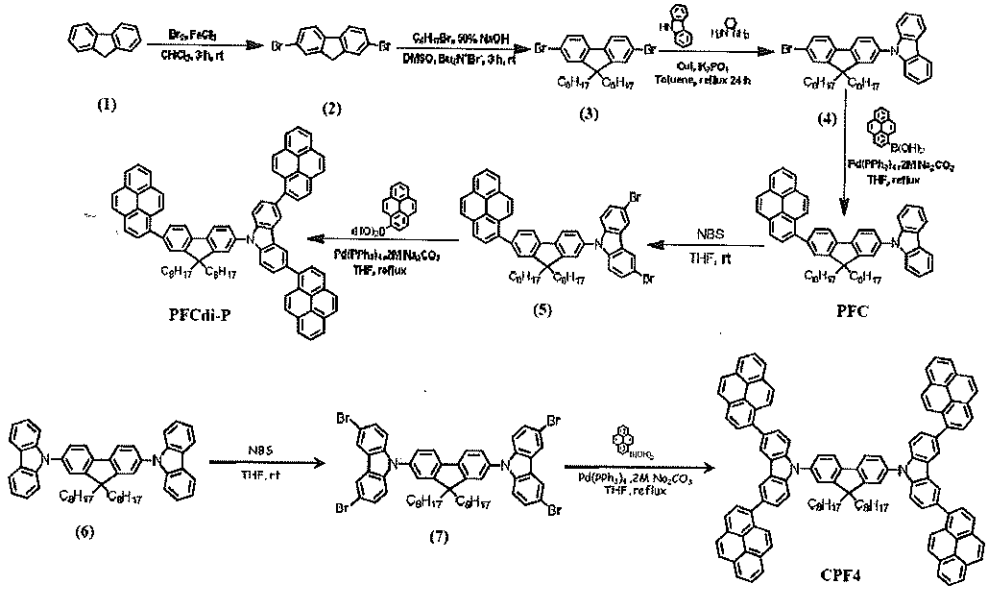

Scheme 1.Synthesis of blue light-emitting diode materials

water (100 ml) was added. The mixture was extracted with CH2Cl2 (50 ml x 3) and sodium thiosulphate, this stirred solution. The reaction mixture was stirred under N_2 atmosphere at room temperature for 3h. After the mixture was cooled to room temperature, then dried over anhydrous Na2SO4. The solvent was finally removed to obtain crude product.The crude product was purified by column chromatography using silica gel elutingwith a mixture of CH_2Cl_2 and hexane gave white solids. Yield 14.807 g (87%). ^{1}H-NMR (300 MHz, $CDCl_3$) δ 7.75(2H, s), 7.65 (2H, d, J = 9.0 Hz), 7.55 (2H, d, J = 9.0 Hz), and 3.85 (2H, s) ppm.

2.1.2 *2,7-dibromo-9,9-dioctyl-9H-fluorene* **(3)**

A mixture of **2** (14.804 g, 46.29 mmol), 1-bromooctane (13.66 ml g, 97.21 mmol), aqueous NaOH solution (50% (w/v), 16.6 ml) and tetrabutyl ammonium bromide (~ 2 g) in DMSO (80 ml) was prepard and stirred at room temperature for 3h. The reaction mixture was then extracted with ethyl acetate (100 ml x 2). The combined organic layer was washed with water (100 ml x 2), HCl (1 M, 50 ml), water (100 ml), brine solution (50 ml),and dried over anhydrous Na_2SO_4. The crude product was obtained after the solvent was removed. The crude product was finally purified by column chromatography using silica gel eluting with hexane gave a colorless viscous. Yield 14.06 g (95%). ^{1}H-NMR (300 MHz, $CDCl_3$) δ 7.50(6H, m), 1.95 (4H, t, J = 8.4 Hz), 1.00-1.40 (24H, m) and 0.95 (6H, m) ppm.

2.1.3*9-(7-bromo-9,9-dioctyl-9H-fluoren-2-yl)-9H-carbazole (4)*

A mixture of **3**(1.0620 g, 1.9364 mmol), carbazole (0.1542 g, 0.9221 mmol), copper(I) iodide (0.1756g, 0.9221 mmol), potassium phosphate (0.5173g, 4.6105mmol) and trans-diaminocyclohexane (0.1053 ml, 0.9221 mmol) in toluene (20 ml)was degassed with N_2 for 5 min. The mixture was heated to reflux under N_2 atmosphere for 24h. After the mixture was cooled to room temperature, water (50 ml) was added and the mixture was then extracted with CH_2Cl_2 (50 ml x 2). The combined organic layer was washed with water (50 ml), brine solution (50 ml), and dried over anhydrous Na_2SO_4. The solvent was removed to obtain crude product. The crude product was finally purified by column chromatography using silica gel eluting with a mixture of CH_2Cl_2 and hexane afforded a colorless viscous product. Yield 0.9468 g (89%) ; ^{1}H-NMR δH (300 MHz, $CDCl_3$) 0.78-0.88(10H, m), 1.15-1.30 (20H, m), 1.99-2.04 (4H, m), 7.32-7.43 (2H, m), 7.47 (4H, d, J = 3.9 Hz), 7.56 (4H, t, J = 6.0 Hz), 7.67 (1H, d, J = 8.7 Hz), 7.91 (1H, d, J = 7.8 Hz), 8.21 (2H, d, J = 7.8 Hz) ppm.

2.1.4 *9-(9,9-dioctyl-7-(pyren-1-yl)-9H-fluoren-2-yl)-9H-carbazole (PFC)*

A mixture of **4** (0.9468 g, 1.4917 mmol), 1-pyrene boronic acid (0.2169 g, 0.4972 mmol), $Pd(PPh_3)_4$ (34.3 mg, 0.0447 mmol) and an aqueous Na_2CO_3 solution (2 M, 10 ml) in THF (20 ml) was degassed with N_2 for 5 min. The mixture was heated to reflux under N_2 atmosphere for 24h. After the mixture was cooled to room temperature, water (50 ml) was added. The mixture was extracted with CH_2Cl_2 (50 ml x 2). The combined organic layer was washed with water (50 ml), brine solution (50 ml),and dried over

anhydrous Na_2SO_4. The crude product was obtained after solvent removal and purified by column chromatography using silica gel eluting with a mixture of CH_2Cl_2 and hexane to afford a white solid product. Yield 0.8517 g (90%):^{1}H-NMR δH (300 MHz, $CDCl_3$) 0.82-0.86 (6H, m), 0.94-0.96 (4H, m), 1.19-1.28 (20H, m), 2.07-2.11 (4H, m), 7.35 (2H, t, J = 7.5 Hz), 7.45-7.53 (4H, m), 7.62 (2H, d, J = 5.7 Hz), 7.70 (2H, d, J = 7.8 Hz),7.97-8.15 (7H, m), 8.21-8.31 (6H, m) ppm.

2.1.5 *3,6-dibromo-9-(9,9-dioctyl-7-(pyren-1-yl)-9H-fluoren-2-yl)-9H-carbazole* ***(5)***

N-Bromosuccinimide (0.4209 g, 2.3655 mmol) was added in small portions to a stirred solution of **PFC** (0.8517 g, 1.1264 mmol) in THF (25 ml). After initiative stirred at room temperature for 3h, water (50 ml) was added. The mixture was extracted with CH_2Cl_2 (50 ml x 3). The combined organic layer was washed with water (50 ml), brine solution (50 ml),and dried over anhydrous Na_2SO_4, sodium thiosulphate. The solvent was then removed to obtain crude product which was then purified by column chromatography using silica gel eluting with a mixture of CH_2Cl_2 and hexane affording a white solid product. Yield 0.8517 g (90%)

2.1.6 *9-(9,9-dioctyl-7-(pyren-1-yl)-9H-fluoren-2-yl)-3,6-di(pyren-1-yl)-9H-carbazole* ***(PFCdi-P)***

A mixture of **5** (0.95 g, 2.03 mmol), 1-pyrene boronic acid (1.23 g, 4.26 mmol), $Pd(PPh_3)_4$ (47 mg, 0.041 mmol) and an aqueous Na_2CO_3 solution (2 M, 10 ml) in THF (15 ml) was degassed with N_2 for 5 min. The mixture was heated to reflux under N_2 atmosphere for 24h. After the mixture was cooled to room temperature, water (50 ml) was added. The mixture was extracted with CH_2Cl_2 (50 ml x 2). The combined organic layer was washed with water (50ml), brine solution (50 ml), and dried over anhydrous Na_2SO_4. After solvent removing, the crude product was purified by column chromatography using silica gel eluting with a mixture of CH_2Cl_2 and hexane afforded light yellow solid product. Yield 1.36 g (82%)

2.1.7 *2,7-Bis[3,6-dipyrenecarbazol-9-yl]-9,9-bis-n-octylfluorene* ***(CFP4)***

A mixture of **7**(0.50 g, 0.48 mmol), pyrene-1-boronic acid)0.53 g, 2.17 mmol(, tetrakis (triphenylphosphine)palladium(0)(0.01g, 0.009 mmol),in THF (20 ml) and 2M Na_2CO_3 4.8 mLwas degassed with N_2 for 5 min. The mixture was heated to reflux under N_2 atmosphere for 24 h. After the mixture was cooled to room temperature, water (50 ml) wasadded. The mixture was extracted with CH_2Cl_2 (50 mlx2). The combined organic layer was washed with water (50 ml), brine solution (50 ml), dried overanhydrous Na_2SO_4. The solvent was then removed to obtained crude product. The crude product was finally purified by column chromatography using silica gel eluting with a mixture of CH_2Cl_2 and hexane to give yellow solids. Yield 0.085 g (11%). ^{1}H-NMR δ_H (ppm) (300 MHz, $CDCl_3$) 0.73-0.75 (10H,m), 1.07-1.28 (20H, m), 2.23 (4H, s), 7.77-7.88 (6H, m), 8.00-8.23 (36H, m), 8.29 (4H, d, J = 7.8 Hz), 8.38 (4H, d, J = 9.3 Hz), 8.52 (4H, s)) ppm.

3. Result and Disscussion

3.1 Synthesis and Characterization

The synthesis procedure of target materials is outlined in Scheme 1. The target materials **PFC**, **PFCdi-P** and **CFP4** were synthesized using a combination of bromination, alkylation, Ullmann coupling and Suzuki cross-coupling. The synthesized materials were characterized by ^{1}H-NMR, ^{13}C-NMR, UV-Vis and Fluoresence spectroscopy.

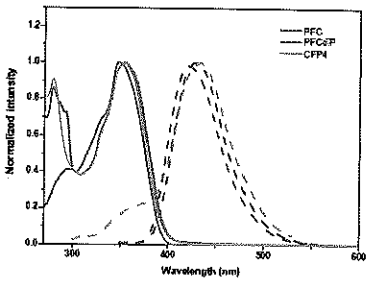

Figure 2.Absorption spectra and PL spectra of **PFC**, **CFP4** and **PFCdi-P** in CH_2Cl_2 solution

3.2. Optical properties

The optical properties of PFC, CFP4 and PFCdi-P were investigated using UV–vis and hotoluminescence spectroscopy in solutions as shown in Figure 2. The UV-Vis absorption spectra of PFC, CFP4 and PFCdi-P exhibit two strong characteristic bands: 280 nm (absorption band corresponds to the absorptions of carbazole unit) and 355 nm (absorption band corresponds to the absorptions of the fluorene unit). The emission spectra of PFC, CFP4 and PFCdi-P located in the blue-green region with emission peaks at 440 nm.

4. Conclusions

In this work,we successfully synthesized PFC, PFCdi-P and CFP4of blue light-emitting materials that conveniently prepared using bromination, alkylation , Ullmann coupling and Suzuki coupling reaction for use as blue light-emitting materials in organic light-emitting diodes (OLEDs)

Acknowledgements

The Thailand Research Fund (TRF) and the Commission on Higher Education (CHE), Center of Excellence for Innovation in Chemistry (PERCH-CIC), Department of Chemistry, Faculty of Science and Center for Organic Electronic and Alternative

Energy (COEA), Ubon Ratchathani University are acknowledged for the support.

References

[1]S. A. Vanslyke and et al. *Applied Physics Letters*.**51** (1987) 913-916.
[2] S. R. Forrest and et al. *Applied Physics Letters*.**75** (1999) 888-890.
[3]V .Promarak and et al. *Optical Materials*. **30** (2007) 364-369.
[4] V. Promarak and et al. *Thin Solid Films*. **516** (2008) 2881–2888.
[5] Y. Chen and et al. *Tetrahedron*.**65**(2009). 4455-4463.

Proceedings of the 38th Congress on Science and Technology of Thailand

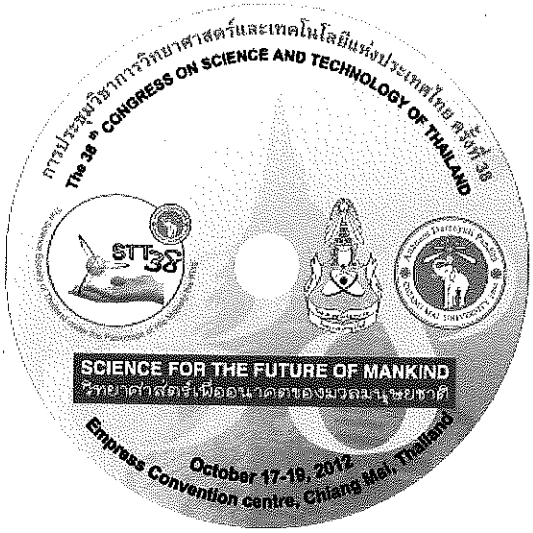

Venue : Empress Convention centre, Chiang Mai, Thailand
October 17-19, 2012

Supporters

NARIT

Sivadon

Lanna Products

Siam Photon

วช. NRCT

Chevron

สวทช. NSTDA

THAI Smooth as silk

PROGRAM FOR INVITED LECTURES AND ORAL PRESENTATIONS
19th October 2012

SESSION D (MATERIALS SCIENCE)
ROOM: ECC-Chiangmai 2

Chair Person: Supon Ananta
Co-chair Person: Anurak Prasatkhetragarn

Time	ID	Title	Speaker	Language
09:00-9:30	D_INV003	STRUCTURAL INVESTIGATIONS OF POLYMER COMPOSITES USING SAXS AND WAXS WITH SYNCHROTRON RADIATION	Taweechai Amornsakchai	Thai
09:30-9:50	D_D0057	SURFACE ANALYSIS OF THIN DLC FILM ON 304 STAINLESS STEEL DEPOSITED BY FCVA TECHNIQUE FOR TRIBOLOGICAL APPLICATION	Naksit Saenphinit	Thai
09:50-10:10	D_D0033	TRIBOLOGICAL PROPERTIES OF AS-RECEIVED FLY ASH-REINFORCED POLYESTER COMPOSITES	S. Zahi	English
10:10-10:20		coffee break		
10:20-10:40	D_D0010	PORPHYRIN MODIFIED TiO_2 FOR PHOTODEGRADATION OF ORANGE II DYE	Cheewita Suwanchawalit	English
10:40-11:00	D_D0053	THE COLORIMETRIC RESPONSE TO pH OF POLYDIACETYLENE/ZnO NANOCOMPOSITES	Kunruethai Faisadcha	Thai
11:00-11:20	D_D0054	VERSATILE ROUTE FOR FINE TUNING COLOR-TRANSITION TEMPERATURE OF POLYDIACETYLENE VESICLES BY USING LONG CHAIN ALCOHOLS AS ADDITIVES	Anothai Kamphan	Thai
11:20-11:40	D_D0055	EFFECT OF POLYMERIC ADDITIVES ON PHOTOPOLYMERIZATION PROCESS OF POLYDIACETYLENE ASSEMBLIES	Chittima Kamrak	Thai
11:40-12:00	D_D0065	SYNTHESIS AND CHARACTERIZATION OF BULKY D-D-pi-A TYPE ORGANIC DYES FOR DSSCs	Teadkait Kaewpuang	English

SYNTHESIS AND CHARACTERIZATION OF BULKY D-D-π-A TYPE ORGANIC DYES FOR DSSCs

Teadkait Kaewpuang, Siriporn Jungsuttiwong, Taweesak Sudyoadsuk, Tinnagon Keawin, Vinich Promarak*
Center for Organic Electronic and Alternative Energy (COEA), Department of Chemistry and Center of Excellence for Innovation in Chemistry, Faculty of Science, Ubon Ratchathani University, Ubon Ratchathani 34190. Thailand
*e-mail: teadkaitkanwpuang@gmail.com

Abstract: Novel organic dyes, namely **Dye2** and **Dye3**, containing di(carbazole fluorenethiophenyl)amine as bulky donor moiety are designed and synthesized. The oligophenylthiophenes and cyanoacrylic acid are used as π-conjugated bridge and electron-withdrawing anchoring group, respectively. The target molecules were characterized by NMR, IR, UV-vis and fluorescence techniques.

Introduction: Dye sensitized-solar cells (DSSCs) have been intensively investigated since the report of highly efficient ruthenium complex-sensitized TiO2 solar cells by the Swiss scientists. To date, overall conversion efficiencies of up to 12% were achieved from the ruthenium complex device. However, pure organic dyes exhibit not only higher extinction coefficient, but simple preparation and purification procedure with a low cost. Recently, enormous progress has been made in this field and the highest overall photoelectric conversion efficiency of solar cells sensitized by organic dyes containing an electron donor (D) and an electron acceptor (A), separated by a π-conjugation bridge (π) has reached 9.8%. This indicates the promising perspective of metal-free organic dyes. Therefore, in this work, we develop bulky D-D-π-A type organic dyes having di(carbazole fluorenethiophenyl)amine as bulky donor moiety, cyanoacrylic acid as acceptor and oligophenylthiophenes as π-conjugated bridge

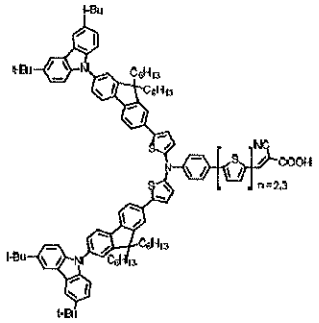

Figure 1. Chemical structures of the designed dyes.

Methodology: All reagents were purchased from Aldrich, Acros or Fluka and used without further purification. All solvents were supplied by Thai companies and used without further distillation. THF was refluxed with sodium and benzophenone, and freshly distilled prior to use. ^{1}H and ^{13}C NMR spectra were recorded on a Bruker AVANCE 300 MHz spectrometer. Infrared (IR) spectra were measured on a Perkin-Elmer FTIR spectroscopy Spectrum RXI spectrometer. Ultraviolet-visible (UV-Vis) spectra were recorded on a Perkin-Elmer UV Lambda 25 spectrometer and photoluminescence spectra were recorded with a Perkin-Elmer LS 50B Luminescence Spectrometer as dilute CH_2Cl_2 solution

Results, Discussion and Conclusion: The **Dye2** and **Dye3** were synthesized as shown in Scheme 1. Ullmann coupling reaction of **BrF (1)** with *t*-Bu-carbazole using K_3PO_4 as base, CuI catalyst and used *trans*-diaminocyclohexane as co-catalyst in toluene gave **CFBr (2)** in 72% yield. Suzuki cross coupling reaction of **CFBr (2)** with 2-thiopheneboronic acid was carried out using $Pd(PPh_3)_4$ as a catalyst, Na_2CO_3 as a base in THF resulting in **CFT (3)** in 77% yield. Iodination reaction of **CFT (3)** with NIS in mixed solvent of choroform:acetic acid (1:1) to gave **CFTIodo (4)** in 90% yield. Ullmann coupling reaction between **CFTIodo (4)** and 4-bromoaniline afforded **CFTA (5)** in 45% yield. Suzuki cross coupling reaction of **CFTA (5)** with 2-thiopheneboronic acid was carried out using $Pd(PPh_3)_4$ as a catalyst, Na_2CO_3 as a base in THF resulting in **CFTAT (6a)** in 66% yield. Bromination reaction **CFTAT (6a)** with NBS in THF gave **CFTATBr (7a)** in 86% yield. Suzuki cross coupling reaction of **CFTATBr (7a)** with 2-thiopheneboronic acid gave **CFTAdi-T (6b)** in 90% yield followed by bromination of the resultant with NBS in THF gave **CFTAdi-TBr (7b)** in 99% yield. Suzuki cross coupling reaction of **CFTATBr (7a)** and **CFTAdi-TBr (7b)** with 5-formyl(thiophen-2-yl)boronic acid yielded **CFTAdi-T-aldehyde (8a)** and **CFTAtri-T-aldehyde (8b)** in 98% and 88% yields, respectively. Finally, Knovenagel condensation reaction of **CFTAdi-T-aldehyde (8a)** and **CFTAtri-T-aldehyde (8b)** with 2-cyanoacetic acid using piperidine catalyst in chloroform produced **Dye2** and **Dye3** in 97% and 98% yields, respectively.

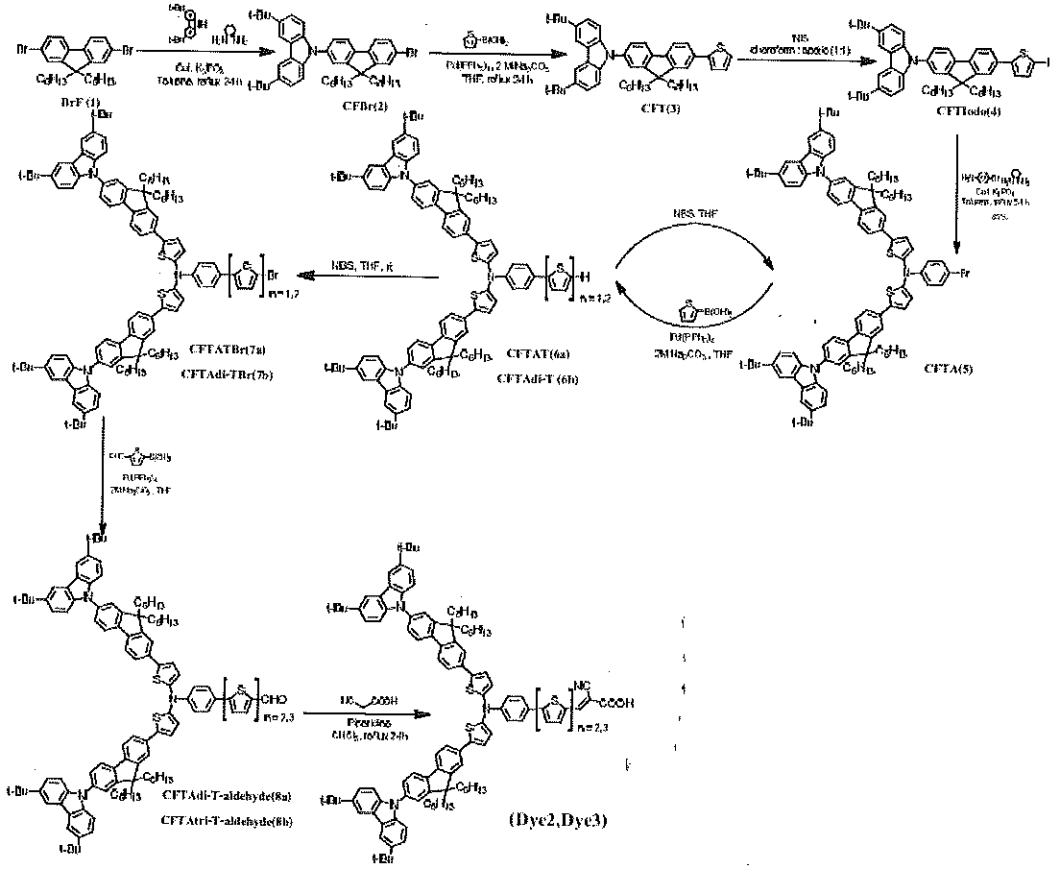

Scheme 1. Synthetic route to the target dyes.

The **Dye2** and **Dye3** were characterized by NMR, IR, UV-vis and fluorescence techniques. They are soluble in chlorinated solvents, THF and acetone and exhibit absorption band cover UV and visible regions.

References:

1. O'Regan B, Gratzel M: Nature 1991;353:737–740.
2. Duckhyun K, Jae Kwan L, Sang Ook K, Jaejung K: Tetrahedron 2007;63: 1913–1922

Acknowledgements: PERCH-CIC, TRF (MRU5080052), UBU, CHE.

Keywords: dye-sensitized solar cell, carbazole, fluorene, thiophene, donor-π-acceptor

VITAE

NAME	Mr. Teadkait Kaewpuang
BORN	28 July 1982, Sisaket, Thailand
EDUCATION	2008-2009, Bachelor of Science Chemistry, Ubon Ratchathani Rajabhat University
	2009-2011, Master of Science Chemistry, Ubon Ratchathani University
SCHOLARSHIPS	Research Prize from Center of Excellence for Innovation in Chemistry: Postgraduate Education and Research Program in Chemistry (PERCH-CIC), 2008